Functional and structural diversity of the microbial communities associated with the use of Fischer-Tropsch GTL Primary Column Bottoms as process cooling water

B.F. VAN NIEKERK

12248053

Dissertation submitted in partial fulfilment of the requirements for the degree of

Master of Environmental Sciences (Microbiology)

in the School of Environmental Sciences and Development at the Potchefstroom Campus of the North-West University

Supervisor: Mr. P.J. Jansen van Rensburg

Co-supervisor: Prof. C.C. Bezuidenhout

Co-supervisor: Mr. J.J. Bezuidenhout

November 2011

TABLE OF CONTENTS

ACKNOWLEDGEMENTS

Mr. Peet Jansen van Rensburg, for all his guidance and technical assistance with various aspects of this project. It is greatly appreciated.

Prof. Carlos Bezuidenhout for all his patience and willingness to help whenever things got overwhelming.

Mr. Jaco Bezuidenhout for being a true friend as well as supervisor. Your help and advice was invaluable.

Dr. Karl-Heinz Riedel, Sasol R&D Sasolburg.

Dr. Lourens Tiedt for assistance with electron microscopy.

Mr. Alfonso Palazzo, Buckman Laboratorius, Hammarsdale, KwaZulu-Natal.

Mr. Don Watt Pringle, Improchem, Sasolburg.

NRF and Sasol R&D (Sasolburg) for funding of this project.

My beloved family and friends, especially my husband Lourens, for their prayers, motivation, support and love.

DECLARATION

I declare that the dissertation submitted by me for the degree of *Master of Environmental Sciences* in Natural Sciences at the North-West University (Potchefstroom Campus), Potchefstroom, North West, South Africa, is my own independent work and has not previously been submitted by me at another university. I further concede copyright of the dissertation in favour of the North-West University.

Signed in Potchefstroom, South Africa

Signature: ..... Date: .....

Bertina Freda van Niekerk

ABSTRACT

Despite emerging water shortages, most water is only used once, and often with low efficiency. However, with appropriate treatment, water can be re-used to reduce the demand on freshwater sources. The Department of Water Affairs, South Africa, promotes industries to reduce discharges into water resources in order to sustain an overall good water quality of all water systems. All of this ultimately leads to industries striving towards zero effluent discharge. Primary Column Bottoms (PCBs) is a wastewater stream derived from the Fischer-Tropsch Gas to Liquid process and consists mainly of organic acids, but no nitrogen or phosphorous, which by implication excludes possible biodegradation. In the operation of cooling towers in industrial processes, cooling water quality has a direct impact on the cooling performance of the system, where nutrient levels may affect fouling, scaling and corrosion observed in the cooling towers. Fouling, scaling and corrosion affect the operating efficiency of cooling water systems and may necessitate the addition of chemical agents to control these phenomena. This has a financial and labour time impact on the operation of these systems.

In this study a mini cooling tower test rig was operated with a synthetic PCB effluent as cooling water and various cycles of concentration, pH and linear flow velocities (LFVs). A constant delta temperature of 10 °C was maintained. Cycles of concentration (COC) evaluated included 2, 4 and 6 cycles of concentration and linear flow velocities evaluated was 0.6 m/s, 0.9 m/s and 1.2 m/s. Fouling, scaling and corrosion rates were determined using corrosion coupons and heat exchanger tubes for mild steel and stainless steel. Besides the evaluation of the various operational parameters for fouling, scaling and corrosion, the possibility for chemical oxygen demand (COD) removal by operating the cooling tower as a bioreactor was also evaluated. To this end nutrient correction was applied to the reactor to allow for a CNP ratio of 100:10:1.

With regard to fouling, scaling and corrosion, mild steel was more affected by fouling, scaling and corrosion compared to stainless steel where almost no fouling, scaling and corrosion was observed. Overall increased linear flow velocities resulted in higher fouling and scaling rates, whereas lower linear flow velocities resulted in decreased corrosion rates. In terms of cycles of concentration, increased COC resulted in higher fouling, scaling and

corrosion rates. Despite the high nutrient removal levels, the accompanying fouling, scaling and corrosion was still below the particular industry's guidelines.

Besides physical-chemical evaluation of the towers under the various operational conditions, culture-dependent and culture-independent methods were also employed. Concerning culture-dependent approaches the study demonstrated that aerobic and anaerobic organisms are present in both the planktonic and sessile phase of the cooling tower reactors. Heterotrophic aerobes were found to be the most abundant under all the operating conditions. Sulphate reducing bacteria were more abundant in the sessile phase of the cooling towers, and the presence of high sulphate levels in the experiments could be indicative of the sulphate reducing bacteria actively participating in the microbial community. Lower than expected corrosion levels, however, suggest that a combination of the organisms in the biofilm rather than sulphate reducing bacteria alone, contributed to the corrosion rates observed. Culture-independent methods, specifically phospholipid fatty acid analysis supported the results from the culture-dependent methods. Furthermore results demonstrated that linear flow velocity had a greater effect on the community structure than cycles of concentration. Finally molecular methods, specifically denaturing gradient gel electrophoresis, found that increasing cycles of concentration resulted in increased microbial community diversity, while increasing linear flow velocity resulted in decreased microbial community diversity.

Regarding COD removal, nutrient correction of the synthetic PCB effluent achieved 89.35 % COD removal at 2 COC and 1.2 m/s LFV, while 80.85 % COD removal was achieved at 4 COC at 1.2 m/s LFV. From these results it was recommended that the operation of the cooling tower should be at 4 COC and 1.2 m/s, which despite slightly lower % COD removal, were characterised by fouling, scaling and corrosion rates well within guidelines.

Keywords: cooling towers; bioreactor; fouling; scaling; corrosion; denaturing gradient gel electrophoresis; phospholipid fatty acid analysis

LIST OF FIGURES

LIST OF TABLES

ABBREVIATIONS

ANOVA	Analysis of variance
Bp	Base pair
CNP ratio	Carbon, nitrogen, phosphorous ratio
COC	Cycles of concentration
COD	Chemical oxygen demand
DGGE	Denaturing gradient gel electrophoresis
DNA	Deoxyribonucleic acid
DO	Dissolved oxygen
DWA	Department of Water Affairs
EC	Electrical conductivity
EDTA	Ethylenediaminetetraacetic acid
eV	Electron volt
FAME	Fatty acid methyl esters
GC	Gas chromatography
GTL	Gas-to-liquid
HET	Heat exchanger tube
HSD	Honest significant difference
IOB	Iron oxidising bacteria
IRB	Iron reducing bacteria
kPa	Kilopascal
LFV	Linear flow velocity
LSCI	Larson-Skold corrosion index
LSI	Langelier saturation index
m/s	metre/second
mg/l	milligram per litre
MIC	Microbiologically induced corrosion
mm	Millimetre
Monos	Monounsaturated fatty acids
MPN	Most probable number
mS/cm	milliSiemens per centimetre

Nsats	Normal saturated fatty acids
PCB	Primary column bottoms
PCR	Polymerase chain reaction
PLFA	Phospholipid fatty acid analysis
Polys	Polyunsaturated fatty acids
PSI	Puckorius scaling index
RDA	Redundancy analysis
rDNA	Ribosomal DNA
RP	Redox potential
RSI	Ryznar stability index
SA	South Africa
SASOL	South African Synthetic Oil Limited
SEM	Scanning electron microscopy
SRB	Sulphate reducing bacteria
TAE	Tris-acetate-EDTA
TDS	Total dissolved solids
TSS	Total suspended solids
UK	United Kingdom
w/v	Weight per volume
ΔT	Temperature difference between inflow and outflow from heat exchanger

CHAPTER 1 - INTRODUCTION

1.1 GENERAL INTRODUCTION

South Africa is classified as a semi-arid country with an average rainfall of approximately 480 mm per year compared to the world's average of 860 mm per year (DWAF, 2004; Karlberg and Penning de Vries, 2004). This water is utilised for agriculture, industries, mining as well as domestic purposes (Benzaoui and Bouabdallah, 2004; DWAF, 2004), resulting in a significant demand for this resource. However, pollution is threatening the available supply of fresh water, and coupled with a rapid increase in population, greater pressure is being exerted on this precious and limited resource (Milovanovic, 2007). These rising demands for water are leading to competition for the allocation of limited freshwater resources (Anon, 2001b; Jewitt *et al*., 2004; Adewumi *et al.*, 2010).

In a country such as South Africa, economical development is closely linked with the wellbeing of its industries and as such industries in turn need to know that there would be sufficient amounts of water available to them (DWAF, 2004). Global interests as well as the interests of all water users should be considered when determining methods to optimise water usage (Anon, 2001a) and this is especially applicable for arid and semi-arid areas such as South Africa (Jewitt *et al*., 2004). With the growing need for water (Yang and Abbaspour, 2007; Panjeshahi and Ataei, 2008), a shortage of freshwater in South Africa can be foreseen and ways to preserve water need to be initiated (Jewitt *et al*., 2004). Some of these possible solutions include amongst others water conservation, desalination, weather modification, reallocation and reuse of water (Benzaoui and Bouabdallah, 2004; Jewitt *et al*., 2004; Karlberg and Penning de Vries, 2004).

Despite emerging water shortages, most water is used only once and generally with low efficiency (Benzaoui and Bouabdallah, 2004), but when water is treated appropriately it can be reused in order to reduce the high demand on freshwater sources (Anon, 2001b; Van Der Bruggen and Braeken, 2006; Alva-Argáez *et al*., 2007). However, reuse is mostly limited to use within industries. Because of the large volumes of water used in petroleum industries such as SASOL (South African Synthetic Oil Limited), water reuse can lead to huge savings in terms of freshwater intake and treatment costs involved before discharge into receiving

water systems (Koppol *et al*., 2003; Saha *et al*., 2005; Van der Bruggen and Braeken, 2006; Alva-Argáez *et al*., 2007; Ataei *et al.*, 2009). The Department of Water Affairs, South Africa, promotes industries to reduce discharges into water resources in order to sustain an overall good water quality of all water systems (DWAF, 2004). With this in mind industries, including SASOL, strive towards zero effluent discharge.

1.2 PROBLEM STATEMENT

Due to new restrictions on water usage by industries (Koppol *et al*., 2003; DWAF, 2004; Van der Bruggen and Braeken, 2006; Panjeshahi and Ataei, 2008) the reuse of process water is becoming essential (Alva-Argáez *et al*., 2007; Adewumi *et al.*, 2010; Gunson *et al.*, 2012) and will have significant social, environmental as well as economical consequences (Koppol *et al*., 2003). One possible application of process water is in the cooling of other industrial streams (Saha *et al*., 2005; Gunson *et al*., 2012), specifically through the use of cooling towers. Normally, the water used during this process is mostly freshwater derived from river water and sometimes reclaimed municipal water. Thus, the reuse of process water would minimise the water intake by the industry significantly (Gunson *et al.*, 2012).

In the case of SASOL, primary column bottoms (PCB) is a wastewater stream of the Fischer-Tropsch gas-to-liquid (GTL) conversion processes (Overett *et al*., 2000). This reaction water was expected to contain large quantities of hydrocarbons as well as oxygenated compounds and the chemistry is very complex (Dry, 1999). Although PCBs have high amounts of carbon in the form of organic acids, it does not contain any nitrogen (Dry, 1999). A carbon, nitrogen and phosphate (CNP) ratio of 100:10:1 is considered appropriate for biodegradation processes (Burgess *et al*., 1999; Schmidt *et al*., 2007). Since no nitrogen is expected to be present in the PCBs the biodegradation may be compromised. This phenomenon was demonstrated by Slabbert (2006).

Increased nutrient loads within the cooling tower system may cause certain problems such as increased biological and non-biological fouling, scaling and microbial and chemically induced corrosion (Lutey, 1996; Mohsen, 2004) which may result in high operational and maintenance costs (Meesters *et al*., 2003; Neria-González *et al*., 2006). Fouling is the accumulation of deposits on surfaces in contact with an aqueous solution (Flemming, 1997)

and different types of fouling are found in cooling water systems, including biofouling which are caused by organisms (micro- and macro-organisms) found in the system (Videla, 2002).

Formation of hard, crystalline mineral deposits is called scaling, and is usually caused by the precipitation of mineral deposits, which in turn are influenced by the water quality (pH, temperature and hardness); (Rakanta *et al*., 2007). Corrosion can be described as the deterioration of a metal caused by one, or a combination of chemical, physical and biological factors (Rakanta *et al.*, 2007). One of the biggest concerns of process cooling water systems is microbiologically induced corrosion (MIC) that are caused by microorganisms (biological factors) (Angell and Urbanic, 2000; George *et al*., 2003).

When the impact of process water reuse on the fouling and corrosion of cooling systems are being studied, both the planktonic and sessile communities should be considered (Ludensky, 2003). Various methods are available to study microbial community structure and functional dynamics. Conventional microbiological techniques include methods such as the most probable number (MPN) technique and plate counts. Most probable number technique provides the user with an estimated amount of bacteria found within a liquid medium (Prescott *et al.*, 2002). Plate counts are done on solid selective media. Both of these techniques (MPN and plate counts) are culture-dependent methods making use of various nutrients and incubation conditions in order to enumerate microorganisms. The main disadvantage associated with the use of conventional methods is the fact that not all microorganisms can be cultured (Wang *et al*., 2006; Sanz and Köchling, 2007). This gives rise to the now common approach of using culture-dependent methods in conjunction with culture-independent methods (such as phospholipid fatty acid analysis, or PLFA and denaturing gradient gel electrophoresis, or DGGE) (Lagacé *et al*., 2006; Soares *et al*., 2006; Wang *et al*., 2006). The use of PLFA is becoming an increasing popular method for microbial community analysis (Werker and Hall, 1998; Hill *et al*., 2000; Wang *et al*., 2006; Sanz and Köchling, 2007). It is based on the principle that all microbial groups have characteristic fatty acids that are unique to that group. By detecting these fatty acids in a sample, the specific microbial communities are revealed (Hill *et al*., 2000; Sanz *et al*., 2007). Denaturing gradient gel electrophoresis (DGGE), on the other hand, determines the structure of microbial communities on the basis of the type and relative abundance of the various phylogenetic groups found within the community (Forney *et al*., 2001). Combined application of both culture-dependent and culture-independent methods for the study of the

microbial communities present in the cooling towers should provide a more thorough characterisation of the microbial communities than either method in isolation.

1.3 AIM AND OBJECTIVES

The aim of this study was to determine the functional and structural diversity of the microbial communities associated with the use of Fischer-Tropsch GTL synthetic PCB as process cooling water and its implication on fouling, scaling and corrosion. The objectives for this study were to:

1. optimise cooling tower operational conditions (COC and LFV) using C:N:P corrected synthetic PCB.
2. determine the effect of operational parameters on the rate of fouling, scaling and corrosion when using water cooling systems operated of GTL Fischer-Tropsch PCB.
3. determine the functional and structural diversity of microbial communities (planktonic and sessile) found within the cooling tower by making use of culture-dependent (conventional) and culture-independent (PLFA and DGGE) methods as well as scanning electron microscopy (SEM).

The mentioned objectives are expanded on in chapters 3, 4 and 5 respectively.

CHAPTER 2 - LITERATURE REVIEW

2.1 INTRODUCTION

Water is an extremely limited resource in South Africa. This can be ascribed to the low average rainfall and high evaporation rates (DWAF, 2004; Jewitt *et al.*, 2004; Karlberg and Penning de Vries, 2004). Furthermore, the distribution of rainfall and water availability across the country vary greatly from east to west, resulting in sub-humid conditions with high rainfall at the eastern coastal regions and desert or semi-desert conditions with low rainfall along the western regions (DWAF, 2004). Current and predicted future global temperature increases may lead to even lower annual rainfall, resulting in up to 10 % decreased runoff water in the west as soon as 2015 and spreading towards the eastern coastal areas by 2060. If this occurs, availability and quality of water could decrease even further (DWAF, 2004).

In order to achieve better water management in South Africa, nineteen catchment-based water management areas has been identified by the Department of Water Affairs (DWA). Most of these catchment areas are interlinked by rivers and tributaries. An example of this is the Vaal River system which extends over several of these catchment areas (DWAF, 2004). The Vaal River system stretches over 1300 km, running from east to west (Tempelhoff, 2009). The central component of this river system is located in the Upper Vaal management area in the eastern inland part of the country (DWAF, 2004). Water from the Vaal River has great economic value, as the river is situated in the main mining and industrial sectors of the country and supplies drinking water to the largest metropolitan area in South Africa. Agriculture can also be found in the surrounding areas (DWAF, 2004; Tempelhoff, 2009; Wepener *et al.*, 2011). The Vaal River Barrage is located in the Upper Vaal management area and is the receptor of industrial and municipal wastewater discharges (DWAF, 2004; Tempelhoff, 2009). Water quality of the Vaal River is greatly affected by these discharges. Mining activities and industrial discharges leads to increased acidity of water with raised levels of metals, toxins and chemicals. If municipal wastewater is not treated appropriately before discharge it could result in increased salinity, nutrient levels and microbiological pollution. Agriculture may also give rise to increased nutrient loads within the river system (DWAF, 2004).

One policy created by the DWA to reduce the discharge of wastewater into freshwater resources is the polluter-pay-policy. This policy states that pollution costs should be the responsibility of the polluter (discharger). Rebates should also be available in cases where the discharged water quality is better than the quality of the water abstracted from the river systems. Hopefully this policy could lead to reduced waste discharge and promote sustainable water use (DWAF, 2004).

Industries use enormous quantities of water. With increased costs and stricter environmental laws concerning wastewater discharge, industries are forced to collect and treat their wastewater streams so that it may be possible to use in other applications (Van der Bruggen and Braeken, 2006; Wang *et al.*, 2006; Alva-Argáez *et al.*, 2007; Adewumi *et al.*, 2010). Reuse of these waste streams by industry could have significant impacts, such as decreased water usage and wastewater discharge as well as lower discharge fees, ultimately resulting in reduced operating costs (Koppol *et al.*, 2003; Mohsen, 2004; Miller, 2006; Van der Bruggen and Braeken., 2006; Wang *et al.*, 2011). Zero liquid discharge has become a strategy for industries to conserve their water use/abstraction profile. Despite the obvious financial savings with the implementation of zero liquid discharge, treatment of wastewaters might be necessary before reuse, which in turn could raise operational costs (Koppol *et al.*, 2003). Therefore, appropriate technologies should be tested for each industry. Studies performed in India and South Africa on the improvement of industrial water use, found that the optimisation of cooling tower conditions can lead to the reuse of wastewater, and ultimately to a reduction in water intake (Saha *et al.*, 2005; Swart and Engelbrecht, 2007).

Vast amounts of water are used by the petroleum industry for cooling and other purposes to such a degree that water is considered its most extensively used raw material (Ataei *et al.*, 2009). Wastewater from the petroleum industry is complex and may contain high levels of organic substrates, nutrients, calcium carbonate, chlorides as well as high TDS levels (Rebhun and Engel, 1998; Van der Bruggen and Braeken, 2006). Water with increased nutrient loads is suitable for microbial growth. Furthermore, microorganisms are capable of degrading organic compounds under favourable growth conditions (Burgess *et al.*, 1999). Primary nutrients that should be available include carbon, nitrogen and phosphorus (CNP), with the optimum CNP ratio for microbial growth 100:10:1. The presence of these primary nutrients all improves nutrient removal/degradation (Burgess *et al.*, 1999; Dhamole *et al.*, 2009; Kampas *et al.*, 2009).

2.2 FISCHER-TROPSCH WASTE WATER STREAM

The South African Synthetic Oil Limited (SASOL) GTL conversion projects, converts natural gas to diesel and other products by making use of the Fischer-Tropsch, (FT) reaction (Dry, 1999). During the FT reaction, synthesis gas (syngas), which consists of carbon monoxide and hydrogen, are converted into hydrocarbons and oxygenates (such as alcohols, aldehydes, ketones and acids) (Dry, 1999; 2002). This waste stream has potential to be used as cooling water which could ultimately lead to the "zero discharge" phenomena (Mohsen, 2004). However, due to the organic nature of the waste stream it requires treatment before it is suitable for use (Dry, 1999).

2.3 COOLING TOWER OPERATION

In industrial systems, cooling towers are used to cool hot process water and to steer clear of thermal pollution (Kim *et al.*, 2001; Mohsen, 2004). This process starts with cold make-up water that moves from the basin of the cooling tower towards the heat exchangers by means of a pump (Figure 2.1) (Bott, 1998). Cold water within the heat exchanger tubes absorbs the process heat and warm water returns to the cooling tower to be cooled down (Qureshi and Zubair, 2006). Warm water enters the top of the cooling tower and moves over the fill (packing material). At the same time air is blown upwards through the cooling tower where heating of the air and evaporation takes place (Figure 2.1) (Bott, 1998; Meesters *et al.*, 2002). The fill (packing material) in cooling towers are used to expand the air-water interface in order to ensure maximum cooling of water.

Circulating water lost through evaporation needs to be replaced with make-up water (Bott, 1998; Meesters *et al.*, 2002; Rakanta *et al.*, 2007). There are three types of water loss in cooling towers, namely, water lost through evaporation, windage (drift) and leakage (Figure 2.1) (Bott, 1998). Water lost through drift within conventional cooling towers is generally considered to be less than 0.2 % of the inlet water and leakage is minimal (Kim *et al.*, 2001). Since water is lost during cooling tower operation, the remaining water is concentrated with dissolved mineral salts. The amount of mineral salts compared to the mineral salt content of the make-up water is called the COC (Lee and Young, 2002; Videla, 2002; Anon, 2005). Make-up water is considered to be one COC. Every time the basin needs to be refilled with

make-up water the dissolved mineral concentration doubles (You *et al.*, 2001). Blowdown is considered a means of controlling the COC, and can be described as the removal of concentrated water from the cooling tower basin at a specific rate (Figure 2.1). This water is then replaced with fresh make-up water, thus keeping mineral salts at a given COC (Lee and Young, 2002).

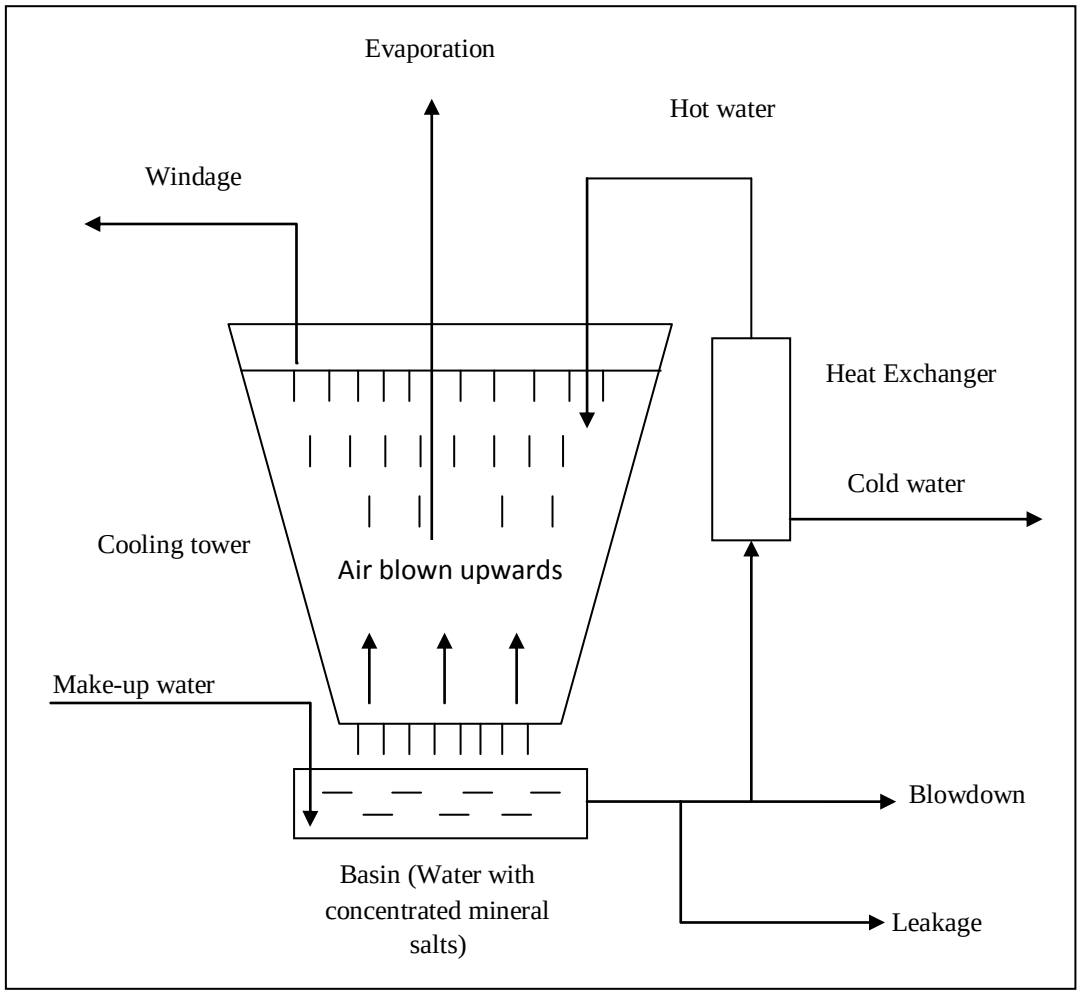

Figure 2.1: Schematic representation of a typical cooling tower, also demonstrating water loss during cooling tower operation (Adapted from Bott, 1998).

2.4 COOLING TOWER WATER QUALITY

Physical-chemical properties of cooling water play an important role in the fouling, scaling and corrosion rate as well as the microbial community present in these sytems (Lutey, 1998; Rakanta *et al.*, 2007). These properties include the pH, temperature and dissolved as well as suspended solids found within the cooling water (Lutey, 1998). Operating pH values can influence the solubility of most salts, for example, high pH levels may might lead to

increased mineral salt deposits, whereas pH levels lower than four (4) will increase the corrosive properties of the water (Anon, 1994; Rakanta *et al.* 2007). Increased temperatures beyond the optimum range for microbial growth within the cooling tower may lead to decreased COD removal rates and also an increase in all chemical reactions, including corrosion (Anon, 1994; Lapara *et al.*, 2001). Solids in cooling water can be found as dissolved solids and suspended solids (APHA, 1985). Because the water in a cooling tower system is concentrated by evaporation, high levels of solids can be expected which in turn may lead to increased scaling within the system, especially on the heat exchangers (Anon, 1994; Mohsen, 2004; Rakanta *et al*., 2007).

2.5 BIOFILMS IN COOLING TOWERS

Biofilms can be described as localised concentrations of microorganisms consisting of multi-species community attached to a substratum (White *et al.*, 1999; Singh *et al.*, 2006). Bacteria initialise biofilm formation when the environmental conditions such as nutrient and oxygen availability are suitable and a liquid comes in contact with a solid surface (Chen and Chai, 2006; Morikawa, 2006). There are advantages to organisms found within the biofilm. Organisms within biofilm secrete a layer of extracellular polymeric substances (EPS) which is responsible for the attachment of the biofilm to the substratum (Lutterbach and De França, 1996). The EPS also trap nutrients, reduce convection processes and controls permeation rate of water through the biofilm (Flemming, 1997; Neu and Lawrence, 1997; Keresztes *et al.*, 2001; George *et al.*, 2003), whilst offering protection against environmental assaults such as high flow velocity (Cloete *et al.*, 1994; Melo and Bott, 1997; Morikawa, 2006).

When investigating the impacts of biofilms in industrial processes, research emphasises the role of biofilms over the role of the planktonic phase in damage to water based technological processes (Ludensky, 2003; Ilhan-Sungur and Çotuk, 2010). This might be due to the fact that the planktonic organisms are more affected by changes in pH, nutrient concentrations and toxic substances (Lazarova and Manem, 1995). Cooling water systems provide the ideal environment for biofilm formation, namely nutrients, favourable temperatures, high residence time, high ratio of surface area to volume, availability of air, heat and light (Melo and Bott, 1997; Choudary, 1998; Chen *et al.*, 2005; Ilhan-Sungur and Çotuk, 2010). The movement of water through the cooling tower affects the biofilm greatly. Thicker biofilms can be found at increased hydrodynamic strengths caused by increased biomass production. The increased

biomass may result from higher mass transfer and increased biofilm cohesion strength in response to high detachment forces (high flow velocities) (Melo and Bott, 1997; Chen *et al.*, 2005; Rochex *et al*, 2008). However, increased flow velocities also lead to lower community diversity within the biofilm (Rochex *et al.*, 2008). Problems caused by biofilms in cooling towers include the reduced transfer of heat at heat exchangers and altered fluid transfer through the system. This results in higher energy requirements as well as more operational downtime for maintenance cleaning, and ultimately leads to increased operational costs (Bott, 1998; Ludensky, 2003; Morikawa, 2006; Ilhan-Sungur and Çotuk, 2010). Biofilms may enhance localised corrosion of metals by creating differences in the ion concentration, pH and oxygen levels at the metal surface (Lutterbach and De França, 1997; Xu *et al.*, 2007; George *et al.*, 2003).

2.6 FOULING

Fouling can be described as the accumulation of deposits on surfaces in contact with an aqueous phase (Flemming, 1997). These materials can be chemically generated or it can either be dissolved or suspended within the aqueous solution (Yang *et al.*, 2002). With regard to cooling water systems, fouling is mostly observed at the heat exchangers (Flemming, 1997). Because of different types of deposits found on heat exchangers, one can distinguish between five different types of fouling, namely, biological (biofouling), chemical, corrosion, particulate and precipitation fouling (Videla, 2002). Chemical fouling can be described as originating from chemical reactions found within the system, but excludes reactions of the structural metal. On the other hand, particulate fouling is caused by the fluid transport of particulate solids, which may accumulate on metal surfaces. Precipitation fouling is typically caused by the precipitation of dissolved substances on metal surfaces and can also be referred to as encrusting (Videla, 2002). In an industrial setting, biofouling seems to be the most widely found type of fouling (Ludensky, 2003). It can be described as the accumulation of deposits containing micro- or macro-organisms on a surface in contact with an aqueous phase (Flemming, 1997; Videla, 2002). Two of the major problems associated with biofouling are that biofilms may reduce heat transfer in heat exchangers and cause numerous other problems in water processing systems (Pasmore *et al*., 2001). These include damage to equipment caused by biocorrosion of metals (Azis *et al*., 2001; Meesters *et al*., 2003) as well as accelerated scale formation (Al-Ahmad *et al.*, 2000).

2.7 SCALING

Scaling can be defined as hard, crystalline mineral deposits (Videla, 2002). It is formed when water saturated with calcium and magnesium salts are either heated or cooled, causing the precipitation of these salts (Lee and Young, 2002; Videla, 2002; Rakanta *et al.*, 2007). Scale is therefore a frequent problem associated with heat exchangers and cooling towers (Lee and Young, 2002; Marín-Cruz *et al*, 2006; Li *et al.*, 2011). Scaling mainly occurs in the form of calcium and magnesium carbonates, sulphates or silicates, with calcium carbonate being the most commonly found form of scaling in cooling waters (Lee and Young, 2002; Videla, 2002). Main parameters influencing scale formation are pH, temperature and hardness (Anon, 1994; Videla, 2002; Omar *et al.*, 2010; Li *et al*., 2011). Within cooling water systems, scaling deposits can cause decreased capacity for thermal exchange and may even lead to corrosion caused by its porous structure (Lee and Young, 2002; Videla, 2002; Marín-Cruz *et al.*, 2006; Rakanta *et al.*, 2007).

2.8 CORROSION

Corrosion is a variation of redox reactions, which occurs when a metal comes in contact with a non-metal substance and the metal is then oxidised and the non-metal substance is reduced (Anon, 1994; Shreir *et al*., 2000). According to Melidis *et al* (2007) all waters may be classified as corrosive and the degree thereof is influenced by the physical and chemical characteristics of the given water. Corrosion is one of the major problems associated with the use of cooling towers (Marín-Cruz *et al.*, 2006; Rakanta *et al.*, 2007; Xu *et al.*, 2007.) Three main factors (chemical, physical and biological) influence the corrosion process in cooling systems (Anon, 1994). Chemical factors which influence the corrosion process are dissolved carbon dioxide, dissolved oxygen, high mineral salt content and the pH value of water (Anon, 1994). High levels of oxygen in cooling water can damage the protective oxide layer on metals (Anon, 1994; Rakanta *et al.*, 2007). The aeration of water during circulation further increase the dissolved oxygen levels (Anon, 1994; Shreir *et al.*, 2000). Higher pH levels tend to increase scaling, whist lower pH levels may increase the corrosive tendency of the water (Anon, 1994; Melidis *et al.*, 2007; Rakanta *et al.*, 2007. Dissolved carbon dioxide can further lower the pH level by combining with water to form carbonic acid which may cause acid attack of the metal (Anon, 1994; Rakanta *et al.*, 2007). High concentrations of chloride and

sulphate within the system might lead to pitting corrosion (Doche *et al.*, 2006; Rakanta *et al.*, 2007).

Physical factors that influence the corrosion process are temperature and water velocity (Anon, 1994; Englert and Müller, 1996; Shreir *et al*., 2000; Rakanta *et al.*, 2007). It was demonstrated that increased temperatures would increase the corrosion rate (Anon, 1994; Shreir *et al*., 2000). Heat exchangers are thus especially prone to corrosion (Anon, 1994). The effect of water velocity on the other hand can either be direct or indirect. Direct effects are when extreme water velocity lead to corrosion as well as erosion of the metal, and indirect effects are when the high water velocity cause suspended solids to intensify erosive corrosion attack (Anon, 1994). On the other hand, in situations with a low water velocity the suspended solids will settle and may lead to pitting corrosion (Anon, 1994).

Various bacterial groups also affect the corrosion process. The major groups are discussed in Section 2.9.1.

2.9 MICROBIOLOGICALLY INDUCED CORROSION (MIC)

Microbiological induced corrosion (MIC) can be defined as any corrosion that is caused by microorganisms or their enzyme-mediated reactions (Iverson, 1987; Lutey, 1998). It is a major problem in the operation of cooling towers around the world (Lutey, 1996; George *et al*., 2003; Ilhan-Sungur and Çotuk, 2010). Cooling water systems possess a number of characteristics that favour, and provide the perfect environment for the formation of biofilms and therefore, MIC (Lutey, 1998). The structure of the biofilm has a direct influence upon the mechanisms as well as the rate of corrosion (Lutterbach and De França, 1997; George *et al*., 2003). Although it may be difficult to visually observe MIC, there are several criteria that may aid in the recognition thereof. These include the observation of pitting corrosion, presence of a biofilm at corroded areas, hydrogen sulfide and ferric hydroxide production in anaerobic and aerobic conditions respectively, high bacterial counts in the planktonic phase, tubercles with pits underneath as well as corrosion in non-corrosive water (Lutey, 1996). When several of the above mentioned criteria are visible it is a good indication of uncontrolled microbial growth and possible MIC (Lutey, 1996).

2.9.1 Organisms responsible for microbiologically induced corrosion

Different products produced by microorganisms (including bacteria, microscopic plants or plant like organisms) could lead to corrosion (Lutey, 1998; Dubey and Upadhyay, 2001). Although sulphate reducing bacteria (SRB) are the main contributors to MIC (Iverson, 1987; Angell and Urbanic, 2000), there are plenty of other less well known organisms involved in biocorrosion (Johansson and Saastomoinen, 1999). According to Lutey (1996) microorganisms involved in MIC includes: SRBs (*Desulfovibrio* sp. and *Desulfotomaculum* sp.), iron-oxidising bacteria (*Gallionella* sp., *Shaerotilus* sp. and *Arthrobacter* sp.), anaerobic acid/H_2 producing bacteria (especially *Clostridium* sp.) as well as slime-forming organisms (acid or alkali producing bacteria, algae and fungi).

2.9.1 (a) Sulphate reducing bacteria

The SRB is one of the most famous corrosion-causing bacterial groups (Gonzalez *et al*., 1998; Johansson and Saastomoinen, 1999; Angell and Urbanic, 2000). Sulphate reducing bacteria can be described as a heterotrophic anaerobic group which is able to reduce sulphate to sulphide (Peng and Park, 1994; Dzierzewicz *et al*., 1997). The sulphide may then lead to metal surface deterioration (Anon, 1994; Keresztes *et al*., 2001). These organisms can survive under extreme conditions and can therefore be found in various environments (Peng and Park, 1994; Dzierzewicz *et al*., 1997). Sulphate reducing bacteria may lead to the corrosion of various types of metals, including cast iron, carbon steel, stainless steel as well as some alloys (Morikawa, 2006; Ilhan-Sungur and Çotuk, 2010). These organisms may induce corrosion by consuming hydrogen and promote the formation of ferrous sulfide (Neria-González *et al.*, 2006). Among the different genera of SRB, *Desulfovibrio* sp. is the most widely recognised (Dzierzewicz *et al*., 1997; Ilhan-Sungur and Çotuk, 2010).

2.9.1(b) Iron reducing / Iron-oxidising bacteria

Iron reducing bacteria (IRB) are responsible for the reduction of ferric iron to ferrous iron (Neria-González *et al.*, 2006; Papassiopi *et al.*, 2010; Hallberg *et al.*, 2011). These IRB include *Acidi-thiobacillus ferrooxidans* and *Desulfuromonas palmitatis* (Papassiopi *et al.*, 2010; Hallberg *et al*, 2011). When the protective ferric oxide layer on a steel surface is reduced, it leaves the steel surface susceptible to corrosion (Neria-González *et al.*, 2006).

Iron oxidation, on the other hand, is the transformation of ferrous iron to ferric iron (Ojumu, *et al.*, 2009; Pathak *et al.*, 2009). In acidic conditions and in the presence of oxygen, ferrous iron is more stable than in alkaline to neutral conditions. Under these conditions the ferrous iron may thus serve as electron donor for some acidophilic bacteria (e.g. *Thiobacillus* sp. and *Leptospirillum* sp.) (Ojumu *et al.*, 2009). The ferric iron that is produced, precipitates out of the solution and encrusts the cells, which may lead to high amounts of iron deposits.

2.10 CORROSION AND SCALING INDICES

Corrosion and scaling indices are used by industries to determine how corrosive or scale forming given water that is used in industrial processes is (Anon, 2006a; Swart and Engelbrecht, 2007). This is achieved by calculating the calcium carbonate saturation level of the water. If the water is saturated with calcium carbonate, it may be considered stable (You *et al.*, 2001; Anon, 2006a; Melidis *et al.*, 2007). Four of the more frequently used indices are described in the following sections and mentioned in Chapter 3. These include the Langelier saturation index (LSI), the Ryznar stability index (RSI), the Puckorius scaling index (PSI) as well as the Larson-Skold corrosion index. All four of these indices have been used in a study conducted at SASOL R&D on cooling tower operation (Swart and Engelbrecht, 2007). These indices are also used in industries to predict the scale-forming and corrosive tendencies of water (Swart and Engelbrecht, 2007).

2.10.1 Langelier saturation index (LSI)

The Langelier saturation index (LSI) is an equilibrium model which predicts whether certain water would dissolve or deposit calcium carbonate (Anon, 1994; Anon, 2006c; Antony *et al*., 2011). It is also the most commonly used index for the prediction of calcium carbonate scale (Antony *et al.*, 2011). Evaporation as well as changes in temperature and water quality could change the LSI value (Yan *et al.*, 2010). Seeing as this index is a qualitative rather than quantitative indicator, it should not be used to indicate the amount or rate of calcium carbonate precipitation, but rather to predict whether the solution is under-saturated or super-saturated (Antony *et al.*, 2011). The equation for LSI is as follows:

$$LSI = pH - pH_s \quad \text{(Equation 1)}$$

In this equation pH denotes the actual measured pH of the water and pH_s denotes the calcium carbonate saturation value. The parameter pH_s can be calculated using the following equation:

$$pH_s=(pK_2\text{-}pK_s)+pCa+pAlk \text{ (Equation 2)}$$

In the above equation pK_2 denotes the negative log of the second dissociation constant for carbonic acid; pK_s denotes the negative $\log_{10}$ of the solubility product for calcite; whilst pCa and pAlk represent the negative $\log_{10}$ of the calcium and total alkalinity measured in the water respectively (Anon, 2006d; Omar *et al*., 2010; Antony *et al*., 2011; Prisyazhniuk, 2007). Interpretation of the LSI value is as follows, negative LSI predicts that the water has no potential to scale and will rather dissolve calcium carbonate. A positive LSI means that the water is likely to be scale-forming and calcium carbonate precipitation may occur. If the LSI value is close to zero the water has borderline scaling potential (Prisyazhniuk, 2007; Rakanta *et al.*, 2007; Antony *et al.*, 2011).

2.10.2 Ryznar stability index (RSI)

The Ryznar stability index is also based on the concept of saturation level (Anon, 2006d). This index quantifies the relation between $CaCO_3$ saturation and alkaline scale formation and predicts the potential of the water to be corrosive or scale forming (Anon, 1994; 2006d; Omar *et al.*, 2010). The equation for RSI values is:

$$RSI=2(pH_s)\text{-}pH \text{ (Equation 3)}$$

In this equation pH represents actual measured pH of the water and pH_s the calcium carbonate saturation value. The pH_s value can be calculated using the same equation as described in section 2.10.1 (Equation 2). An RSI result of 6 or less predicts scaling, whilst an RSI value of 7-8 predicts that calcium carbonate will be deposited resulting in less corrosion because of the layer of $CaCO_3$ that forms (Anon, 2006c). If the RSI value is above 8, intensity of corrosion will increase with the increasing value (Anon, 2006d; Prisyazhniuk, 2007).

2.10.3 Puckorius scaling index (PSI)

Most scaling and corrosion indices overlook the buffering capacity of the water, as well as the amount of deposits that water can form at equilibrium conditions (Prisyazhniuk, 2007). The PSI works on the same basis as LSI and RSI, the only difference is that it also incorporates the estimated buffering capacity of the water making it possible to measure the relationship between supersaturation and scale formation (Anon, 2006d; Prisyazhniuk, 2007). This index does not use the measured system pH, but rather an equilibrium pH (Silbert and Associates, 2006; Prisyazhniuk, 2007). The equation used to calculate the PSI value is as follows:

$$PSI = 2(pH_s) - pH_{eq} \quad \text{(Equation 4)}$$

In this equation, pH_s is once again the calcium carbonate saturation value and pH_{eq} is calculated using the following equation:

$$pH_{eq} = 1.465 \times \log_{10}[Alk] + 4.54 \quad \text{(Equation 5)}$$

where alkalinity is calculated as follows:

$$[Alk] = [HCO_3^-] + 2[CO_3^{2-}] + [OH^-] \quad \text{(Equation 6)}$$

Interpretation of the calculated PSI values is that a PSI value above 6 tends to be scale-forming, with values below 6 considered as corrosive (You *et al.*, 2001).

2.10.4 Larson-Skold corrosion index (LSCI)

The corrosivity of any given water towards mild steel can be determined by the use of the LSCI (Anon, 2006c; Prisyazhniuk, 2007; Ishii and Boyer, 2011). Corrosivity of the water is calculated using concentration of chloride, sulphate and bicarbonate (Silbert and Associates, 2006). This is apparent in Equation 7:

$$LSCI = \frac{C_{Cl^-} + C_{SO_4^{2-}}}{C_{HCO_3^-} + C_{CO_3^{2-}}} \quad \text{(Equation 7)}$$

At values below 0.8 the chlorides and sulphates within the water do not hinder the formation of a protective film on the steel surface. However, values between 0.8 and 1.2 is where chlorides and sulphates do block the formation of this protective layer and corrosion rates above normal can be expected. As the value increases from 1.2, the corrosion rates increase accordingly (Prisyazhniuk, 2007).

2.11 COOLING TOWER AS BIOREACTOR

Cooling towers are ideal for the growth of microorganisms, as by its design and function, it constantly supplies air, heat and light. By making use of wastewater streams with high nutrient loads (preferably with a CNP ratio in the order of 100:10:1) as make-up water, the conditions in the cooling tower will also be favourable for microbial degradation of organics (COD removal) (Burgess *et al.*, 1999; Ludensky, 2003; Kosińska and Miśkiewicz, 2009).

2.12 METHODS USED TO MONITOR BACTERIAL GROWTH

2.12.1 Culture dependent methods

Industries make use of conventional microbiological techniques such as plate count and MPN methods to investigate bacterial levels in water systems (Lutterbach and De França, 1997; Okabe *et al*., 1998). However, there are limitations associated with the use of conventional microbiological techniques. One of the limitations is that microorganisms need to be culturable (Sanz and Köchling, 2007). Up to date less than 1 % of all known bacteria can be cultured (Sanz and Köchling, 2007). Conventional methods are also time consuming (Beloti *et al.*, 2003; Garcia-Armisen and Servais, 2004).

2.12.1 (a) Plate count method

The plate count method has been used for more than 100 years as a means of enumerating bacterial cells in water as well as other materials (Reasoner, 2004). According to Reasoner (2004) three types of heterotrophic plate count procedures are available, namely the pour plate method, the spread plate method and the membrane filter method. When using the plate count method, there are four different aspects that need to be taken into account. These

include medium composition, incubation time and temperature as well as oxygen tension (Reasoner, 2004). Because of this, there is no single set of conditions that is suitable for the optimal growth of all the bacterial species found within a water sample (Reasoner, 2004). When using the plate count method, different media formulations as well as conditions are used, depending on the target species. A problem associated with the plate count method is the counting of bacterial colonies. The counting process makes this approach subjective (Le Blay *et al*¸2004).

2.12.2 (b) Most probable number technique

The most probable number (MPN) method can be described as a method that estimates, without direct count, the number or density of bacteria found in a liquid (Cochran, 1950; APHA, 1985; Prescott *et al*., 2002). It is a culture- based method (Garcia-Armisen and Servais, 2004), which involves the inoculation of diluted samples into selective media. Five replicates of each dilution used (Garcia-Armisen and Servais, 2004; Li *et al*., 2006) that then needs to be incubated between 24 and 48 hours (Beloti *et al*., 2003; Garcia-Armisen and Servais, 2004). After incubation, statistical analysis results in a number. This number reflects the most probable number of organisms present within the sample (APHA, 1985; Prescott *et al*., 2002). A limitation of the MPN method is the fact that it is not capable of detecting viable but non-culturable bacteria (Garcia-Armisen and Servais, 2004).

2.12.2 Culture independent methods

Conventional microbiological techniques will not give a complete picture of the microbial communities found within complex ecological niches such as cooling water systems. Therefore one should consider using alternative techniques that would enable the study of both the planktonic as well as the sessile microbial communities. Alternative techniques such as PLFA and DGGE can be used in addition to culture dependent methods (Li *et al*., 2006).

2.12.2 (a) Phospholipid fatty acid analyses

Phospholipids are located in the membranes of all living cells (Palojarvi *et al*., 1997; Smith *et al*., 2000). In microorganisms, however, phospholipids are found in their membranes exclusively (Hill *et al*., 2000; Lei and VanderGheynst, 2000) where it is then degraded upon cell death (Smith *et al*., 2000). Thus, analysing the PLFA composition will give a good estimate of the viable microbial biomass within a specific environmental sample (Hill, *et al*., 2000; Lei and VanderGheynst, 2000; Smith *et al*., 2000). Signature lipid biomarkers, such as PLFA, provides a measure of the microbial community composition, functional descriptors such as the stress and status of the microbial community (Smith *et al*., 1999; 2000; Pelz *et al*., 2001). This method is suitable for the analysis of environmental samples, such as soil, water and air (Macnaughton *et al.*, 1997). When one is making use of PLFAs, gas chromatography (GC) and mass spectrometry (MS) is used to quantitatively and qualitatively identify the lipids (Werker and Hall, 1998; Smith *et al*., 2000; Widmer *et al*., 2001; Sanz and Köchling, 2007). The data obtained from the GC and MS can then be compared to data found within a fatty acids database, and the PLFAs can be identified (Widmer *et al*., 2001). A limitation with this specific approach is that appropriate signature molecules are not yet known for all organisms and as such this technique cannot be used to characterise microorganisms to species level (Hill *et al*., 2000).

2.12.2 (b) Denaturing gradient gel electrophoresis

Denaturing gradient gel electrophoresis (DGGE) is used to identify specific populations within an environment, without the need to isolate them (Sanz and Köchling, 2007) and is widely used within industry (Rolleke *et al*., 1999; Sanz and Köchling, 2007). It is used to determine the structure of microbial communities (Sanz and Köchling, 2007; Zhao *et al*., 2006), based on the type and relative abundance of the various phylogenetic groups found within the community (Forney *et al*., 2001). It is possible to use DGGE to determine the microbial community diversity in numerous research fields/industries (Sanz and Köchling, 2007), such as soil, water (Rolleke *et al*., 1999) alcohol distillery, unbleached pulp plant wastewater, as well as other wastewater treatment systems (Zhao *et al*., 2006).

The DGGE technique involves a four-step process which includes: (i) the extraction of DNA from the sample (Aguilera *et al*., 2006); (ii) the amplification of partial 16SrRNA genes

(Muyzer *et al.*, 1993; Rolleke *et al*., 1999; Sanz and Köchling, 2007); (iii) electrophoretic separation on an acrylamide gel that contains an increasing urea/formamide gradient (Skopek *et al*., 1999; Li *et al*. 2006; Sanz and Köchling, 2007) and (iv) the analysis of the banding patterns obtained. There is however certain limitations associated with the use of the DGGE technique. For instance, DGGE is not a quantitative measure (Forney *et al*., 2001), it can detect similar diversity patterns within ecosystems, but it cannot give a definitive estimate of the species distribution within the microbial community (Sanz and Köchling, 2007).

2.12.2 (c) Scanning electron microscopy (SEM)

Although SEM cannot be used to identify specific fungal and bacterial members of the biofilm, it is a valuable tool to visualise adhesion and biofilm structure (Lagacé *et al.*, 2006; Ilhan-Sungur and Çotuk, 2010). This method is based on the dehydration of a sample and subsequent coating with gold or palladium. After preparation the sample is placed in an electron microscope equipped with a probe to scan the sample (Lagacé *et al.*, 2006; Andermark *et al*., 1991). One drawback of this approach is its lengthy and complex sample preparation process (Lazarova and Manem, 1995)

Various studies have found SEM can reveal some complimentary information on biofilm structure. SEM has been applied in various industries including wastewater treatment (Lazarova and Manem, 1995), biofilms within cooling tower system (Ilhan-Sungur and Çotuk, 2010) and biofilms within water distribution systems (Feng *et al*., 2005).

2.14 SUMMARY

Literature presented in this chapter illustrated that South Africa is generally water stressed and that strategies should be put in place to protect water resources. These strategies include the reuse of industrial effluent as make-up water in cooling towers. Problems described in literature that is associated with the use of industrial effluent within cooling towers include increased corrosion, scaling and fouling rates. With CNP correction of the make-up water to 100:10:1, the probability of COD removal and degradation of hydrocarbons and organic acids within the effluent increases. However, with CNP correction, there is the possibility that fouling, scaling and corrosion might increase. Optimisation of cooling tower conditions are therefore of utmost importance. The optimum conditions should be where fouling, scaling

and corrosion are within set limits, with accompanying COD removal. Literature was presented that gave an introduction to methods that could be used to monitor bacterial growth as well as the fouling, scaling and corrosion rates. Methods used to monitor bacterial growth include culture dependent methods (plate counts and MPN) and culture independent methods (PLFA, DGGE and SEM). Whereas the fouling, scaling and corrosion rates can be monitored by making use of corrosion and scaling indices as well as the physical and chemical data. Should an optimum balance in the operating conditions be achieved, water usage and water discharge by industry will be considerably less and may even approach zero discharge levels.

CHAPTER 3 - OPTIMISATION OF COOLING TOWER OPERATIONAL CONDITIONS

3.1 INTRODUCTION

Different factors influence corrosion and scaling rates found within a cooling system. These include the type of metal used (Englert and Müller, 1996) as well as the water quality (Rakanta *et al*., 2007). Although stainless steel is more expensive than mild steel it is becoming an increasingly popular choice in cooling water systems because it exhibits greater resistance towards corrosion (Xu *et al*., 2007). It is therefore expected that the fouling, scaling and corrosion rate would be less for stainless steel coupons than for mild steel coupons.

Water quality plays a significant role in corrosion rate as well as in the fouling and scaling tendencies of water systems (Rakanta *et al*., 2007; Hawthorn, 2009; Ilhan-Sungur and Çotuk, 2010). For example, hard waters (or water with high alkalinity) would result in lower corrosion rates but may increase scale formation (Melidis *et al*., 2007; Rakanta *et al*., 2007). The pH of water will affect the corrosion and scaling rates, where a lower pH will increase the rate of corrosion and decrease scale formation (Li *et al.*, 2006; Rakanta *et al*., 2007; Al-Rawajfeh, 2010). When chloride and sulphate levels are high, an increase in the corrosion rate can be expected (2006; Melidis *et al*., 2007; Rakanta *et al*., 2007; Xu *et al*., 2007). High levels of dissolved oxygen will also increase the corrosion rate (Rakanta *et al*., 2007; Yan *et al.*, 2010).

An aspect that affects biodegradation by microorganisms is the ratio of carbon, nitrogen and phosphorus. When waters from an industrial wastestream are used for cooling purposes this aspect (CNP) should be determined. According to Schmidt *et al* (2007) an adequate ratio of CNP is 100:10:1 for biodegradation.

Accelerated corrosion tests simulate corrosion conditions within a system. Conditions are created to allow corrosion to occur at an increased rate (Doche *et al*., 2006; Wang *et al.*, 2010). Corrosion rates can then be calculated by the weight loss method (Rao *et al*., 2000; Choi *et al*., 2002; Ilhan-Sungur and Çotuk, 2010; Wang *et al.*, 2010) in conjunction with corrosion and scale indices (Swart and Engelbrecht, 2007). Various corrosion and scale

indices can be used to calculate the expected corrosion rate and/or scale forming tendencies of water (Hawthorn, 2009; Khatami *et al.*, 2010).

The LSI and RSI are probably the most common methods used in industry to predict the corrosiveness of water (Melidis *et al*., 2007; Rakanta *et al*., 2007). However, both indices calculate the expected scale forming tendency of water and thus the corrosion rate is based on the assumption that water which is scale forming will have little tendency to corrode (Rakanta *et al*., 2007). The LSI calculates the tendency of water to deposit or dissolve $CaCO_3$. It is a qualitative method and gives no indication of the amount of scale formed or the actual precipitation of $CaCO_3$ (Anon, 1994; Prisyazhniuk, 2007; Rakanta *et al*., 2007). This index predicts scale formation based on pH, alkalinity, calcium, TDS and temperature. Researchers have different opinions on what the optimum LSI value should be. However, most agree that a value between 0 and 0.5 would indicate relatively stable water, while a negative value indicates corrosion and a positive value scale formation (Anon, 1994; You *et al*., 2001; Lee and Young, 2002; Melidis *et al*., 2007; Prisyazhniuk, 2007; Rakanta *et al*., 2007; Yan *et al.*, 2010).

The RSI predicts the scaling or corrosivity of water in terms of $CaCO_3$ saturation. The main difference between the LSI and RSI is the fact that the latter is a qualitative as well as quantitative method. It combines empirical data with theory. Values smaller than 6 gives a strong tendency for scaling and values above 7 a strong tendency for corrosion (Anon, 1994; Rakanta *et al*., 2007; Al-Rawajfeh, 2010). Researchers agree that LSI and RSI should be seen as general indications of scale formation and corrosion, and not as an absolute guide (Anon, 1994; Hawthorn, 2009; Khatami *et al.*, 2010).

According to You *et al.* (2001), the PSI is a much more accurate method than LSI and RSI when determining scale formation and corrosion in alkaline waters. It can be described as a measurement of the relationship between supersaturation state and scale formation (Prisyazhniuk, 2007). A PSI index value of 6.00 is considered to be neutral, whilst values higher than 6.00 tend to precipitate $CaCO_3$ and are thus scaling. Water with a PSI value smaller than 6.00 is considered to be corrosive (You *et al.*, 2001).

The LSCI determines the corrosiveness of water towards mild steel by measuring the chloride, sulphate and bicarbonate concentrations of the water. In order to avoid corrosion,

values smaller than 0.8 should be maintained. The rate of corrosion increases as the value increase to above 0.8 (Melidis *et al*., 2007; Prisyazhniuk, 2007). Thus by using the indices described above, water can be stabilised up to a point where the water is saturated. This will result in water which is neither strongly corrosive, nor scale forming (Anon, 2004). Water can also be stabilised by maintaining the pH between 8.0 and 8.3 (You *et al*., 2001; Anon, 2004; Melidis *et al*., 2007; Rakanta *et al*., 2007).

In cooling towers there are several factors that contribute to water loss. These include 1) water that is lost through evaporation, 2) blow-down; 3) drift (or windage) and 4) leakage through the system (Bott, 1998; Anon, 2004; Mohsen, 2004). Most of the water loss can be attributed to evaporation (almost 1 % of inlet water) whereas water loss caused by drift is usually only a very small amount (about 0.2 % of inlet water) and can therefore be considered negligible (Kim *et al*., 2001). Leakage can be controlled by general maintenance of the cooling water system.

When water evaporates, the dissolved ions in the water concentrate (Rakanta *et al*., 2007). This concentration of water can also be described as the COC of the system. Cycles of concentration is therefore the ratio between the concentration of dissolved ions in the cooling tower compared to the concentration of dissolved ions within the make-up water (You *et al*., 2001; Yan *et al.*, 2010). Blow-down is needed to maintain a specific COC within a cooling tower. It operates by continuously removing water from the cooling tower to prevent the concentration effect of evaporation (Lee and Young, 2002; Swart and Engelbrecht, 2007; Hawthorn, 2009).

3.2 AIM AND OBJECTIVES

The aim of this chapter was the optimisation of the operational conditions of laboratory scale mini cooling tower test rigs by making use of CNP corrected synthetic PCB as process cooling water. The objectives for this chapter were to:

1. determine the fouling, scaling and corrosion rates of stabilised and non-stabilised PCB by making use of various indices as well as water quality (water chemistry) data.
2. analyse results obtained from corrosion and scaling indices as well as the water quality to ascertain which operational parameters would be best suited for this particular study.

3.3 MATERIAL AND METHODS

3.3.1 Make-up water composition

During this study synthetic make-up water resembling PCB produced during the FT reaction GTL conversion process at SASOL was used. At the time of the study no PCB effluent was available, thus the need for synthetic PCB make-up water. This water consisted of all the components that were expected in PCB effluent as provided by SASOL Research and Development, Sasolburg. It consisted of acetic acid, formic acid, methanol, hydrocarbons, butyric acid, propionic acid and pentanoic acid (in order of quantities added to 100 litres of make-up water). During this experiment the water was also CNP corrected, by making use of phosphoric acid and urea to achieve a molar ratio of CNP (100:10:1). The make-up water was drained and the containers cleaned and refilled daily to avoid growth of microorganisms in the make-up water.

3.3.2 Stabilisation of make-up water

The synthetic PCB make-up water contained high concentrations of acid and it can therefore be expected that the pH would be extremely low. In this case the pH average was 3.7 and after CNP correction 4.4. Water with such a low pH would promote rapid corrosion within the system (Li *et al.,* 2006; Rakanta *et al.,* 2007) and therefore it was decided to stabilise the

water by adjusting the pH. This was done by adding 10 % NaOH to the recirculating water in the cooling tower until a pH between 8.0 and 8.3 was reached. The pH was maintained between these two set points, by making use of a pH controller (Hanna HI S04, USA) and a pH probe (Hanna HI 1006-32, USA). The pH probe was situated in the sump. On the other hand the pH controller was connected to two peristaltic pumps (Watson Marlow 101 U/R, England) dosing 10% NaOH and 10 % HCl, respectively. During the accelerated corrosion tests, the pH of the non-stabilised water was maintained between 6.0 and 6.5 by this same method.

3.3.3 Determining drift loss

When determining drift loss it is important to turn off the heat exchangers as this would lead to water loss through evaporation which would interfere with the results. For the same reason the blowdown was also turned off. A 5 % TRASAR® solution was prepared by adding TRASAR® 2 solution to distilled water. Then 8 ml of the 5 % TRASAR® solution was added to the recirculating water of the cooling tower. This resulted in a total concentration of 5 mg/L TRASAR® in the cooling tower. Ten millilitre samples were taken from the cooling tower sump every 6 - 8 hours for approximately 72 hours. After the samples were taken the amount of fluorescent radiation was measured immediately, by making use of a TRASAR® hand-held fluorometer. The sample was then returned to the cooling tower. Readings obtained from the fluorometer were used to calculate the drift loss of the cooling tower by making use of the following equation:

$$\%\ \text{Drift Loss} = \frac{\text{Drift Loss}\ \left(\frac{\text{L}}{\text{hr}}\right)}{\text{Flow Rate}\ \left(\frac{\text{L}}{\text{hr}}\right)}\ \text{x}\ \frac{100}{1}$$

3.3.4 Determining the cycles of concentration (COC)

During this study the cooling towers were run at different COC (2, 4 and 6 COC). The COC were determined by calculating the ratio of LiCl (mg/L) in the circulating water/blow-down to that in the make-up water. It was decided to use Lithium chloride (LiCl) to determine COC because the PCB (make-up water) was devoid of Lithium. Lithium chloride (LiCl) was added to the make-up water until a value of 1 mg/L LiCl was present in the make-up water. Lithium chloride (LiCl) levels were obtained by inductively coupled plasma mass

spectrometry (ICPMS) (Agilent 7500C, Agilent, America). The ratio of LiCl (make-up:blow-down) was indicative of the COC. For example, if the ratio LiCl in the make-up and blow-down was 1:4, the COC would be 4 (Lee and Young, 2002; Yan *et al*., 2010).

3.3.5 Blow-down rate

A peristaltic pump (Watson Marlow 10l/U/R, England) connected to the sump of the cooling tower was used to control the blowdown rate. The actual blow-down rate needed to maintain a specific COC, was determined by first measuring the amount of make-up water used to replenish the cooling tower during one hour. This was done in triplicate to determine the average make-up water used as fill during one hour. The value obtained from the measurement was the amount of water that had to be extracted from the cooling tower during an hour to maintain the specific COC. Secondly, the amount of water that was extracted at different pumping rates was determined, until the peristaltic pump extracted the precise amount of water during an hour. This was done for each different LFV used during the experiment.

3.3.6 Accelerated corrosion tests

Accelerated corrosion tests were performed on both stabilised water and non-stabilised water. After stabilisation, the make-up water was released into the cooling tower until the various COC was reached (2, 4 and 6 COC). This water was then used to perform the accelerated corrosion tests. For the non-stabilised samples, the make-up water was directly cycled up in the cooling tower until the required COC were reached. Mild steel as well as stainless steel (316 L) corrosion coupons were used during the accelerated corrosion process. The mini cooling tower test rigs were used to cycle up to the required COC. The pH controller (Hanna HI S04, USA) and peristaltic pumps (Watson Marlow 10 l/U/R, England) of the cooling towers were used to maintain the pH between 8.0 and 8.3 for the stabilised water, and between 6.0 and 6.5 for the non-stabilised water. When the water reached the required COC and was at the correct pH range it was collected and used as samples for the accelerated corrosion tests. Excess water was stored at 4 °C for further use during the experiment.

The water samples that were at the correct COC and pH were then poured into 250 ml Erlen-Meyer flasks (Figure 3.1). Mild steel and stainless steel corrosion coupons were rinsed with

acetone and dried in an oven at 104 °C. These were allowed to cool to room temperature in a desiccator and then weighed (Weight 1). After weighing the coupons, they were inserted into separate flasks (one per flask). This was done since different metals can affect each other and lead to galvanic corrosion, where the "less noble" metal will be corroded (Anon, 1994). Coupons were then tied to a piece of string attached to the top of the Erlen-Meyer flask, allowing the coupon to hang freely in the water (Figure 3.1). The flasks were placed into a water bath where the surrounding water was kept at 60 °C. Accelerated corrosion tests were performed for 28 days. During this period some of the water in the flasks was lost due to evaporation. Because of this loss of water the flasks were replenished every three days. The samples were not aerated during the accelerated corrosion tests.

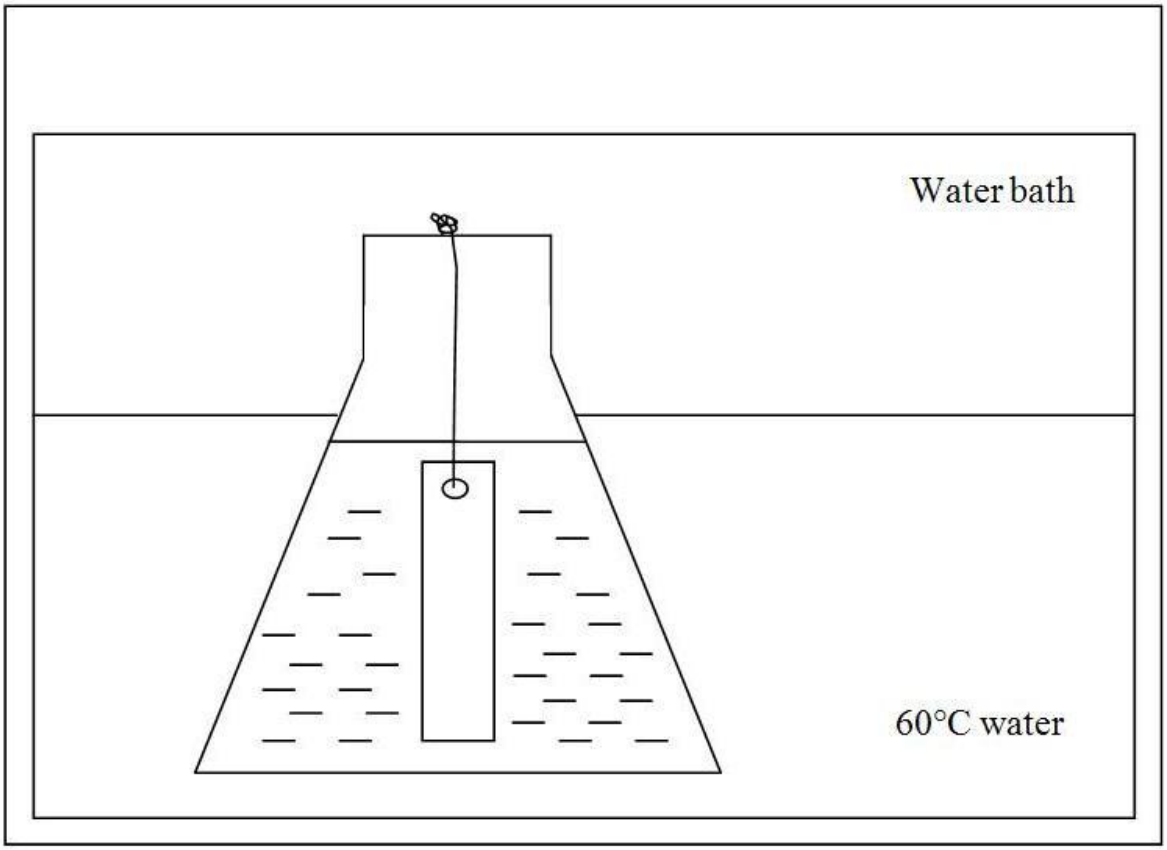

Figure 3.1: Schematic representation of the accelerated corrosion test setup showing the 250 ml Erlen-Meyer flask (with corrosion coupon attached) situated inside the 60 °C water bath.

3.3.6.1 Daily measurements and analyses done during accelerated corrosion test

Dissolved oxygen (DO), pH, and electrical conductivity (EC) values were obtained by making use of a standard WTW handheld meter (WTW, Germany) and corresponding probes. Redox potential (RP) was determined by making use of a Metrohm 704 handheld meter (Hanna, USA). Furthermore total suspended solids (TSS) and total dissolved solids (TDS) were also determined. These measurements were used for the determination of corrosion-, scaling- and fouling rates.

The TSS and TDS were done separately for every sample. Schott bottles and evaporating dishes were cleaned and dried in an oven at 104 °C, allowed to cool to room temperature in a desiccator and weighed on a balance that is accurate to the nearest 0.0001 g. Whatman GF/A glass filter paper (110 mm diameter) was rinsed with distilled water and then placed on the cleaned evaporation dish. Filter papers were then dried at 104 °C and allowed to cool in a desiccator and weighed.

The weighed filter paper was placed in a clean Buchner filter funnel (120 mm) with a rubber stopper that was attached to a Buchner filtering flask. The filter paper was then washed three consecutive times with distilled water. Complete drainage was allowed between each wash. After the last drainage step, the vacuum was kept on for another three minutes ensuring that all the distilled water was removed. A hundred millilitres of the sample was filtered through the Buchner filtering flask until filtration was completed. The filter paper was placed in the same evaporation dish and the filtrate poured into the cleaned Schott bottles. Both the Schott bottles and the filter papers were then placed in an oven at 104 °C and left to dry. The dried bottles and filter papers were removed from the oven and allowed to cool to room temperature in a desiccator. After this, the bottles and filter papers were weighed again.

The TSS (by using weight of the filter papers) and TDS (by using the weight of the Schott bottles) were calculated using the following equations (APHA, 1985):

$$\text{TSS mg/L} = \frac{(m_2 - m_1) \times 10^6}{V_1}$$

and

$$\text{TDS mg/L} = \frac{(m_4 - m_3) \times 10^6}{V_2}$$

Where:

m_1	=	initial mass of GF/A filter paper (g)
m_2	=	mass of GF/A filter paper with residue (g)
m_3	=	mass of empty evaporating dish (g)
m_4	=	mass of evaporating dish with residue (g)
V_1	=	volume of sample used for filtration (ml)
V_2	=	volume of sample evaporated (ml)

The fouling-, scaling- and corrosion rates were calculated by the weight loss method. This method uses the various weights of the corrosion coupons in combination with the area, density and time of exposure (Rao *et al.*, 2000; Choi *et al.*, 2002; Ilhan-Sungur and Çotuk, 2010; Wang *et al.*, 2010). The corrosion indices were used as shown in Section 2.11.

3.3.7 Cleaning procedures

The cleaning procedures were followed as directed and optimised by SASOL (SASOL Research and Development, Sasolburg) by making use of a modified NACE and ASTM method. The various sections of the cooling towers that required cleaning, were cleaned using methods described below.

3.3.7.1 Heat exchanger tubes (HETs)

Before the HETs were inserted into the cooling tower system, they were rinsed with acetone and dried in an oven at 104 °C for 24 hours. It was allowed to cool to room temperature, and weighed (weight 1). The HETs were then sprayed with a dry lubricant (Teflon; enhanced insertion) and inserted into the cooling tower system. After each experimental run the HETs

were carefully removed from the system and placed in oven at 104 °C, where they were dried for 24 hours. They were allowed to cool to room temperature and weighed (weight 2). The HETs were cleaned with a pipe cleaner under running tap water and afterwards rinsed with acetone. Heat exchanger tubes were then placed in a 10 % sodium hydroxide (NaOH) solution for three minutes, removed, rinsed with running tap water and then with acetone. After this treatment the HETs were dried in an oven (104 °C) for 24 hours and allowed to cool and weighed (weight 3). Stainless steel HETs were then placed in a 15 % citric acid solution for two hours, and the mild steel HETs in 22 % Hibatex (inhibitory HCl) for 25 minutes. The HETs were then rinsed under running tap water and yet again rinsed with acetone. Heat exchanger tubes were then placed in the oven (104 °C) for 24 hours, allowed to cool and the final weight (weight 4) of the HETs were taken.

3.3.7.2 U-bends

All the U-bends were stainless steel and were therefore cleaned in the same manner as HETs. The only difference in the cleaning methods were the fact that U-bends were only cleaned and not weighed as they were not used to determine the corrosion, fouling and scaling rates.

3.3.7.3 Corrosion coupons

Cleaning procedures for the corrosion coupons were similar to the cleaning procedures for the HETs. Corrosion coupons however, were dried for two hours instead of 24 hours. A soft toothbrush was used to mechanically brush the corrosion coupons clean after each rinsing step.

3.3.7.4 Packing material

The packing material was carefully removed from the cooling tower system and rinsed with running tap water. It was then placed in a 30 % HCl solution and left for three hours. After this they were rinsed with tap water to wash off remaining acid. This step was then repeated until the packing material appeared visually clean.

3.3.7.5 Cooling tower

Cooling towers were cleaned by firstly filling the cooling tower sump with tap water and then recycling it through the system whilst bypassing the heat exchanger. This water was drained after an hour, and the system again filled with tap water. Fifty millilitres concentrated HCl was then added to the sump water and the water was allowed to recycle through the system for a period of 24 hours. After this the system was drained and repeatedly rinsed with tap water to remove all remaining acid from the system. The cooling tower was then mechanically cleaned with a soft brush and tap water.

3.4 RESULTS AND DISCUSSION

Loss of water through drift (as determined by the TRASAR® method) was calculated as 0.03 L/hr. Research by Kim *et al.* (2001) on the design of cooling systems for effluent temperature deduction compared the amount of water loss through drift and evaporation in a cooling tower. In conventional cooling towers, water loss through drift is on average less than 0.2 % of the inlet water, whilst water loss through evaporation is much higher (more than 1 %). For this reason Kim *et al*. (2001) decided to regard water loss through drift negligible. Drift loss for this particular study was extremely low (0.05 % at 0.6 m/s LFV, 0.03 % at 0.9 m/s LFV and 0.025 % at 1.2 m/s LFV) even when compared to the average of 0.2 % found in conventional cooling towers. Therefore the drift loss during this study was also disregarded.

Results of the PCB (make-up water) and circulating water at specific COC, as determined by the corrosion and scaling indices can be found in Table 3.1. The Larson-Skold (LI) index is the only index used that actually predicted corrosion (Melidis *et al*., 2007). The other indices used are designed to predict scale formation. Their prediction of the corrosion rate is only based on the assumption that higher scale formation would lead to less corrosion (Rakanta *et al*., 2007).

Make-up water (PCB) had an extremely low LSI value (-4.63) and very high RSI, PSI and LI values (13.67, 11.06, 17.34, respectively). Thus, the make-up water (PCB) was predicted to be extremely corrosive. In Table 3.1, the stabilised water in all cases had higher LSI values. All the LSI values (stabilised water) were positive, indicating supersaturated water that would

tend to precipitate a $CaCO_3$ layer. The LSI values and prediction trends were similar to that observed by Melidis *et al.* (2007). In the latter study on the control of corrosion and deposition within drinking water, it was observed that the drinking water samples were supersaturated and would precipitate $CaCO_3$. This was demonstrated in a study by Al-Rawajfeh (2010) to simulate the CO_2 release rates and simultaneously $CaCO_3$ scale formation from evaporation in distillers. Results from the study suggested that RSI values below 5 would have high scale-forming tendencies and values above 5 only slight scale-forming tendencies. In the present study LSI and RSI indices predicted that the circulating stabilised water would generally be more scale forming, and the circulating, non-stabilised water more corrosive.

Negative LSI values were found at the non-stabilised water samples of 2 COC and 6 COC (-0.12 and -0.27, respectively). The non-stabilised sample of 4 COC also had a relatively low LSI value (0.45). A review study on the different corrosion and scale-forming properties of water was done by Prisyazhniuk (2007). This review found that the LSI gives qualitative and not quantitative results. It was suggested that values in the range of -0.4 and +0.4 should be regarded as zero. It can therefore be assumed that according to the LSI, all of the non-stabilised water samples will be relatively stable with slight corrosion.

Larson-Skold corrosion index (LSCI) values for stabilised water at 2, and 4 COC (0.39 and 0.62, respectively) are the lowest LSCI values found for the different COC samples (stabilised and non-stabilised water). The highest LSCI value (stabilised water) was found at 6 COC (0.96). All the non-stabilised water (regardless of COC) had very high LSCI values (higher than 4). The review by Prisyazhniuk (2007) stated that at LSCI values below 0.8, a protective layer will be formed on steel surfaces, whilst values between 0.8 and 1.2 would lead to some degree of corrosion. Values higher than 1.2 would have increased corrosion rates as this value increases. In the present study LSCI predicted that the stabilised water from COC 2 and 4 would form a protective film against corrosion, whilst the stabilised water from 6 COC would lead to higher than normal corrosion rates. All of the non-stabilised water is predicted to have high rates of localised corrosion.

Table 3.1: Various corrosion indices' results obtained during the acceleration corrosion test.

	LSI	RSI	PSI	LSCI
Make-up water	-4.63	13.67	11.06	17.34
2COC,S	0.9	6.36	5.73	0.39
4COC,S	1.26	5.79	5.11	0.62
6COC,S	1.33	5.73	5.08	0.96
2COC,N	-0.12	7.68	7.01	4.17
4COC,N	0.45	6.62	5.75	4.21
6COC,N	-0.27	7.63	6.79	42.66
*** COC = Cycles of concentration; S = Stabilised water; N = Non-stabilised water * LSI = Langelier saturation index; RSI = Ryznar stability index; PSI = Puckorius and LSCI = Larson-Skold Index**				

From Table 3.1 it can be concluded that all indices predicted that the stabilised water would generally be more scale-forming and the non-stabilised water more corrosive. Highest scale formation was predicted to occur at 6 COC for the stabilised water, and at 4 COC for the non-stabilised water. Corrosion was predicted to occur in non-stabilised water with the highest corrosion rates predicted for the non-stabilised water at 6 COC.

Actual fouling, scaling and corrosion rates obtained during the accelerated corrosion test are found in Table 3.2. Results from Table 3.2 illustrate that all fouling rates were within the SASOL standard guideline (20 mg/dm^2/d; SASOL Research and Development, Sasolburg). The mild steel sample of stabilised water at 6 COC (17.52 mg/dm^2/d), and the mild steel sample of non-stabilised water at 4 COC (17.68 mg/dm^2/d) that had the highest fouling values were also within this guideline. With regard to the scaling rates observed, it can be seen that all the stainless steel samples had extremely low scaling rates (less than 0.1 mg/dm^2/d), whereas all the mild steel samples were higher than the SASOL standard guideline (2 mg/dm^2/d). The scaling rates for all the mild steel samples ranged from 4.29 to 12.97 mg/dm^2/d. All the corrosion rates were also below the SASOL standard guideline (0.2 mm/y). The highest corrosion rates for both the stabilised and non-stabilised water samples were observed at 4 COC (mild steel; 0.048 and 0.038 mm/y, respectively). Although the scaling rates of the mild steel coupons are much higher than the SASOL standard guideline,

research done by Swart and Engelbrecht (2007) on the use of mine water as cooling medium also had scaling rates that were much higher than the SASOL standard guideline. Furthermore Swart and Engelbrecht (2007) demonstrated that the actual process cooling towers from Sasol One had higher scaling rates than the SASOL standard guideline.

From Table 3.2, the stainless steel samples from the stabilised and the non-stabilised water had extremely low fouling, scaling and corrosion rates. All values were within the SASOL standard guidelines. The highest fouling rate was observed for stabilised water samples from 6 COC (0.12 mg/dm^2/d) and the scaling rate for non-stabilised water samples at 4 COC (0.06 mg/dm^2/d). None of the stainless steel corrosion coupons showed any evidence of corrosion (0.00 mm/y). This implies that stainless steel offers protection against corrosion, an observation that is similar to that of Xu *et al.* (2007). These authors investigated the corrosion behaviour of 316 L stainless steel. According to their research, stainless steel corrosion coupons showed no sign of corrosion, unless it was in a solution which also contains SRB and iron oxidising bacteria. In the light of the observations by Xu *et al.* (2007) and the findings of the present study, only the mild steel corrosion coupon results for fouling, scaling and corrosion rates will be further discussed.

Table 3.2: Fouling, scaling and corrosion results from corrosion coupons, obtained during the accelerated corrosion process.

	Fouling ($mg/dm^2/d$)	**Scaling ($mg/dm^2/d$)**	**Corrosion (mm/y)**
SASOL Guidelines	**20.00**	**2.00**	**0.20**
2COC,S,ss	0	0.02	0
2COC,S,ms	13.48	8.68	0.03
4COC,S,ss	0	0	0
4COC,S,ms	8.58	5.15	0.05
6COC,S,ss	0.12	0.04	0
6COC,S,ms	17.52	10.33	0.04
2COC,N,ss	0.10	0	0
2COC,N,ms	6.65	4.29	0.03
4COC,N,ss	0.10	0.06	0
4COC,N,ms	17.68	11.00	0.04
6COC,N,ss	0.10	0.04	0
6COC,N,ms	14.20	12.97	0.02
Legend: COC = Cycles of concentration; S = Stabilised water; N = Non-stabilised water; ss = Stainless steel; ms = Mild steel			

For stabilised water the highest fouling and scaling rates on mild steel was at 6 COC (17.52 and 10.33 $mg/dm^2/d$, respectively). The highest corrosion rate was observed at 4 COC (0.05 mm/y). On the other hand, the lowest fouling and scaling results for stabilised water was found at 4 COC (8.58 and 5.15 $mg/dm^2/d$, respectively) and the lowest corrosion rate at 6 COC (0.03 mm/y). Table 3.2 also illustrate that for the non-stabilised water, the highest fouling and corrosion rates were found at 4 COC (17.68 $mg/dm^2/d$ and 0.04 mm/y, respectively) and the highest scaling rates at 6 COC (12.97 $mg/dm^2/d$). The lowest corrosion rate (non-stabilised water) was found at 6 COC (0.02 mm/y). This phenomenon was also demonstrated by Swart and Engelbrecht (2007). The samples with the highest scaling and fouling rates also had the lowest corrosion rates. Corrosion predictions by the LSI and RSI are based on the notion that the formation of scale offer protection against corrosion by the formation of a protective barrier between the metal and the medium (Rakanta *et al.*, 2007). It

can therefore be said that these observations are in accordance with the presented research which found that scale formation can protect metals against corrosion.

The chemistry and some physical parameters of the CNP (100:10:1) corrected non-stabilised and stabilised PCBs was determined (Table 3.3). Results from this table (Table 3.3) show that stabilised water had higher amounts of total alkalinity, sulphate and dissolved oxygen compared to the results of the non-stabilised water. Research by Melidis *et al.* (2007) found that an increase in alkalinity levels reduced the amount of corrosion and simultaneously increased scaling tendencies of water. However, higher sulphate and dissolved oxygen levels can result in higher corrosion rates. Ilhan-Sungur and Çotuk (2010) performed a study to determine microbial corrosion of steel within simulated recirculating cooling towers. Their results demonstrated that high sulphate levels might increase corrosion rates, this was also demonstrated in the study done by Swart and Engelbrecht (2007). Rakanta *et al.* (2007) and Yan *et al.* (2010) found that during their research, increased dissolved oxygen levels also increased the aggressive tendencies of water with regards to corrosion. Based on the example from literature, the water chemistry contained in Table 3.3 suggests that the non-stabilised water, particularly due to the high alkalinity levels, will be have high scaling tendencies and lower corrosion tendencies. Consequently stabilisation of the water is recommended.

Table 3.3: Water chemistry of raw feed (PCB) as well as the stabilised and non-stabilised water used during the accelerated corrosion process.

Variable	PCB	Stabilised water	Non-stabilised water
Total alkalinity (mg $CaCO_3$/L)	**10**	**605 – 1 050**	**88 – 235**
Total hardness (mg $CaCO_3$/L)	391	428 – 958	561 – 1 792
Total dissolved solids (mg/L)	143	1 000 – 2 300	1 300 – 5 400
Total suspended solids (mg/L)	22	42 – 92	31 – 117
Total iron (mg Fe/L)	2.30	1.10 – 4.30	1.60 – 7.20
Chloride (mg Cl/L)	33	68 – 292	265 – 2 365
Sulphate (mg SO_4/L)	122	132 – 576	142 – 386
Dissolved oxygen (mg/L)	2.21	0.29 – 0.90	0.23 – 0.74
Electrical conductivity (mS/cm)	0.79	2.12 – 4.24	1.85 – 8.72
pH	4.4	8.0 – 8.3	6.0 – 6.3

The values in Table 3.3 indicate that in comparison to stabilised water, the non-stabilised water had higher levels of total hardness and chloride. The study by Melidis *et al.* (2007) also demonstrated that increased hardness reduces corrosion and increases the scale formation rate. Furthermore, their results indicate that an increase in the chloride levels might lead to increased corrosion rates. Rakanta *et al.* (2007) found similar results. They (Rakanta *et al.*, 2007) also demonstrated that increase in scale formation caused by increased hardness levels could also increase the corrosion rate if the scale that was formed is porous (corrosion caused by differential airing). Implications of this for the current study might be increased scale formation caused by the high total hardness values, or increased corrosion caused by high levels of chloride.

Predictions of the various indices (Table 3.1) as well as the assumptions from the water chemistry results (Table 3.3) do not correlate well with the actual fouling, scaling and

corrosion results obtained for the stabilised and non-stabilised water during accelerated corrosion (Table 3.2). The need to interpret each sample individually (various COC, stabilised as well as non-stabilised water) is necessary in order to explain the results more thoroughly (Appendix A, Table A1).

The highest fouling and scaling rates observed for stabilised water was found at 6 COC (17.52 and 10.33 mg/dm^2/d, respectively) (Table 3.2). This trend was also predicted by all four indices (Table 3.1). A possible explanation for this can be coupled with the higher COC. Results in Appendix A, Table A1 clearly illustrates that 6 COC (stabilised water) had the highest levels of total alkalinity, total hardness, TDS, chlorides and sulphates as well as the highest pH and EC. These high values for various salts/ions suggests an increase in scale forming tendencies (Melidis *et al*., 2007; Rakanta *et al*., 2007) of PCB at 6 COC, however, at 6 COC the corrosion rate was small (Table 3.2). This could be ascribed to the combined effect of elevated chloride and sulphate levels (Melidis *et al.*, 2007; Ilhan-Sungur and Çotuk, 2010).

The non-stabilised water with the highest actual levels of scale formation was also observed at 6 COC (Table 3.2). The indices however, predicted (Table 3.1) that 4 COC would have the highest scaling rates of the non-stabilised water samples. By comparing the water chemistry (Appendix A, Table A1) of 4 COC and 6 COC (non-stabilised water), the major differences between the two samples may be the cause for the difference in the actual and predicted values. Table A1 (Appendix A) shows that the major differences between these two samples were the total hardness, and TDS levels. These parameters are also associated with scaling. The levels of both of these variables were considerably higher at 6 COC than at 4 COC. Both these variables suggest a negative influence on scale formation at raised levels (Rakanta *et al*., 2007).

3.5 CONCLUSION

The highest corrosion rate for stabilised water as well as non-stabilised water was found to be at 4 COC (Table 3.2). This is contrary to what was predicted by the various indices in Table 3.1. All four indices predicted that the highest corrosion rates (stabilised and non-stabilised water) would be at 6 COC. The reason for this may be that 6 COC (stabilised and non-stabilised water) had the highest scaling rates (also predicted by the indices). These high corrosion and scaling rates could also be related to the high total hardness and TDS values found at 6 COC (Appendix A, Table A1).

According to available literature, there are differences in opinion between researchers with regard to the effectiveness of the use of indices in the prediction of scaling and corrosion (Melidis *et al.*, 2007; Swart and Engelbrecht, 2007; Hawthorn, 2009; Khatami *et al.*, 2010). Hawthorn (2009) did a study to interpret heat transfer problems, by using scaling equations to better understand scaling within recirculated evaporatively cooled river water. This author suggested that predictions made by these indices were not valid for recirculating water concentrated by evaporation, especially at raised pH levels. Khatami *et al.* (2010) did research on the development of a new saturation index, chiefly because of the limitations of the scale indices used. Others, such as Swart and Engelbrecht (2007) and Melidis *et al.* (2007), found the indices to be an excellent tool in the prediction of scaling and corrosion. Results from the present study suggest that the scaling and corrosion indices could be useful in the prediction of scaling tendencies and not in the prediction of corrosion. Indices should rather be viewed as an indication of what could be expected, bearing in mind the limitations associated with them.

Results also illustrated that on average, the stabilised water had a higher fouling and corrosion rate as opposed to the higher scaling rate observed for non-stabilised water Table 3.2). These differences between the stabilised and non-stabilised water were, however, very small and could have been caused by overdosing of NaOH by the pH controlling pumps. The values obtained for fouling and corrosion rates were within the SASOL standard guidelines, suggesting that fouling and corrosion were less problematic than scaling in this particular experiment. Therefore, the water with the lowest scaling tendencies (in this case the stabilised water) would be the preferred water for the experiments in Chapter 4.

CNP correction did not have an effect on the fouling, scaling and corrosion results with regard to the LFV and COC, when considering the chemical data. This can be expected, since the CNP was corrected in order for microorganisms to be able to survive within the cooling tower system. The full effect of CNP correction will therefore be demonstrated in the results in Chapter 5.

Based on the accelerated corrosion results obtained through chemical analyses as well as the predictions made by various scaling and corrosion indices, it can be concluded that:

1. Water loss through drift for the specific cooling tower is minimal and should not affect the COC.
2. Stainless steel offers a higher level of protection against fouling, scaling and corrosion than mild steel.
3. Predictions made by corrosion and scaling indices should rather be seen as general guidelines and not as absolutes.
4. Stabilising of the PCB is necessary if this wastewater stream is used as cooling medium within cooling towers.

After the accelerated corrosion tests were done, the results were presented to SASOL R&D (Sasolburg). At this meeting it was decided that the water used in the actual cooling tower experiment, would be stabilised CNP corrected PCB. The COC used should be 2, 3 and 4 COC instead of 2, 4 and 6 COC as was done for the accelerated corrosion test. SASOL R&D (Sasolburg) further decided that H_2SO_4 instead of HCl should be used to maintain the pH in the cooling tower system.

CHAPTER 4 - THE EFFECT OF OPERATIONAL PARAMETERS ON THE RATE OF FOULING, SCALING AND CORROSION USING CNP CORRECTED GTL FISCHER-TROPSCH PCB

4.1 INTRODUCTION

Fouling, scaling and corrosion are three major problems that are associated with cooling towers (Marín-Cruz *et al.*, 2006; Rakanta *et al.*, 2007). It is responsible for reduced plant reliability and efficiency (Johnson, 2001; Rakanta *et al.*, 2007). Currently, most industries control/manage these problems by the addition of chemicals (Johnson, 2001; Li *et al.*, 2011). Managing fouling, scaling and corrosion in this way is very expensive and could also lead to environmental concerns (Bott, 1998; George *et al.*, 2003; Swart and Engelbrecht, 2007). Cost effective and environmentally friendly alternative methods to control these effects thus need to be found.

A study by Lee and Young (2002) on the effect of velocity on antifouling technology to decrease fouling within heat exchanger tubes, demonstrated that the LFV can greatly affect fouling, scaling and corrosion rates within a cooling tower. The effect that fluid velocity has on corrosion may be both direct and indirect. High LFV may directly lead to combined erosion and corrosion. Indirect LFV effects may occur when low LFV lead to suspended matter being deposited and thus creating aeration cells. The latter condition may induce pitting corrosion (Anon, 1994). A study was done by Swart and Engelbrecht (2007) on the use of mine water as cooling medium. They found that an increase in LFV would result in a decrease in fouling, scaling and corrosion rates. These authors (Swart and Engelbrecht, 2007) thus identified LFV as a suitable operational parameter for managing fouling, scaling and corrosion rates.

Another way is to operate cooling towers at higher COC which would not only benefit the environment, but it may also be of economic benefit to industries. Higher COC could, however, lead to higher scaling and corrosion rates (and to a lesser degree, fouling) within the cooling tower system (Anon, 2005; Swart and Engelbrecht, 2007). Any increase in the COC could lead to increased opportunity for precipitation and the resultant high scaling and corrosion rates (Bott, 1998; Rakanta *et al.*, 2007). Cycles of concentration can be controlled by means of blow-down (Bott, 1998; Johnson, 2001; Lee and Young, 2002; Anon, 2005;

Swart and Engelbrecht, 2007). Blow-down is the process where a specific amount of concentrated recirculating cooling water is removed from the system and replenished by make-up water. The amount of blow-down removed controls the COC within the cooling system (Anon, 2005; Rakanta *et al*., 2007).

In summary, it is apparent from literature that control of LFV and COC represent the two main parameters for optimisation when operating cooling towers systems to moderate fouling, scaling and corrosion. As such the influence of these parameters was the main focus in this chapter.

4.2 AIM AND OBJECTIVES

The aim of this chapter was to determine the effect of operational conditions (COC and LFV) on fouling, scaling and corrosion rates when CNP corrected Fischer-Tropsch GTL PCB was used as cooling water. The objectives of this chapter were therefore to:

1. determine the fouling, scaling and corrosion rates of corrosion coupons (stainless steel and mild steel) and heat exchanger tubes (stainless steel and mild steel) that were exposed to the cooling water under varying COC and LFV conditions over a period of 30 days per experiment.
2. analyse the statistical values obtained from different corrosion and scaling indices, water chemistry, the weight loss method and COD removal to ultimately determine the effect that COC and LFV had on the fouling, scaling and corrosion rates.

4.3 MATERIALS AND METHODS

4.3.1 Make-up water preparation, CNP correction, water stabilisation and pH control

PCB (make-up water) preparation and CNP correction was done as previously described in Section 3.3.1. Water stabilisation and pH control was performed as described in Section 3.3.2. The pH was maintained between two set pH levels (8.0 and 8.3) and that pH control was achieved by using 10 % NaOH (as in section 3) and with 10 % H_2SO_4 instead of HCl, as requested by SASOL R&D (Sasolburg, South Africa).

4.3.2 Cooling tower design and operation

The mini cooling tower test rig used in this experiment was supplied by Nucleus Engineering (Durban, South Africa) (Figure 4.1). The test rig was used to simulate conditions typically found within industrial-sized open recirculating cooling towers. Mini cooling tower test rigs used were made of PVC and have an internal diameter of 18 cm. The total volume of the cooling tower is 11.8 L and the volume of the sump 9.65 L.

When the process started, make-up water was pumped from the basin next to the tower into the cooling tower sump (Figure 4.1 and 4.2) and then through a heat exchanger containing eight heat exchanger tubes (length: 750 mm; outer diameter: 10 mm; wall thickness: 1 mm) (Figure 4.1 and 4.2). Four of the heat exchangers were mild steel and four were stainless steel (316 L). The water was heated in the heat exchanger to a temperature not exceeding 60 °C (block temperature). From there the water passed through two corrosion coupon racks (Figure 4.1 and 4.2) each containing three mild steel corrosion coupons and three 316 L stainless steel corrosion coupons. The coupons had the following dimensions: 74 mm x 11.5 mm x 1.6 mm. Water then passed through a 30 cm biocell (polyvinyl chloride pipe; internal diameter: 12 mm) where it then reached the spray nozzle and was sprayed into the tower (Figure 4.2). From here it dripped down passing the microscope slide holders and through the packing material (25 mm Pall V-rings; polypropylene with a surface area of 1 m^3; Mass and Heat Transfer Technology (Pty) Ltd., Roodepoort, South Africa) into the sump (Figure 4.1 and 4.2). A constant ΔT (temperature difference between inflow and outflow from heat

exchanger) of 10 °C was maintained for the various experimental conditions during this project. Figure 4.2 provide a schematic diagram to demonstrate the water flow process.

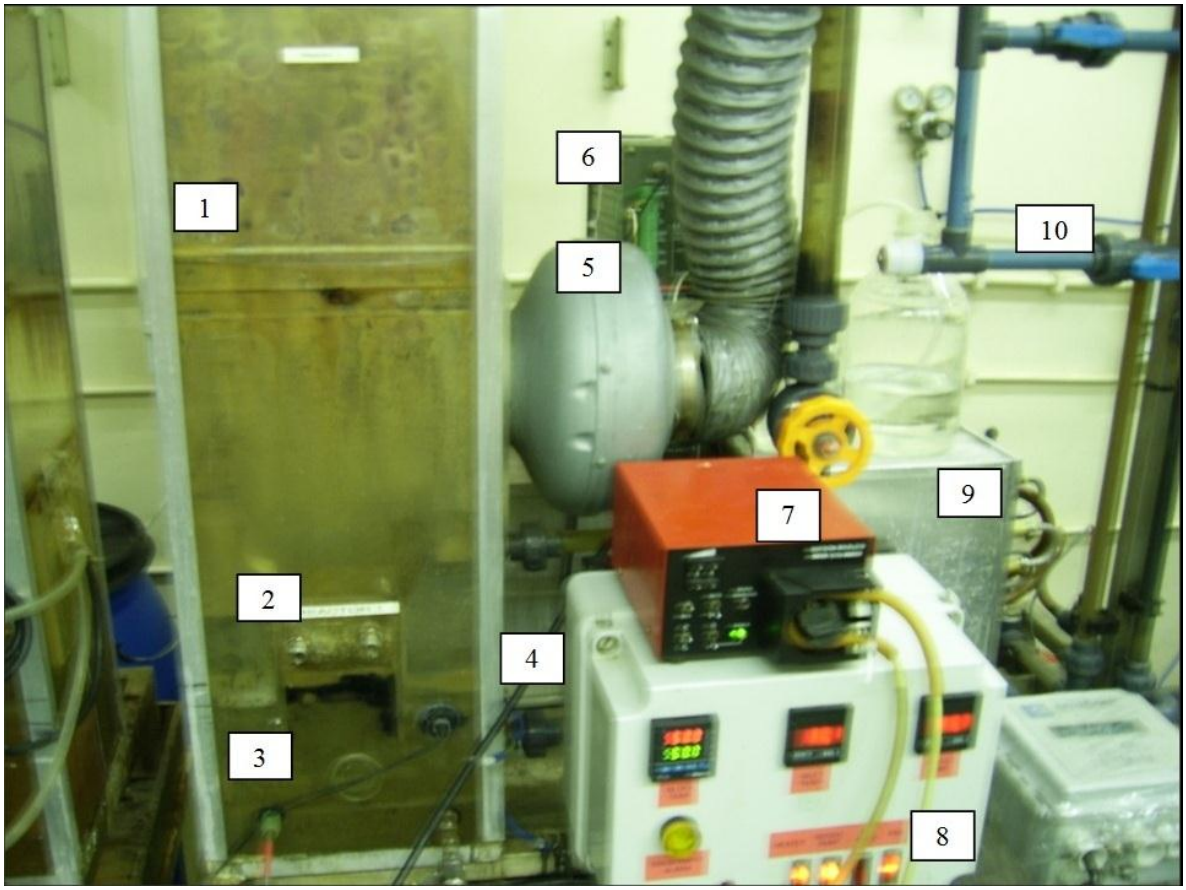

Figure 4.1: Photograph of lab-scale mini cooling tower test rig. (Legend: 1 = Fill (packing materials); 2 = Water level regulator; 3 = Sump; 4 = Pump; 5 = Fan; 6 = pH controller; 7 = Blowdown pump; 8 = Control Unit; 9 = Heat exchanger; 10 = Corrosion coupon racks)

Each experimental run lasted 30 days during which the cooling tower was operated continuously. The experimental runs differed with respect to LFV and COC. Linear flow velocity was controlled by a flow meter attached to the cooling tower (Figure 4.2). In order to control the COC, a blow-down pump removed water from the sump at a predetermined rate in order to keep the COC within the sump constant (Donald, 2001; Swart and Engelbrecht, 2007).

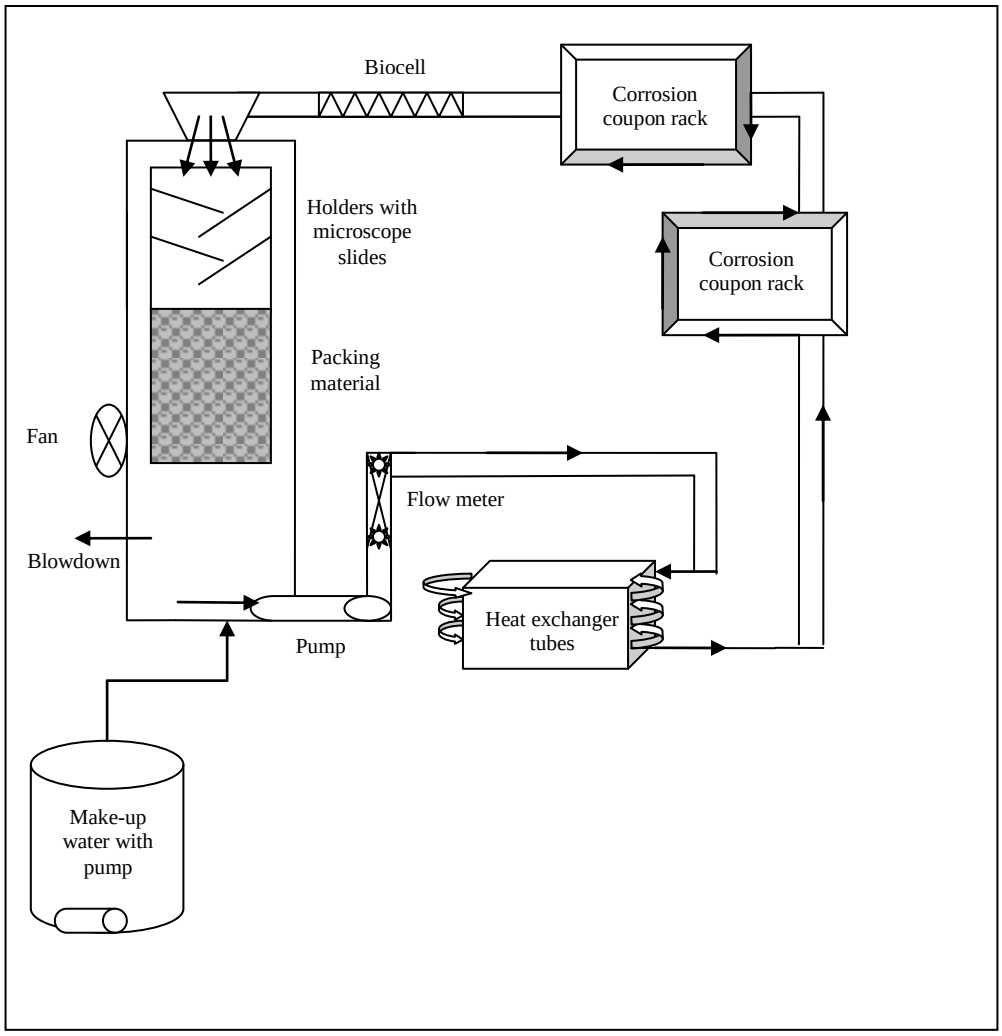

Figure 4.2: Schematic representation as well as dimensions of laboratory scale mini cooling tower test rigs used.

The cooling tower test rig operated at a ΔT of 10 °C by adjusting the block temperature. This was achieved by trial and error (Swart and Engelbrecht, 2007). Before each experimental run the U-bends, heat exchanger tubes and corrosion coupons were cleaned, dried and weighed according to specifications described previously (Sections 3.3.7.1, 3.3.7.2 and 3.3.7.3), and were then inserted into the cooling tower. After each experimental run the corrosion coupons, heat exchangers as well as the biocell were removed for analyses. Samples of the sump were also taken and represented the planktonic community. All samples were analysed for microbial community dynamics using conventional microbiological techniques, as well as DGGE and PLFA analyses. The biocell was cut into 2 cm pieces and the biofilm removed with a sterile spatula, for analyses of the sessile microbial community. Microscope slides were also removed from the tower. These were used for SEM and represented the planktonic

microbial community. A section of biocell was analysed by SEM and represented the sessile microbial communities. The methods are described in Chapter 5. The cooling tower was then thoroughly cleaned before the next experimental run (Sections 3.3.7.4 and 3.3.7.5).

4.3.3 Routine measurements taken and analyses done during each experimental run

Daily measurements included DO, pH, EC and the RP of both the make-up (PCB) water as well as the blow-down water (sump). These results together with the TSS and TDS were done as described in Section 3.3.6.1.

4.3.4. Statistical analysis

Physico-chemical results from the make-up water as well as the sump was recorded and used to determine indices values. Results obtained from the weight loss method for corrosion coupons and heat exchanger tubes were used in an Excel spreadsheet (obtained from SASOL Research & Development, Sasolburg) to calculate the fouling, scaling and corrosion rates (Swart and Engelbrecht, 2007; Ilhan-Sungur and Çotuk, 2010). These rates were then used to determine the average and standard error by means of breakdown and one-way ANOVA, using STATISTICA 10 (StatSoft Inc ©, 2011). The statistical difference between samples was determined using the Tukey Honest Significant Difference (HSD) test. Where applicable, superscript suffixes indicate statistically significant differences in the results obtained, where no statistically significant differences would be indicated by matching superscript characters. Multivariate analysis, specifically Redundancy Analysis (RDA), was performed on the data using Canoco for Windows 4.5 (Ter Braak and Smilauer 1998).

4.4 RESULTS AND DISCUSSION

From previous research it is clear that the physico-chemical properties of water can be used to determine the water quality in terms of fouling, scaling and corrosion. A study performed by Swart and Engelbrecht (2007) on mine water as a cooling medium, made use of these parameters to predict scaling and corrosion by applying these properties in scaling and corrosion indices equations. In Table 4.1, averages of the physico-chemical properties of the synthetic PCB used as make-up water during the different experiments are shown. These are averages of experiments which were performed for 30 days.

It is apparent that there were variations among values of certain experiments. Swart and Engelbrecht (2007) used mine water as a cooling medium and fluctuation within their make-up water quality was also found. This suggests that there will be some degree of differences in the physico-chemical properties of make-up water, especially when using effluent or wastewater. This might be so because of the large array of factors present within cooling systems, each of which may alter the water quality.

Table 4.1: Physico-chemical properties of make-up water (PCB) during experiments.

PARAMETER	EXP. 1	EXP. 2	EXP. 3	EXP. 4	EXP. 5
Ca Hardness (mg $CaCO_3$/L)	**102.80**	**130.09**	**142.10**	**118.08**	**107.31**
Mg Hardness (mg $CaCO_3$/L)	192.10	177.15	214.17	220.18	198.18
Total Hardness (mg $CaCO_3$/L)	**249.90**	**307.24**	**356.27**	**338.26**	**305.49**
M Alkalinity (mg $CaCO_3$/L)	39.00	104.50	224.00	89.00	90.00
Total Alkalinity (mg $CaCO_3$/L)	**75.00**	**139.50**	**228.00**	**120.00**	**129.50**
Electrical Conductivity (mS/cm)	0.70	0.70	0.71	0.76	0.71
pH	**4.80**	**5.68**	**7.43**	**6.11**	**5.20**
Chloride (mg Cl/L)	46.01	36.67	35.28	36.23	36.77
Sulphate (mg SO_4/L)	**101.22**	**102.03**	**103.73**	**87.45**	**108.54**
Phosphate (mg PO_4/L)	18.71	11.80	7.91	3.45	4.82
Nitrate (mg NO_3/L)	**0.04**	**0.63**	**0.98**	**1.29**	**0.13**
Nitrite (mg NO_2/L)	< 0.01	1.59	0.88	< 0.01	< 0.01
Fluoride (mg F/L)	**7.67**	**7.57**	**7.98**	**0.21**	**1.19**
Ammonia (mg NH_4/L)	**0.11**	**0.40**	**1.44**	**0.07**	**0.94**
Exp. 1 = 2 COC, 0.6 m/s; Exp. 2 = 3 COC, 0.9 m/s; Exp. 3 = 2 COC, 1.2 m/s; Exp. 4 = 4 COC, 1.2 m/s; Exp. 5 = 4 COC, 0.6 m/s					

The values from Table 4.1 were used to predict the scale-forming and/or corrosive tendencies of the PCB (make-up water) used during each experiment (Table 4.3). The physico-chemical properties of the recirculating water (sump) after each experimental run of 30 days are found in Table 4.2. Results from Table 4.2 were then used to calculate the corrosion and scale indices values of each experimental run, at different COC and LFV (Table 4.3).

Table 4.2: Physico-chemical properties of the recirculating cooling water during each experimental run at different COC and LFV.

PARAMETER	EXP. 1	EXP. 2	EXP. 3	EXP. 4	EXP. 5
Ca Hardness (mg $CaCO_3$/L)	**168.92**	**237.68**	**114.08**	**123.10**	**151.67**
Mg Hardness (mg $CaCO_3$/L)	291.80	458.41	355.30	226.20	262.20
Total Hardness (mg $CaCO_3$/L)	**460.72**	**696.09**	**469.38**	**349.30**	**413.87**
M Alkalinity (mg $CaCO_3$/L)	497.00	131.00	264.00	74.00	550.50
Total Alkalinity (mg $CaCO_3$/L)	**501.00**	**134.50**	**266.50**	**115.00**	**557.00**
Electrical Conductivity (mS/cm)	2.32	4.34	1.44	1.75	2.83
pH	**7.40**	**7.71**	**8.14**	**5.13**	**7.66**
Chloride (mg Cl/L)	57.36	63.14	50.94	36.96	84.18
Sulphate (mg SO_4/L)	**636.31**	**2 360.44**	**399.40**	**88.81**	**907.51**
Phosphate (mg PO_4/L)	23.17	5.14	7.50	< 0.01	< 0.01
Nitrate (mg NO_3/L)	**2.93**	**4.76**	**4.44**	**1.14**	**4.99**
Nitrite (mg NO_2/L)	0.01	< 0.01	< 0.01	< 0.01	< 0.01
Fluoride (mg F/L)	**9.22**	**5.06**	**4.83**	**0.24**	**4.68**
Ammonia (mg NH_4/L)	**20.44**	**58.55**	**23.81**	**0.18**	**18.20**
Exp. 1 = 2 COC, 0.6 m/s; Exp. 2 = 3 COC, 0.9 m/s; Exp. 3 = 2 COC, 1.2 m/s; Exp. 4 = 4 COC, 1.2 m/s; Exp. 5 = 4 COC, 0.6 m/s					

According to the results from Table 4.2, the highest total hardness (696.09 mg $CaCO_3$/L), conductivity (4.34 mS/cm), levels of sulphate (2 360.44 mg SO_4/L) and ammonia (58.55 mg NH_4/L) can be found at experiment 2 (3 COC, 0.9 m/s LFV). This suggests that a high amount of scaling (caused by the high amount of mineral ions and total hardness) as well as corrosion (caused by high sulphate levels) can be expected at experiment 2 (Anon, 1994; Doche *et al.*, 2006; Swart and Engelbrecht, 2007). The lowest levels of hardness (349.30 mg $CaCO_3$/L) and alkalinity (115 mg $CaCO_3$/L) (shown in Table 4.2) was found at experiment 4 (4 COC, 1.2 m/s LFV), which suggests that the water in this experiment would be less corrosive (Melidis *et al.*, 2007). Predictive values of the corrosiveness and/or scale-forming

properties of the make-up water as well as the sump water (recirculating water), as determined by the various corrosion indices are shown in Table 4.3.

Table 4.3: Table showing the various corrosion indices' results (make-up water as well as water from the cooling tower sump).

EXPERIMENT	RSI	LSI	PSI	LSCI
Indices Key	**< 6 Scale forming** **> 6 Corrosive**	**+ Scale forming** **- Corrosive** **0 Borderline**	**6 Stable** **< 6 Scale forming** **> 6 Corrosive**	**< 0.8 Scaling** **> 0.8 Corrosive**
Exp. 1, S	**5.45**	**0.97**	**4.15**	**1.48**
Exp. 1, M	10.06	-2.63	6.98	2.27
Exp. 2, S	**6.16**	**0.77**	**5.74**	**18.94**
Exp. 2, M	8.39	-1.35	5.92	1.13
Exp. 3, S	**5.41**	**1.37**	**5.11**	**1.83**
Exp. 3, M	6.04	0.70	5.11	0.40
Exp. 4, S	**9.25**	**-2.06**	**6.31**	**1.26**
Exp. 4, M	8.19	-1.04	6.21	1.18
Exp. 5, S	**5.38**	**1.44**	**5.09**	**3.51**
Exp. 5, M	7.57	-0.70	5.78	2.38

- **Exp. 1 = 2 COC, 0.6 m/s; Exp. 2 = 3 COC, 0.9 m/s; Exp. 3 = 2 COC, 1.2 m/s; Exp. 4 = 4 COC, 1.2 m/s; Exp. 5 = 4 COC, 0.6 m/s**
- **S = Sump water; M = Make-up water**
- **RSI = Ryznar Stability Index; LSI = Langelier Saturation Index; PSI = Puckorius Scaling Index and**
  LSCI = Larson-Skold Corrosion Index

In Table 4.3 it is illustrated that the make-up water (PCB) was predicted to be corrosive during all experiments except experiment 3 (2 COC, 1.2 m/s LFV). The latter experiment was more likely to be scale-forming. Three indices (RSI, LSI and PSI) predicted that the sump water of all the experiments were scale forming except for experiment 4 S (4 COC, 1.2 m/s LFV) (Table 4.3). The LSCI is the only index that predicted that experiment 2 (3 COC, 0.9 m/s LFV) was the most corrosive (make-up as well as sump water).

Actual fouling, scaling and corrosion rates of each experimental run (as measured on corrosion coupons and heat exchanger tubes), are depicted in Table 4.4. From Table 4.4 it can be seen that the only significant differences for scaling were between mild steel heat exchanger tubes (^{c,b,e,c} and ^{d} for experiments 1, 2, 3, 4 and 5, respectively) and the mild steel corrosion coupons from experiment 3 (^{a,b}). There were no significant difference between the heat exchanger tubes (mild steel) from experiment 1 and 4 (^{c}). A wide variety of significant differences were found within the fouling results. These differences occurred mainly on the mild steel corrosion coupons and heat exchanger tubes. For mild steel corrosion coupons and heat exchanger tubes the only values where there were no statistical difference between samples occurred on the mild steel heat exchanger tubes from experiments 3 and 4 (^{i}). Stainless steel corrosion coupons and heat exchangers showed little significant difference, apart from the heat exchangers from experiment 4 (^{b,c}) and the corrosion coupons and heat exchangers of experiment 5 (^{a,b}). No significant differences were found on stainless steel corrosion coupons and heat exchanger tubes (^{a}), whilst the mild steel corrosion coupons and heat exchanger tubes from experiments 3, 4 and 5 were all found to be significantly different.

Table 4.4: Average fouling, scaling and corrosion rates as determined at different COC and LFV. (Mean value ± standard error, superscript characters denote honest statistical significant differences)

EXPERIMENT	LFV (m/s)	COC	FOULING ($mg/dm^2/d$)	SCALING ($mg/dm^2/d$)	CORROSION (mm/y)
SASOL Guidelines			**20.000**	**2.000**	**0.200**
EXP 1ccss	0.6	2.0	-0.148 ± 0.393[a]	0.105 ± 0.192[a]	-0.001 ± 0.001[a]
EXP 1ccms	**0.6**	**2.0**	**9.127 ± 1.092[b,c]**	**1.740 ± 0.229[a]**	**0.031 ± 0.001[b]**
EXP 1hetss	0.6	2.0	0.221 ± 0.141[a]	0.626 ± 0.284[a]	0.004 ± 0.001[a]
EXP 1hetms	**0.6**	**2.0**	**21.544 ± 1.552[f,g]**	**22.501 ± 2.336[c]**	**0.034 ± 0.001[b]**
EXP 2ccss	0.9	3.0	1.872 ± 0.479[a]	0.016 ± 0.025[a]	0.000[a]
EXP 2ccms	**0.9**	**3.0**	**5.329 ± 0.240[a,b,c]**	**0.969 ± 0.046[a]**	**0.142 ± 0.004[f]**
EXP 2hetss	0.9	3.0	0.836 ± 0.044[a]	0.152 ± 0.062[a]	0.001 ± 0.000[a]
EXP 2hetms	**0.9**	**3.0**	**11.062 ± 0.593[c,d]**	**8.819 ± 0.407[b]**	**0.145 ± 0.003[f]**
EXP 3ccss	1.2	2.0	2.172 ± 0.802[a]	0.006 ± 0.027[a]	-0.001[a]
EXP 3ccms	**1.2**	**2.0**	**26.321 ± 1.482[g]**	**3.271 ± 0.304[a,b]**	**0.050 ± 0.003[c,d]**
EXP 3hetss	1.2	2.0	1.064 ± 0.108[a]	0.418 ± 0.073[a]	-0.001 ± 0.000[a]
EXP 3hetms	**1.2**	**2.0**	**47.974 ± 1.297[i]**	**36.228 ± 0.771[e]**	**0.063 ± 0.002[e]**
EXP 4ccss	1.2	4.0	2.063 ± 0.736[a]	-0.229 ± 0.539[a]	-0.002[a]
EXP 4ccms	**1.2**	**4.0**	**18.195 ± 1.312[e,f]**	**1.099 ± 0.104[a]**	**0.060 ± 0.003[d,e]**
EXP 4hetss	1.2	4.0	4.600 ± 0.521[b,c]	1.673 ± 0.566[a]	-0.002 ± 0.001[a]
EXP 4hetms	**1.2**	**4.0**	**44.782 ± 1.634[i]**	**23.075 ± 2.679[c]**	**0.056 ± 0.003[c,d,e]**
EXP 5ccss	0.6	4.0	3.335 ± 1.246[a,b]	0.006 ± 0.006[a]	-0.003[a]
EXP 5ccms	**0.6**	**4.0**	**15.461 ± 1.270[d,e]**	**2.447 ± 0.110[a]**	**0.031 ± 0.001[b]**
EXP 5hetss	0.6	4.0	3.575 ± 0.118[a,b]	2.043 ± 0.231[a]	0.001 ± 0.001[a]
EXP 5hetms	**0.6**	**4.0**	**37.278 ± 1.710[h]**	**28.872± 0.538[d]**	**0.047 ± 0.002[c]**

- **cc = corrosion coupons; het = heat exchanger tubes**
- **ss = stainless steel; ms = mild steel**

4.4.1 Fouling

According to results in Table 4.4, all the stainless steel corrosion coupons and heat exchanger tubes had fouling rates which were well below the given SASOL standards (Table 3.2, Section 3.4). This suggests that stainless steel is not affected by fouling to the same extent as mild steel. Stainless steel corrosion coupons and heat exchanger tubes from experiment 1, 2 and 3 reacted statistically the same ([a]) in terms of fouling rates. All three these experiments

(1, 2 and 3) were operated at lower COC (2 COC during experiments 1 and 3, and 3 COC at experiment 2); thereby demonstrating that lower COC resulted in lower fouling rates. On the other hand, fouling rates found on mild steel corrosion coupons and heat exchanger tubes were greater than the SASOL standard guidelines (Section 3.4). Experiment 2 (3 COC, 0.9 m/s LFV) was the only experiment where both the mild steel corrosion coupons and heat exchanger tubes had fouling rates that were below the SASOL standards ($9.127 \pm 1.092^{b,c}$ $mg/dm^2/d$ and $11.062 \pm 0.593^{c,d}$ $mg/dm^2/d$, respectively). Mild steel fouling values which reacted statistically the same (^{i}) were the heat exchanger tubes from experiments 3 and 4. Linear flow velocity for experiment 3 and 4 was 1.2 m/s, suggesting that the mild steel heat exchanger tubes reacted statistically the same to the (high) LFV parameter.

From the fouling results in Table 4.4 it can be deducted that the fouling rates are generally higher at high LFV (1.2 m/s), somewhat less at low LFV (0.6 m/s) and the lowest at medium LFV (0.9 m/s). Results in Table 4.4 also demonstrate that lower COC have lower fouling rates, except when it is paired with high LFV (as found at experiment 3). The study done by Swart and Engelbrecht (2007) found that the LFV and COC did not have a statistically significant effect on the fouling rates. They (Swart and Engelbrecht, 2007) suggested that higher LFV and lower COC will lead to a decrease in fouling rates. The effect of LFV on fouling rates during the present study is contradictory to the effect found by Swart and Engelbrecht (2007). However, the effect of COC on fouling rates is in accordance with their (Swart and Engelbrecht, 2007) findings. Although some fouling rates were not within the SASOL standard guidelines, all the fouling rate values obtained in the present study were lower than the fouling rate observed on corrosion coupons (56.41 $mg/dm^2/d$) from the actual Process Cooling Towers from SASOL One as reported by Swart and Engelbrecht (2007).

4.4.2 Scaling

From the scaling results in Table 4.4 it is evident that all corrosion coupons and heat exchanger tubes (mild steel and stainless steel) from experiments 1, 2 and 4 statistically reacted the same (^{a}), except for the mild steel heat exchanger tubes. The mild steel heat exchanger tubes were also the only values during experiments 1, 2 and 4 that were not within the SASOL standards. According to the review by Prisyazhniuk (2009) scaling of heat exchanger tubes is the biggest problem associated with cooling systems in industry. Li *et al.*

(2011) did a pilot scale study on the control of scale deposition within a cooling tower, by using secondary-treated municipal wastewater as cooling medium. They (Li *et al.*, 2011) suggested that scaling had a greater affect on heat exchanger tubes because of the higher temperatures associated with it.

For stainless steel, the highest scaling rates were observed at the heat exchanger tubes of experiments 4 and 5 (1.673 ± 0.566^{a} and 2.043 ± 0.231^{a}). These experiments were operated at high COC (4 COC). Swart and Engelbrecht (2007) found that higher COC lead to increased scaling rates. Results from the present study are similar to the observations by Swart and Engelbrecht (2007), where higher COC ultimately lead to increased scaling rates. The highest scaling rates for mild steel corrosion coupon and heat exchanger tubes were observed during experiment 3 (3.27 $mg/dm^2/d$ and 36.228 $mg/dm^2/d$, respectively). Experiment 3 was operated at 2 COC and 1.2 m/s LFV. These observations suggest that higher LFV leads to increased scaling rates. This is once again in contradiction to research done by Swart and Engelbrecht (2007). They observed that increases in the LFV decreased the scaling rate. In general the lowest scaling rates for mild steel corrosion coupons and heat exchanger tubes (0.969 ± 0.046^{a} $mg/dm^2/d$ and 8.819 ± 0.407^{b} $mg/dm^2/d$) were observed during experiment 2. This experiment was operated at medium LFV (0.9 m/s) and medium COC (3 COC). Thus, scaling results from Table. 4.4 indicate that lower COC decreased the scaling rates, whereas higher LFV increased the scaling rate.

4.4.3 Corrosion

Corrosion results in Table 4.4 show that all stainless steel corrosion coupons and heat exchanger tubes reacted statistically the same (^{a}). All of these values are extremely low and were within the SASOL standard guidelines. Mild steel corrosion coupons and heat exchanger tubes from experiment 1 statistically reacted the same as the mild steel corrosion coupons from experiment 5 (^{b}). Table 4.4 also indicates that experiments 1 and 5 had the lowest corrosion rate for mild steel. Both of these experiments were operated at low LFV (0.6 m/s). It can therefore be deducted that low LFV had a positive effect on corrosion. This observation and deduction is supported by the work of Swart and Engelbrecht (2007) where the samples which were operated at low LFV also resulted in decreased corrosion rates. According to Table 4.4 the highest mild steel corrosion rates can be observed during

experiment 2 (3 COC, 0.9 m/s LFV). These results suggest that slightly higher COC leads to higher corrosion rates. This was also found during the study by Swart and Engelbrecht (2007). Corrosion rates from all five experiments were well below the SASOL standards (Table 4.4). Almost no corrosion was observed on stainless steel corrosion coupons and heat exchanger tubes. The effect of LFV and COC are similar to trends found within literature where an increase in LFV and COC lead to an increased corrosion rate (Swart and Engelbrecht, 2007).

When the values of the various experiments (sump and make-up water) (Table 4.4) are compared to the prediction values in Table 4.3**,** apparent similarities between the data can be seen. Highest fouling and scaling results were found during experiment 3, both on the mild steel corrosion coupons (26.321 mg/dm^2/d and 3.271 mg/dm^2/d, respectively) as well as the mild steel heat exchanger tubes (47.974 mg/dm^2/d and 36.228 mg/dm^2/d, respectively). Three of the indices (RSI; LSI and PSI) predicted that the sump water from experiment 3 would be scale-forming, but none predicted that it would be the most scale-forming (Table 4.3). Another similarity is the mild steel corrosion coupons and heat exchanger tubes of experiment 2, which contained the highest corrosion rates (0.142 mm/y and 0.154 mm/y, respectively). This was also predicted by the high Larson-Skold index value (18.94) seen in Table. 4.3.

4.4.4 Redundancy analysis

Redundancy analysis (RDA) graphs were used to demonstrate the relation between different samples and variables. In the RDA samples that are clustered together are similar and variables are represented as vector arrows. Importance of a variable is shown in the length of the arrow. The angle that forms between arrows can be used to demonstrate the correlation between the two variables. When the angle is 180°, the variables have a negative correlation to each other. An angle of 90° or greater have no correlation whilst less than 90° can be seen as a positive correlation. Environmental data used in Figure 4.3 included corrosion rate, conductivity, redox potential, dissolved oxygen, pH and temperature of the make-up – as well as the sump water. Species data consisted of the fouling, scaling and corrosion rates of the corrosion coupons and heat exchanger tubes from each experiment.

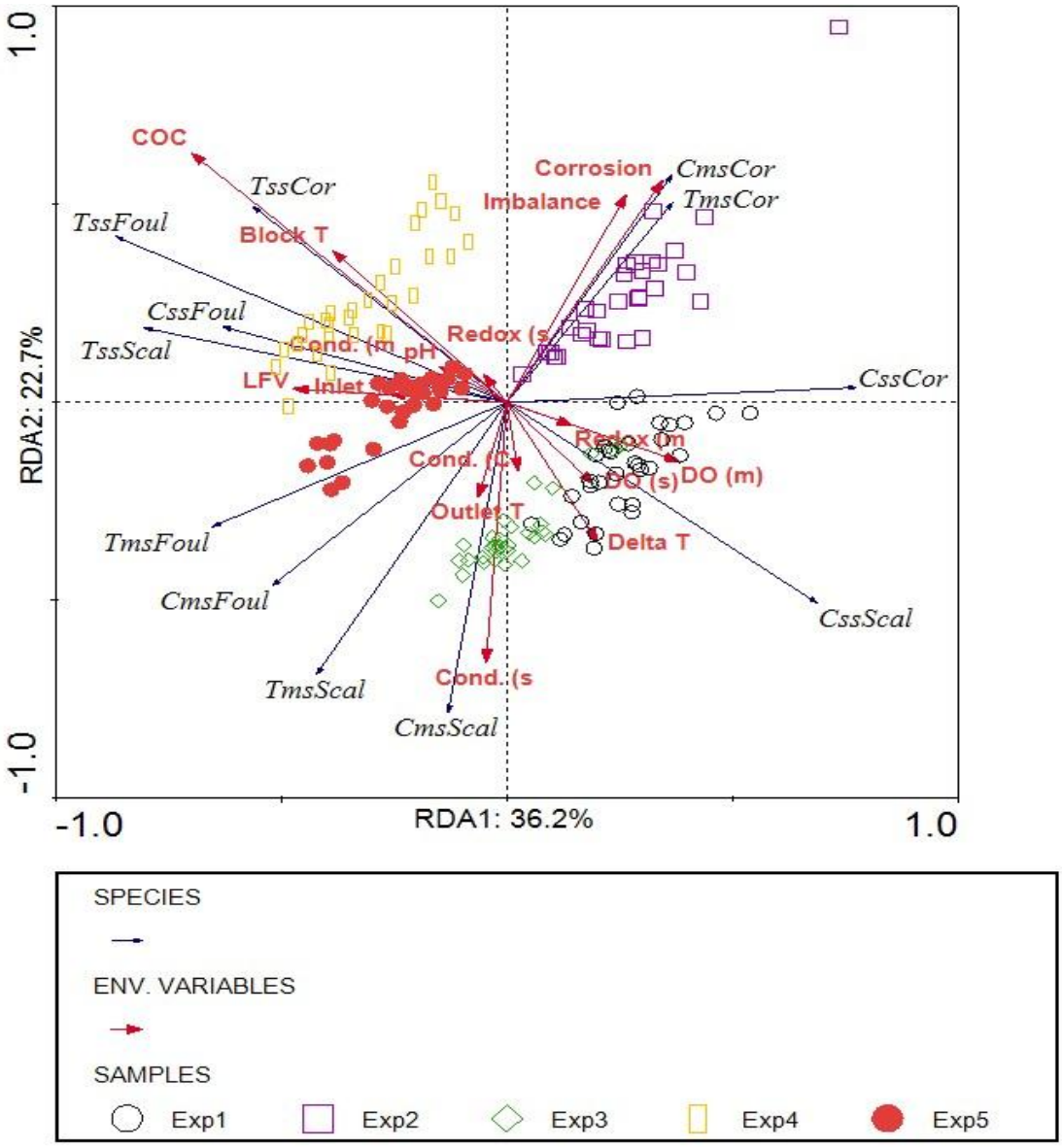

Figure 4.3: Redundancy analysis (RDA) using external operating parameters of experiments 1, 2, 3, 4 and 5. Eigen values for the first canonical axis is 36.2 % and for the second axis is 22.7 %.

The following trends are observed in the ordination graph in Figure 4.3. From this ordination it is apparent that COC is one of the major factors influencing the ordination of the experimental data. The experimental runs during this study form distinct groupings in the ordination. Experiments 1 and 3, which were operated at 2 COC are clustered separately from experiment 2, which was operated at 3 COC and experiments 4 and 5 which were operated at 4 COC. The ordination also shows a gradient with regard to the cycles of concentration.

From the ordination, high COC had a positive correlation with fouling, scaling and corrosion measured on the stainless steel heat exchanger tubing and with fouling observed on the stainless steel coupons. Cycles of concentration (COC) had a weak correlation with fouling and scaling observed on the mild steel corrosion coupons and heat exchanger tubing. Scaling on the mild steel heat exchanger tubing and coupons in particular, seems to be correlated with the ΔT (difference between in and outlet temperatures from the heat exchanger block). This is also true for the stainless steel coupons, but to a lesser degree. Linear flow velocity (LFV) correlates with scaling and fouling on both the mild steel and stainless steel, but not as strongly as the cycles of concentration. The Monte Carlo permutation test, the test of significance for all the canonical axes, had a p-value of 0.002. This indicates that the variation captured by the ordination is statistically significant ($p \leq 0.05$).

4.4.5 COD values within the cooling tower

Table 4.5 gives the COD values found in the make-up water as well as the water from the sump of the cooling tower. Results for percentage COD removal are also summarised in Table 4.5.

Table 4.5: Average COD values of the make-up – and the sump water, including the percentage COD removal during each experiment.

EXPERIMENT	COD (Make-up) (mg/L O_2)	COD (Sump) (mg/L O_2)	% COD REMOVAL
1	**412**	**347**	**15.78**
2	464	370	20.26
3	**526**	**56**	**89.35**
4	518	99	80.89
5	**422**	**161**	**61.85**

The fact that all the values from the sump water were well below the corresponding make-up water values, indicates that COD was removed during the cooling process. Highest percentage COD removal occurred at experiments 3 (89.35 %; 2 COC, 1.2 m/s LFV) and 4 (80.89 %; 4 COC, 1.2 m/s LFV). Experiment 5 (4 COC; 0.6 m/s LFV) also had a high

percentage COD removal (61.82 %). From the results it is evident that the cooling tower can be used as a bioreactor for COD removal.

4.5 CONCLUSION

During this study the physico-chemical properties of the make-up as well as the sump water were measured (Tables 4.1 and 4.2). These values were then used to predict the corrosiveness and scale-forming ability of the water by making use of four predictive indices (Ryznar stability index, Langelier saturation index, Larson-Skold corrosion index and the Puckorius scaling index) (Table 4.3). According to the indices the make-up water was likely to be corrosive, except the make-up water from experiment 3, which was more likely to be scale-forming. The water from the sump was predicted to be scale-forming, with exception of experiment 4, which was predicted to be corrosive. Actual scaling and corrosion rates determined (Table 4.4) during this study showed that the predictions made by the various indices were indeed accurate as the water from the sump did indeed result in scale formation. The highest scaling rates were also observed for the mild steel heat exchanger tubes from experiment 3 (36.228 mg/dm^2/d) and the second highest corrosion rates for the mild steel corrosion coupons from experiment 4 (0.60 mm/y).

Redundancy analyses showed that COC, as a parameter, had a strong correlation (72 %) with fouling, scaling and corrosion, especially on the stainless steel. Thus, higher COC lead to increased scaling, fouling and corrosion potential. Similar trends were observed for linear flow velocity, but the correlation was not as pronounced as with COC. These results are very similar to the results obtained in a study by Swart and Engelbrecht (2007). Contradictions to the study by Swart and Engelbrecht (2007) were related to the effect of LFV on fouling and scaling rates. According to their research, increased LFV would result in a decrease in the fouling and scaling rates. Swart and Engelbrecht (2007) added biocide to the cooling system, which reduced biofouling (fouling caused by microorganisms). In the present study no chemicals were added to the system, therefore microorganisms present in the system could have a marked affect on the fouling rates. According to Melo and Bott (1997), increased mass transfer at high LFV could lead to higher microbial growth. This aspect will be discussed further in Chapter 5.

Results from the present study also demonstrated that stainless steel coupons and heat exchanger tubes were resistant to scaling, fouling and corrosion. This phenomenon was also observed during previous studies (Xu *et al.*, 2007) which monitored localised corrosion on 316 L stainless steel. During all five experiments in the present study COD was removed from the system. It is thus apparent that the cooling tower can be used as a bioreactor.

For best overall performance when using PCB as cooling water, stainless steel should be used and the recommended cooling tower conditions should be those used during experiment 4 (4 COC, 1.2 m/s LFV). Although experiment 4 had higher scaling, fouling and corrosion rates than some of the other experiments, all these values were still within the SASOL guidelines, with the exception of the mild steel heat exchanger tubes. Furthermore, the results obtained in the present study were also lower than those from the actual process cooling towers found at SASOL One (Swart and Engelbrecht, 2007). In the case of experiment 4, the chemical oxygen demand (COD) removal was still high (80.89 %).

CHAPTER 5 - THE FUNCTIONAL AND STRUCTURAL DIVERSITY OF PLANKTONIC AND SESSILE MICROBIAL COMMUNITIES IN A PILOT SCALE COOLING TOWER SYSTEM

5.1 INTRODUCTION

Cooling water systems (including cooling towers) provide ideal growth conditions for microorganisms (Choudary, 1998; Ludensky, 2003; Xu *et al.*, 2007). These conditions include favourable temperature, aerobic and anaerobic conditions as well as light and certain energy sources. When the CNP ratio of the cooling water is corrected (100:10:1) to ensure adequate biodegradation of high COD cooling water, microbial growth is encouraged (Schmidt *et al.*, 2007). Microorganisms present within cooling water systems, can have adverse effects on such a system. These effects include microbiological fouling and induced corrosion (MIC) (Lutey, 1998). Microbiologically induced corrosion (MIC) is the most common problem associated with microorganisms found in cooling water systems (Lutey, 1996). To manage microbial fouling and corrosion it is of critical importance that the microbial dynamics within cooling water systems are understood. Microorganisms involved in MIC which are commonly found in cooling water systems, include members from the sulphate reducing bacteria (SRB) (*Desulfovibrio* sp., *Dusulfotomaculum* sp. and *Shewanella putrefaciens*), iron oxidizing/reducing bacteria (*Gallionella* sp, *Shaerotilus* sp. and *Arthrobacter* sp.) as well as anaerobic acid/H_2 producing bacteria (*Clostridium* sp.) (Lutey, 1996; McLeod *et al.*, 2002; Xu *et al.*, 2007; Ilhan-Sungur and Çotuk, 2010). There are also important slime-forming organisms which can contribute to both corrosion and fouling. These organisms include bacteria (*Pseudomonas* sp., and alkali or acid producing bacteria), algae and fungi (Lutey, 1996; Viera *et al.*, 1999). There are various methods to determine microbial dynamics within cooling water systems. Previous studies on microbial dynamics within cooling water systems used conventional microbiological methods, PLFA and PCR-DGGE (Jack *et al.*, 1992; Villanueva *et al.*, 2004; Neria-González *et al.*, 2006; Wang *et al.* 2006; Ilhan-Sungur and Çotuk, 2010). These methods were mostly done together in order to complement each other.

5.1.1 Culture dependent methods

Conventional microbiological techniques can be described as methods that are based on the isolation of pure cultures (Sanz and Köchling, 2007). Typical conventional microbiological techniques used in previous studies to determine microbial community dynamics, included plate counts (spread plate method) and the MPN technique (Jack *et al.*, 1992; Gagnon and Slawson, 1999; Wang *et al.*, 2006; Ilhan-Sungur and Çotuk, 2010; Li *et al.*, 2011). Bacterial counts for the plate count method are expressed as colony forming units per millilitre (CFU/ml) of sample used. Most probable number technique is used as an estimation of the number of organisms present within a sample, and is expressed as MPN/ml sample used. One limitation associated with the use of these methods is the fact that an entire microbial community within a sample need to be culturable (MacDonald and Brözel, 2000; Soares *et al.*, 2006). This however is not the case. According to Wang *et al* (2006), more than 90 % of microorganisms that occur in nature cannot be detected by these methods. In a study by MacDonald and Brözel (2000) on the community analysis of bacterial biofilms in cooling water systems, it was found that less than 1 % of the bacteria found in the biofilm were culturable. Culture dependent methods need to be used in addition to the culture independent methods.

5.1.2 Culture independent methods

Scanning electron microscopy is also widely used to study bacteria adhering to surfaces (Lagacé *et al.*, 2006; Ilhan-Sungur and Çotuk, 2010. Scanning electron microscopy (SEM) can be used to validate results from other methods (such as conventional methods, DGGE and PLFA). Images obtained from SEM show the morphology of microorganisms as well as the abundance thereof (Ilhan-Sungur and Çotuk, 2010). Adhesion of organisms can also be seen, thus confirming biofilm formation. Extracellular polysaccharide substances (EPS) and corrosion byproducts (if present) will also be apparent (Ilhan-Sungur and Çotuk, 2010). Scanning electron microscopy (SEM) can thus be used to study microbial biofilms. The biofilm samples need to be dehydrated, then critically point dried and finally coated with gold (Lagacé *et al.*, 2006; Perni *et al.*, 2006; Ilhan-Sungur and Çotuk, 2010).

There are various culture independent methods that can be used, two of which are PLFA and DGGE (Hill *et al.*, 2000; Wang *et al.*, 2006; Sanz and Köchling, 2007). Both of these

methods are increasingly being used to determine microbial diversity within environmental samples (Macnaughton *et al.*, 1997; Wang *et al.*, 2006; Sanz and Köchling, 2007). Phospholipid fatty acid analysis (PLFA) is a method that is used to analyse a microbial community for structure and function independently of culturability and viability (Macnaughton *et al.*, 1997; Werker and Hall, 1998; Hill *et al.*, 2000; Smith *et al.*, 2000; Church *et al.*, 2007). It is based on the theory that there are numerous different fatty acids and each is indicative of a specific microbial group (Hill *et al.*, 2000). Although specific fatty acids may be correlated with the presence of some groups of organisms, it might not necessarily be unique to only those specific groups (Hill *et al.*, 2000). Therefore, it is a good method to use in association with 16S based assays (Sanz and Köchling, 2006). It is also described as an effective method to determine functional diversity within a sample because it is affected by low bacterial activities (Pelz *et al.*, 2001) and can also be used to determine the estimated number of viable cells within a sample (Hill *et al.*, 2000; Lei and VanderGheynst, 2000).

Denaturing gradient gel electrophoresis is a genetic fingerprinting technique where each band found may represent a single, dominant species (Sanz and Köchling, 2007; Schwartz *et al.*, 2009). According to Ercolini (2004) and Sanz and Köchling (2007) this is not always the case. Similar positions on a gel could result in similar mobility but may represent different species, whilst single species may have more than one copy of 16S, therefore more than one band could be representative of an individual species (Ranjard *et al*., 2000, Ercolini, 2004). In spite of these infractions, DGGE is still a useful application and is used regularly in different industries, including cooling systems to determine the microbial community structure (Sanz and Köchling, 2007). Denaturing gradient gel electrophoresis is based on DNA extraction, amplification of the nucleic acid by PCR (Muyzer *et al.*, 1993) and separation of the product by electrophoresis (Sanz and Köchling, 2007). The sequences can then be reamplified and data can then be compared to a 16S rDNA database (Gelsomino *et al.*, 1999). The profiles could also be analysed for microbial community dynamics using the Shannon-Weaver index (Zhang *et al.*, 2010).

5.2 AIM AND OBJECTIVES

The aim of this chapter was to determine the functional and structural diversity of both the planktonic as well as the sessile (biofilm) microbial community found within the pilot scale cooling tower system, by making use of culture dependent and culture independent methods. The objectives of this chapter were to:

1. use the plate count method and the MPN technique to determine the microbial levels of different types of microorganisms (IRB; SRB; anaerobic bacteria, aerobic heterotrophic bacteria, *Pseudomonas* spp., fungi and yeasts).
2. determine the structure of the microbial community as well as the biomass of the different groups found within the community by making use of the PLFA method.
3. use DGGE to determine microbial diversity and monitor population dynamics.
4. use SEM to validate results obtained through other methods during the study.
5. use these results to determine the effect of the operational parameters (LFV and COC) on the microbial community structure to ultimately find the optimum parameters that should be used in actual cooling towers.

5.3 MATERIALS AND METHODS

5.3.1 Culture dependent methods (conventional microbiological techniques)

5.3.1.1 Plate count method (Spread plate)

Three different types of agar were used for the plate count method. These included R2A (aerobic heterotrophic bacteria) (Sigma Aldrich, US); King's B Medium (*Pseudomonas* spp.) and Sabouraud Medium (fungi and yeast) (Merck, South Africa). All the types of agar were prepared with distilled water and then autoclaved at 121 °C for 15 minutes. The agar was then allowed to cool to ± 50 °C and then dispensed into sterile petri dishes. Agar plates were then left to solidify. Hundred microliter of diluted sample was added aseptically and spread evenly to cover the surface. Incubation was at room temperature (in order to simulate conditions found within the cooling tower) for a minimum of 24 hours. King's B medium was incubated for 5 days whilst the Sabouraud plates were incubated for 7 days. Only values between 30 and 300 were used for plate counts. Sessile community (biofilm) samples were prepared by scraping the biofilm off a biocell segment with a sterilized spatula and then adding this to sterilised saline solution. A dilution series was prepared to ensure that the values obtained were within the 30 and 300 counts. The planktonic community samples were prepared by taking a sample of circulating water and then diluting this in sterilised saline solution.

5.3.1.2 Most probable number (MPN) technique

Sessile samples were taken by scraping biofilm from the biocells with a sterile spatula. The biofilm was then added to sterile saline solution and a dilution series was prepared. Dilutions of the planktonic samples were prepared by adding circulating water to sterile saline solution. Appropriate liquid media was selected and the dilutions were then added into a test tube containing a specific liquid media. Media used included Modified Postgate medium B (sulphate reducing bacteria) (Church *et al.*, 2007; Winch *et al.*, 2008), B10 broth (iron reducing bacteria) and Thioglycollate medium (Merck, South Africa) (total anaerobic bacteria) (Lutterbach and De França, 1997; Ilhan-Sungur and Çotuk, 2010). Samples inoculated in B10 broth were incubated aerobically at room temperature for two weeks.

Postgate B and Thioglycollate broth samples were incubated anaerobically at room temperature for two weeks. After incubation the pattern of positive and negative tubes was noted, and compared to a standardised MPN table. This table was used to give an estimate of the number of organisms per unit volume of the original sample.

5.3.2 Culture independent methods

5.3.2.1 Scanning electron microscopy (SEM)

Both planktonic as well as the sessile (biofilm) samples were subjected to SEM. The microscope slides that were inserted into the cooling tower at the beginning of each experiment were used to represent the planktonic microbial community. Biocells were used to represent the sessile (biofilm) community. Samples were fixed in 70 % ethanol and processed through an acetone series (at 15 minute intervals) (70 %, 80 %, 90 %, 100 % and 100 %) and then critical point dried with liquid CO_2 and coated with gold/palladium. The samples were then analysed using a FEI Quanta 200 ESEM.

5.3.2.2 Phospholipid fatty acids (PLFA)

Sessile community (biofilm) samples were prepared by scraping the biofilm off of the biocell with a sterilised spatula. The samples were placed into a sterile Falcon tube. The planktonic community samples were prepared by transferring 50 ml of the sump water into a sterile Falcon tube. Samples were frozen and stored at -60 °C until lyophilisation occurred.

5.3.2.2.1 Lipid extraction

A modified version by White and Ringelberg (1998) of the Bligh and Dyer (1959) method was used to extract lipids. After lyophilisation, the dry mass of the samples were taken and the samples were transferred to a 50 ml centrifuge tube. The following was then added to the Kimax tube: 4 ml phosphate buffer; 10 ml methanol and 5 ml chloroform. Samples were then sonicated for 2 minutes and vortexed for 30 seconds after which it was left for 2 – 18 hours and centrifuged at 1800 rpm for a total of 15 minutes. The single phase supernatant was decanted into 50 ml centrifuge tube and 5 ml chloroform added to the original tube. This

was vortexed for 30 seconds and centrifuged at 1800 rpm for 15 minutes. Chloroform was transferred into the pooled (2nd tube) centrifuge tube. Five millilitres (5 ml) of nano-pure water was added and the tube shaken. The tube was left overnight to allow separation of the different phases. After the separation of phases, the samples were centrifuged at 1800 rpm for 15 minutes and the bottom phase transferred with a Pasteur pipette into a 15 ml Kimax tube. The samples were dried under a gentle stream of nitrogen and stored at -20 °C.

5.3.2.2.2 Selective extraction of hydrocarbons

Kimax tubes were removed from -20 °C and 2 ml hexane:chloroform (4:1) and 2 ml nano-pure water was added. Samples were vortexed and centrifuged at 2000 rpm for 5 minutes. The upper phase was removed and transferred to a new Kimax tube. These steps were repeated three times until a recovered volume of 6 ml was reached. The sample was once more dried under a gentle stream of nitrogen and stored at -20 °C.

5.3.2.2.3 Lipid fractionation

Kimax tubes containing 0.5 g silicic acid was dried in an oven at 105 °C for 2 hours. It was allowed to cool in a desiccator, after which 5 ml chloroform was added to the silicic acid tube. This silicic acid mixture was then packed in a column (containing glass wool plug) with the aid of a Pasteur pipette. After packing of the column was completed, the activated silicic acid mixture was flushed with additional 5 ml chloroform as well as 5 ml acetone. The sample was then redissolved with 100 µl chloroform and transferred to the silicic acid column by means of a solvent rinsed glass syringe. This step was repeated three times to ensure that the entire lipid sample was transferred. Fractionation of lipid classes were performed by adding 5 ml chloroform (for neutral fatty acid fraction), 5 ml acetone (for glycolipid fraction) and 10 ml methanol (for the phospholipid fraction. The phospholipid fraction (10 ml methanol) was dried under a gentle stream of nitrogen and stored at -20 ºC.

5.3.2.2.4 Fatty acid methyl ester (FAME) preparation

Phospholipid fractions were removed from -20 ºC storage and 500 µl of both chloroform and methanol was added. One millilitre methanolic KOH (prepared by mixing 0.28 g KOH and

25 ml methanol) was also added to the Kimax tube and vortexed for 30 seconds. The fraction was incubated at 60 ºC for 30 minutes and allowed to cool. Two millilitres hexane was added to the sample and mixed. To this 200 µl 1N glacial acetic acid and 2ml nano-pure water was added. The sample was vortexed for 30 seconds and thereafter centrifuged at 2000 rpm for 5 minutes.

The top organic phase was transferred to a different Kimax tube. Extraction from the bottom phase continued by adding another 2 ml hexane, vortexing for 30 seconds and once again centrifuging the sample at 2000 rpm for 5 minutes. This step was repeated three times. Thereafter the top phase was added to the Kimax tube containing the organic phase and dried under a gentle stream of nitrogen and stored at -20 ºC.

5.3.2.2.5 GC conditions

FAMEs were analysed by capillary gas chromatography with flame ionisation detection on an Agilent 6890 series II gas chromatograph, using a 60 m SPB-1 column (0.250 mm I.D., 0.250 µm film thickness) with the injector and detector maintained at 270 °C and 290 °C, respectively. Hydrogen was used as the carrier gas and sample injection was splitless. The column temperature was programmed to start at 60 °C for 2 min, increased at a rate of 10 °C min^{-1} to 150 °C, then increased at 3 °C min^{-1} to 312 °C. Gas flow was at a constant pressure of 300 kPa. Methyl nonadecanonate (19:0) was used as a quantitative internal standard and definitive peak identification was made for representative samples by gas chromatography/mass spectrometry using an Agilent 6890 series II gas chromatograph interphased with an Agilent 5973 mass selective detector under the same column and temperature programme described. Mass spectra were determined by electron impact at 70 eV (McKinley *et al.*, 2005).

5.3.2.2.6 Data analysis

All samples were analysed in triplicate. Data obtained from GC-MS analysis was used to order to obtain lipid group structure profiles (based on different lipid classes). These profiles were demonstrated as bar graphs in Excel. Furthermore, an RDA ordination diagram was created by making use of Canoco Version 4.5 (TerBraak, 1988). In this particular RDA

diagram the fouling, scaling and corrosion data was combined with the lipid data to demonstrate the reciprocal effect.

5.3.2.3 Denaturing gradient gel electrophoresis (DGGE)

5.3.2.3.1 Sample collection

Both the planktonic as well as the sessile phase samples were collected in duplicate. The planktonic phase samples were obtained by collecting 50 ml sump water in sterile Falcon tubes which were freeze-dried. Sessile phase samples were collected by scraping biofilm from the biocells with the aid of a sterilised spatula. The biofilm was then inserted into a sterile Falcon tube with 10 ml water in order to break up the biofilm and resuspend the organisms to produce a colloidal solution. These samples were also freeze-dried until later use.

5.3.2.3.2 DNA extraction

DNA was extracted by making use of a CTAB-PVP DNA, hot phenol-chloroform-isoamyl alcohol (25:24:1) and salt-ethanol precipitation treatment (Mamlouk *et al.*, 2011). The concentrations and quality (A_{260nm}:A_{280nm} ratios) of the DNA were determined by a NanoDropTM 1000 Spectrophotometer (Thermo Fischer Scientific, US).

5.3.2.3.3 PCR Amplification

An ICycler thermal cycler (Bio-Rad, UK) was used to amplify the DNA. A concentrated PCR master mix which consisted of the following: 2.5 U/µl *Taq* DNA polymerase in 20 mM Tris-HCl, 100 mM KCl, 3.0 mM $MgCl_2$, dNTP mix, final pH 8.3 (20 ºC) (PCR Master; Roche, Germany). In addition to this, Supertherm *Taq* polymerase (1 U/µl) (JM Holdings, UK) $MgCl_2$ (4 mM final) and 50 ng BSA were added to the PCR mixture. After this step, the primers were added to the 100 ng sample DNA for each reaction. All primer sets used in this study were obtained from Inqaba Biotech, SA. Universal eubacterial primer combination (GM5F and 907R) (Inqaba Biotech, SA) was used for the 16S ribosomal DNA (bacterial community). A summary of the primer sets used in the study can be found in Table 5.1.

Cycling conditions were set at 65 ºC for 30 seconds for annealing, 72 ºC for 60 seconds for primer extension and 94 ºC for 30 seconds denaturing. These conditions were repeated for 35 cycles with additional initial denaturing step of 95 ºC for 300 seconds and a final extension that was done at 72 ºC for 300 seconds.

Amplification of the 18S fragments was achieved by using a nested PCR approach. The first combination of primers used was nu-SSU-0017FGC and nu-SSU-1196R (Table 5.1). These primers were used to amplify a 1200 bp fragment. One microliter of this PCR amplicon was then used as a template for the following PCR. The same forward primer (nu-SSU-0017FGC) was used but the reverse primer was substituted for the nu-SSU-0583R (Table 5.1) primer. The second PCR provided 500 bp fragments that would then be used for DGGE analysis. Cycling conditions were set at 60 ºC for 30 seconds for annealing, 95 ºC for 30 seconds for primer extension and 60 ºC for 30 seconds denaturing. These conditions were repeated for 35 cycles with additional initial denaturing step of 72ºC for 60 seconds and a final extension that was done at 72 ºC for 300 seconds.

Table 5.1: Primer sets employed during this study. Primer sets based on Nakagawa *et al.*, 2002 and Muyzer *et al.*, 1993.

Gene	Primer	Primer Sequence
16S rRNA	**GM5F**	5'-CGCCGCCGCGCCCCGCGCCCGTCCCGCCGCCCCCGCCCG CCTACGGGAGGCAGCAG-3'
	907R (506 bp)	5'-CCGTCAATTCCTTTGAGTTT-3'
18S rRNA	**nu-SSU-0017FGC**	5'-CGCCCGCCGCGCGCGGCGGGCGGGGCGGGGGCACGGGGGGCC AGTCATATGCTTGTC-3'
	nu-SSU-1196R	5' -TCTGGACCTGGTGAGTTTCC-3'
	nu-SSU-0583R	5' -GAATTACCGCGGCTGCTGGC-3'

*** Underlined base pairs constitute the GC clamp.**

5.3.2.3.4 Agarose gel electrophoresis

The success of the PCRs (Section 5.3.2.3.3) were determined by electrophoresis. Electrophoresis was conducted in an IBI electrophoresis system model MP 1015 (Shelton Scientific, USA). A one percent (w/v) agarose gel prepared in 1 x TAE buffer (20mM Glacial Acetic acid (Merck, US), 40mM Tris (Sigma Aldrich, US) and 1mM EDTA (Merck, US), pH 8.0) was used. The gel contained 10 mg/l ethidium bromide for visualisation of the bands. Electrophoresis conditions were set at 80 V for 120 min using 1 x TAE as electrophoresis buffer. A Gene Genius Bio Imaging System (Syngene, Synoptics UK) was used to capture the image using GeneSnap (version 6.00.22) software. Analysis of images was done by making use of GeneTools (version 3.00.22) software (Syngene, Synoptics, UK) in order to determine the relative intensities of the bands in each lane.

5.3.2.3.5 Denaturing Gradient Gel Electrophoresis (DGGE) Analysis

Denaturing gradient gel electrophoresis (DGGE) was done using a DCode Universal Mutation Detection System (Bio-Rad, UK). Six percent (w/v) polyacrylamide gel was used for electrophoresis. The electrophoresis process was at 60 ºC, 100V for 16 hours. A 30 – 60 % denaturing gradient was used for 16S and a 20 – 50 % denaturing gradient was used for the 18S samples. Staining was done using 1 x TAE containing ethidium bromide (10 µg/ml) (Bio-Rad, UK) for visualisation of bands using the Bio-Rad DGGE manual.

5.3.2.3.6 Statistical analysis of DGGE profiles

A Gene Genius Bio Imaging System (Syngene, Synoptics, UK) and GeneSnap software (version 6.00.22) were used for visualisation of the DGGE fingerprints obtained. The community structure of each sample was determined by selecting the first single band in each gel as reference band. This band was then allotted an arbitrary quantity value. The relative quantities of the other bands were then normalised in relation to the quantity of the reference band. The DNA quantity of each band was then plotted in relation to their Rf distances along the DGGE gel to determine the microbial community structure of each sample. Structural diversity of both the bacterial as well as the fungal communities was calculated by using the Shannon-Weaver general diversity index:

$$H' = -\sum_{i=1}^{s} p_i \ln p_i$$

H was calculated on the basis of the bands on the gel lane by using the relative intensities of the bands. Pi is the relative probability of the bands in a lane. The relative probability (Pi) was calculated as:

$$Pi = n_i/N$$

Where n_i is the relative intensity of a band and N is the sum of all the relative intensities within a lane (Lagacé *et al.*, 2006; Zhang *et al.*, 2010).

5.4 RESULTS AND DISCUSSION

Operating conditions (favourable temperature, high residence time, large submerged surface area and concentrated nutrients) found in recirculating cooling tower systems, can result in large quantities of microbial growth (Choudary, 1998; MacDonald and Brözel, 2000; Videla, 2002; Ludensky, 2003). According to Rochex *et al.* (2008), formation of thick biofilms can be counteracted by increasing the linear flow velocity (LFV) of a cooling system. This would then lead to improved mass transfer within the system. The flow rate and water chemistry can also influence the type of biofilm formed on the submerged surfaces (Almeida and de França, 1998).

5.4.1 Culture dependent methods (Plate count method and MPN)

The combined plate count and MPN results for the planktonic and sessile samples are found in Figures 5.1 and 5.2, respectively. From these figures it is apparent that, according to the conventional microbiological techniques, the microbial communities were dominated by heterotrophic aerobic bacteria and *Pseudomonas*. Large quantities of fungi were also found at experiments which were operated at lower LFV (experiment 1 and 5 at 0.6 m/s LFV and experiment 2 at 0.9 m/s LFV).

In Figure 5.1 and 5.2 it is demonstrated that the amount of SRB's was generally higher in the planktonic phase than in the sessile phase, except for esperiment 5. The highest SRB count found within the planktonic phase samples occurred at experiment 3 (2 COC, 1.2 m/s LFV). This might be due to the high LFV (1.2 m/s) which could be responsible for removal of SRB's from the biofilm (Rochex *et al.*, 2008). A study done by Rochex *et al.* (2008) on the role of shear stress on the composition and diversity of biofilm bacterial communities using a Conical Couette-Taylor Reactor, found that increased flow velocities results in increased detachment of microorganisms. This is turn results in more compact biofilms with lower diversity. On the other hand, low fluid velocity may promote the formation of biofilm by deposition of suspended materials (Anon, 1994). Sulphate reducing bacteria counts from the sessile samples were the highest during experiment 5 (4 COC, 0.6 m/s LFV). Previous research done by Peng and Park (1994) on the influence of SRBs in aquatic systems on the electrical mechanisms of corrosion found that high sulphate levels may be an indication of SRB participation and could lead to higher corrosion rates. Lutterbach and De França (1997) found the same trend in their study on the formation of biofilms and the variation in the biofilm community in cooling systems fed with seawater. In the present study this was also found in experiment 5 (sessile sample) (Figure 5.2), where a high level of sulphate was found within the cooling water (907.51 mg SO_4/L – Figure 4.2).

A study by Herrera and Videla (2009) compared the corrosive properties and protective effect that IRB within a biofilm may have. Iron reducing bacteria may promote corrosion by reductively dissolving the protective ferric oxide coat that forms on steel surfaces (Peng and Park, 1994; Neria-González *et al.*, 2006). Inhibition of corrosion by IRB's within biofilm might be due to the EPS which may act as a barrier between the metal and the environment (Dubiel *et al.*, 2002; Herrera and Videla, 2009). Species of iron respiring bacteria that generally occurs in cooling water systems are *Gallionella* sp., *Shewanella oneidensis* and *Arthrobacter* (Lutey, 1996; Herrera and Videla, 2009). The bacterial counts for the IRB of the planktonic community (Figure 5.1) and the sessile community (Figure 5.2) follows a similar trend. The highest bacterial counts were found during experiment 3 (2 COC, 1.2 m/s LFV) and then at experiment 2 (3 COC, 0.9 m/s LFV). Whenever non-limiting biofilm growth conditions are present, detachment and biomass accumulation will increasingly occur (Cresson *et al.*, 2006). The ratio of IRB to SRB is also higher during these 2 experiments (Experiments 2 and 3). According to studies done by McLeod *et al.* (2002), facultative anaerobic IRB can successfully out-compete SRB within a microbial community.

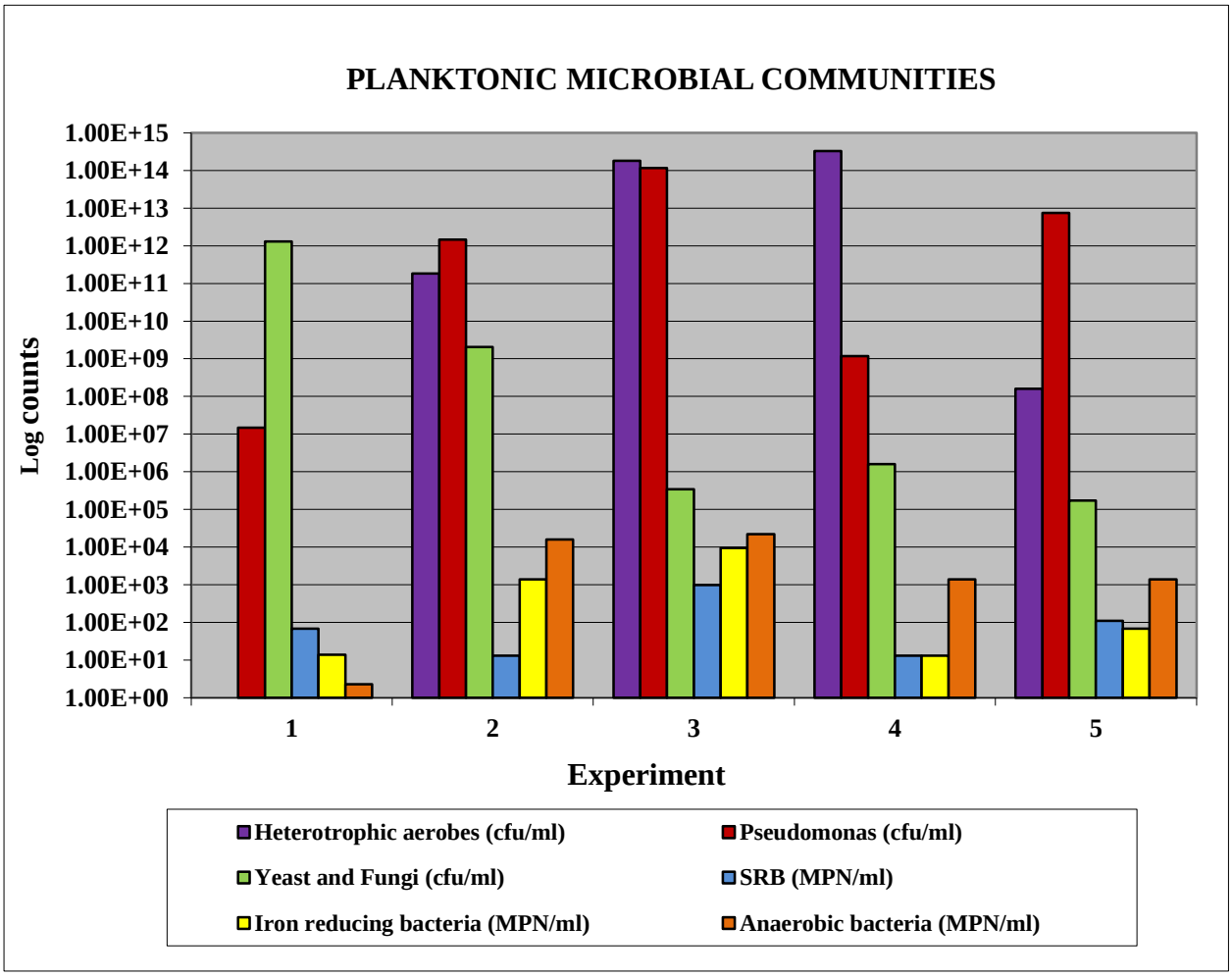

Figure 5.1: Bar chart illustrating log counts of the planktonic microbial communities enumerated by making use of the plate count method as well as the MPN technique.

Pseudomonas sp. which is a common slime-forming microorganism that can be found within all industrial systems, including cooling towers (Viera *et al.*, 1999; McLeod *et al.*, 2002). These organisms occurred abundantly throughout all experiments and also in both phases (planktonic and sessile).

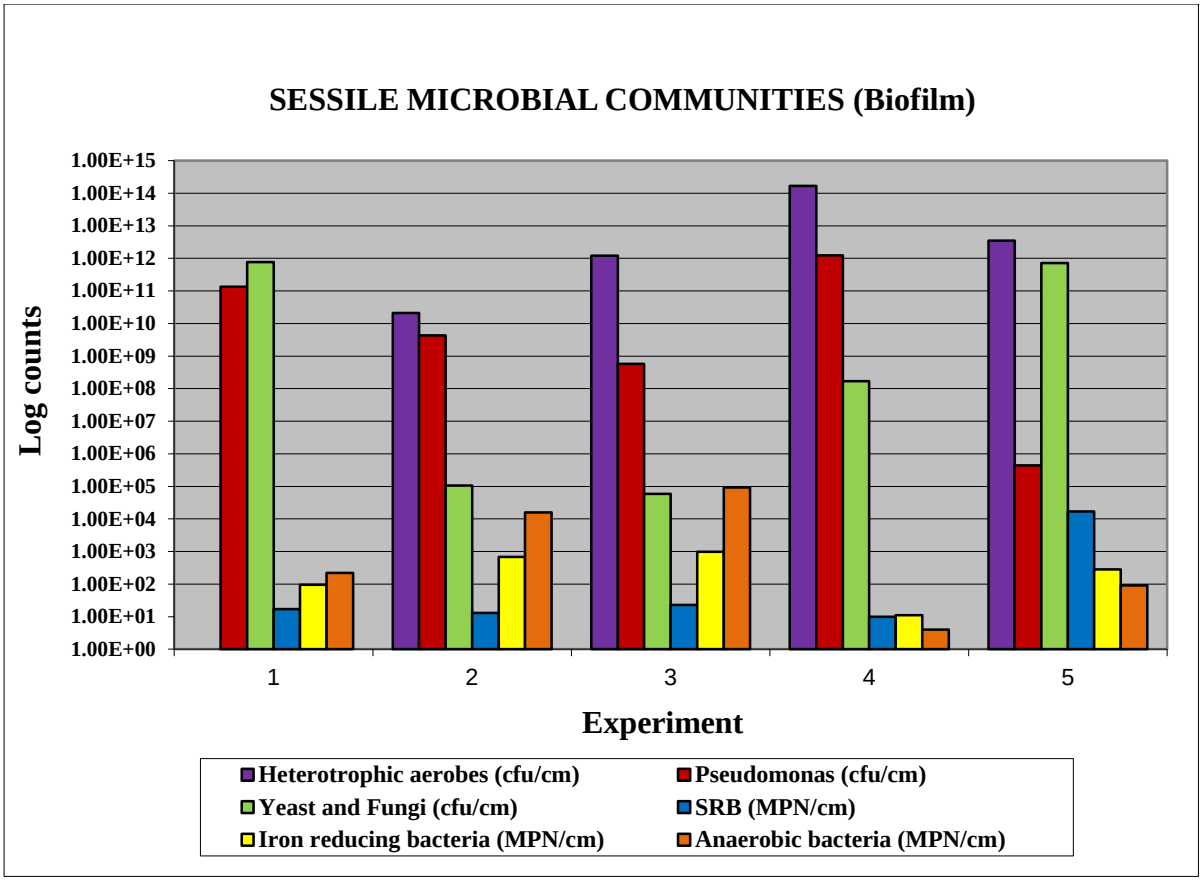

Figure 5.2: Bar chart illustrating log counts of sessile (biofilm) microbial communities enumerated by making use of the plate count method as well as the MPN technique.

Heterotrophic aerobes were the most dominant group found in all the samples apart from experiment 1. This may be ascribed to the fact that aerobic bacteria have a higher growth rate compared to anaerobic bacteria (Brözel *et al.*, 1997). From Figure 5.1 it is clear that the highest heterotrophic aerobes in the planktonic samples were found during experiment 3 and 4 (both was run at 1.2 m/s LFV, and COC of 2 and 4, respectively). Sessile heterotrophic aerobic bacterial counts were also the highest during experiment 4. This is in accordance with the fouling rate results from Table 4.4, where experiment 4 had the highest fouling rate observed during this study. Coincidently these experiments (Experiments 3 and 4) were also the two experiments with the highest COD removal rate (Table 4.5). A COD removal rate of 89.35 % was reported for experiment 3 and 80.89 % for experiment 4.

Yeast and fungi were also well represented throughout the planktonic and sessile samples during this study (Figure 5.1 and 5.2). The highest yeast and fungal counts in the planktonic samples were observed during experiment 1 (2 COC, 0.6 m/s LFV), followed closely by

experiment 2 (3 COC, 0.9 m/s LFV). This would indicate that fungi and yeast preferred lower fluid velocity. The results in Figure 5.2 is demonstrating that the sessile samples where the highest fungi and yeasts counts were found are for experiments 1 (2 COC, 0.6 m/s LFV) and 5 (4 COC, 0.6 m/s LFV).

Conventional microbiological techniques used in the present study illustrated that heterotrophic aerobic bacteria dominated the microbial communities within the planktonic and the sessile samples. Increased LFV resulted in higher heterotrophic aerobic counts. High fungal counts were found at the sessile samples with low LFV (experiments 1 and 5).

5.4.2 Culture independent methods: SEM results

Scanning electron microscopy is a useful tool that can be used to witness bacterial adhesion to surfaces, thus verifying actual biofilm formation (Lagacé *et al.*, 2006; Ilhan-Sungur and Çotuk, 2010). It can also be used to show different cell morphologies found within a specific sample (Neria-González *et al.*, 2006), and give an indication of the microbial diversity found within a specific community (Chongdar *et al.*, 2005). Figures 5.3 -5.7 show SEM images of the planktonic phase (A), and the sessile phase (B) of each experiment during this study. The planktonic phase represents organisms found on the glass microscope slides that occur in the spray zone of the lab scale cooling towers. Biocells were cut in half to represent the microbial community found in the sessile phase.

In Figure 5.3 (A+B), the high microbial biomass of both the planktonic as well as the sessile samples can be seen. Bacterial cell morphologies that were observed in the planktonic phase sample (Figure 5.3; A), included cocci and bacilli shapes. There were also yeast cells visible in the planktonic sample. The sessile community (Figure 5.3; B) consisted of a very thick multilayered biofilm, contained within a thick EPS matrix that also shows the typical distribution channels found in biofilms (Tanji *et al.*, 1999). These channels facilitate the movement of liquid, nutrients and oxygen within a biofilm, thus creating micro niches that enable aerobic as well as anaerobic microbial growth. The cells found within the sessile sample are clustered together to such an extent that identification of different cell morphologies was difficult. There were however, cocci and bacilli shaped cells visible. The thick EPS matrix shown in Figure 5.3 (B), might explain the differences in the heterotrophic

anaerobes count shown in Figure 5.1 and 5.2, where the sessile sample contained higher counts of these organisms.

A)

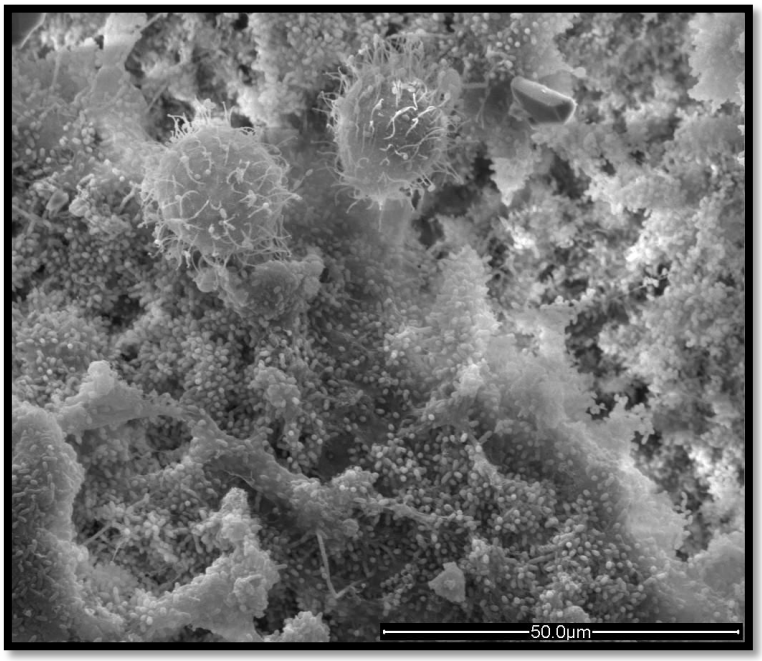

B)

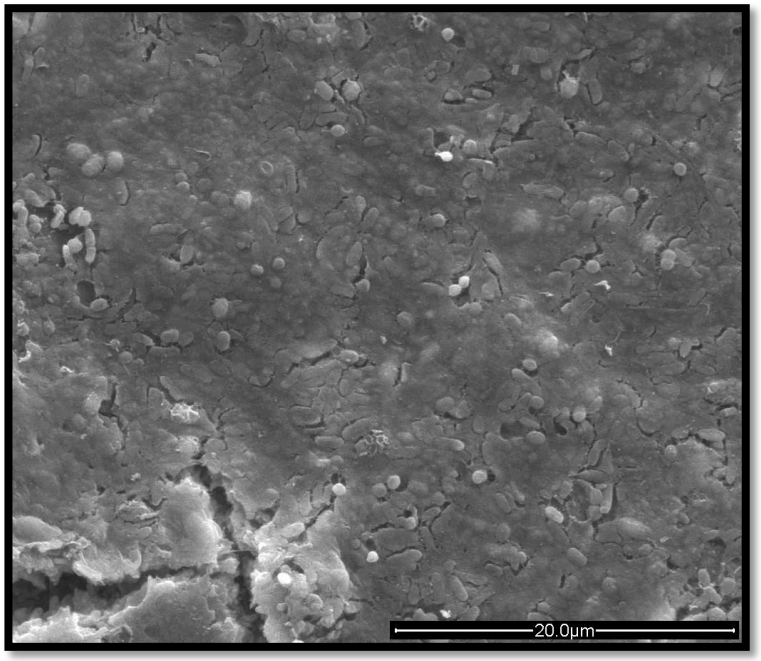

Figure 5.3: Scanning electron micrograph of the planktonic as well as the sessile (biofilm) phase of experiment 1 (2 COC and 0.6 m/s LFV). A) Planktonic phase (2 500x magnification), and B) Sessile phase (biofilm) (6 000x magnification).

Single cells as well as cells that formed part of a micro colony were found during the planktonic phase of experiment 2 (Figure 5.4 A). Once again (as in Figure 5.3 A), cocci,

bacilli and singular yeast cells were present within the planktonic phase. Scanning electron micrograph of the biocell (Figure 5.4 B) shows the thickness and complete coverage of the biofilm found within the biocell. Gaps within the biofilm might be caused either by the detachment of cells or it might just be distribution channels (Viera *et al.*, 1999).

A)

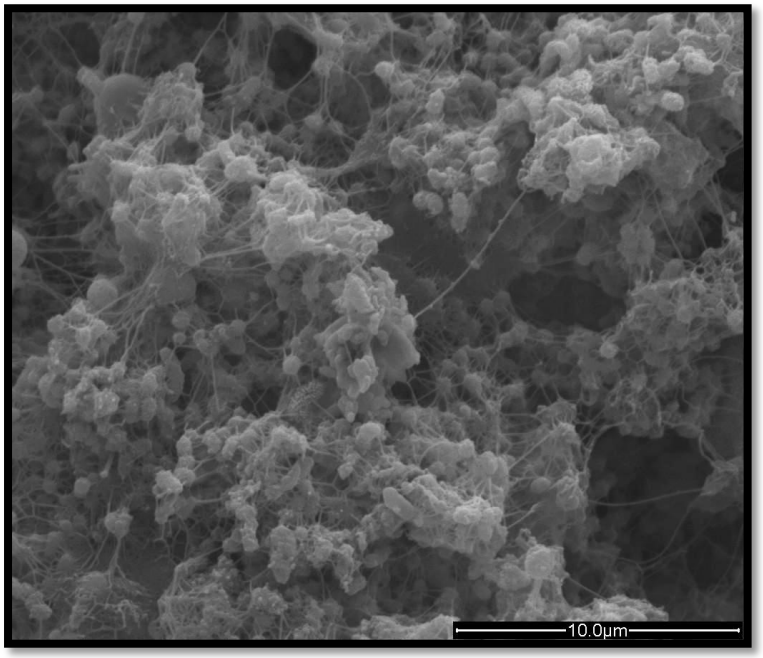

B)

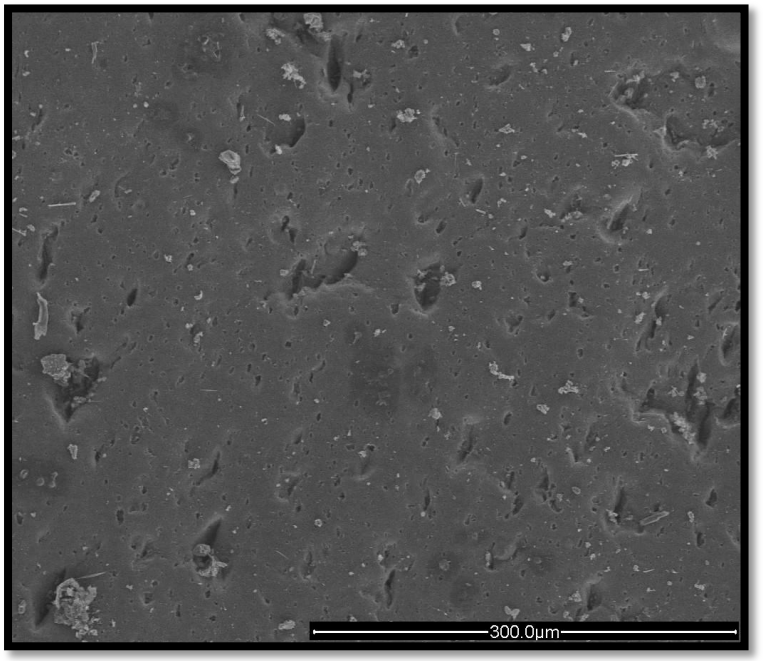

Figure 5.4: Scanning electron micrograph of the planktonic as well as the sessile (biofilm) phase of experiment 2 (3 COC and 0.9 m/s LFV). A) Planktonic phase (10 000x magnification), and B) Sessile phase (biofilm) (500x magnification).

A)

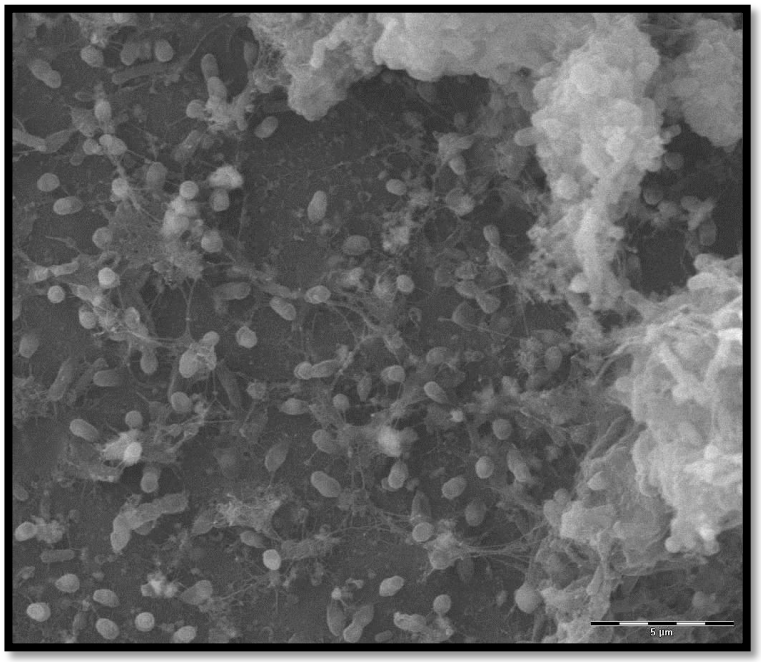

B)

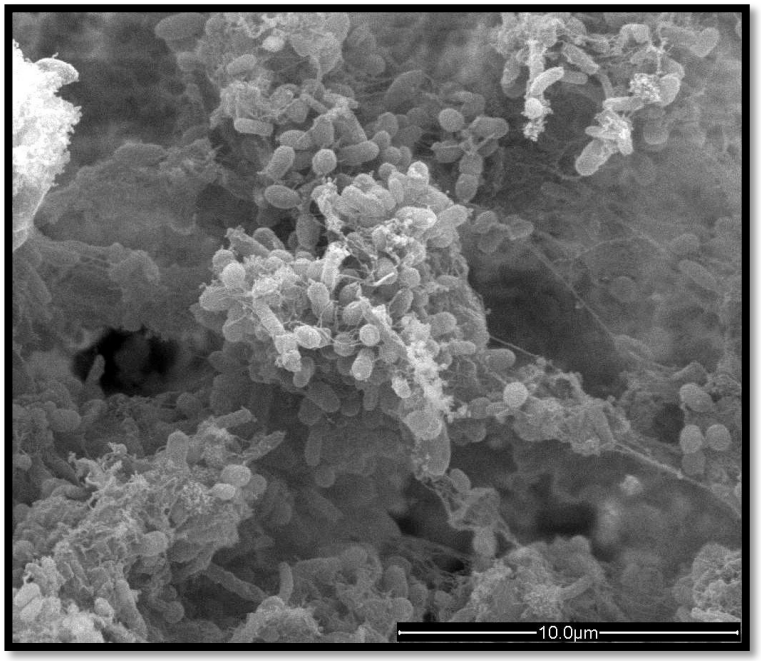

Figure 5.5: Scanning electron micrograph of the planktonic as well as the sessile (biofilm) phase of experiment 3 (2 COC and 1.2 m/s LFV). A) Planktonic phase (10 000x magnification), and B) Sessile phase (biofilm) (12 000x magnification).

From Figure 5.5 (A), the same cell morphologies as in experiment 1 and 2 can be seen. The sessile sample (Figure 5.5; B) shows a multilayer heterogeneous biofilm consisting of bacilli, cocci as well as vibrio cell morphologies. Extra polymeric substances (EPS) matrix can be seen, with some microbial cells distributed within this matrix.

A)

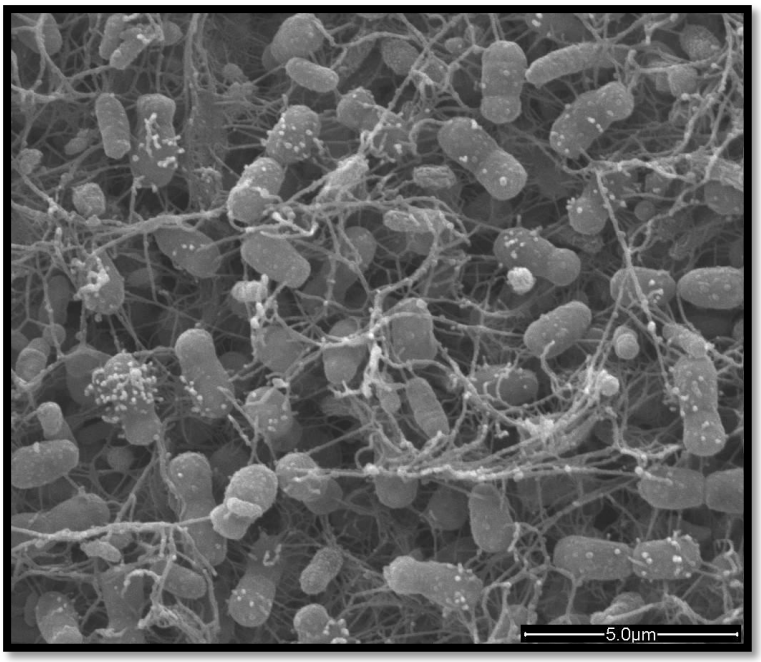

B)

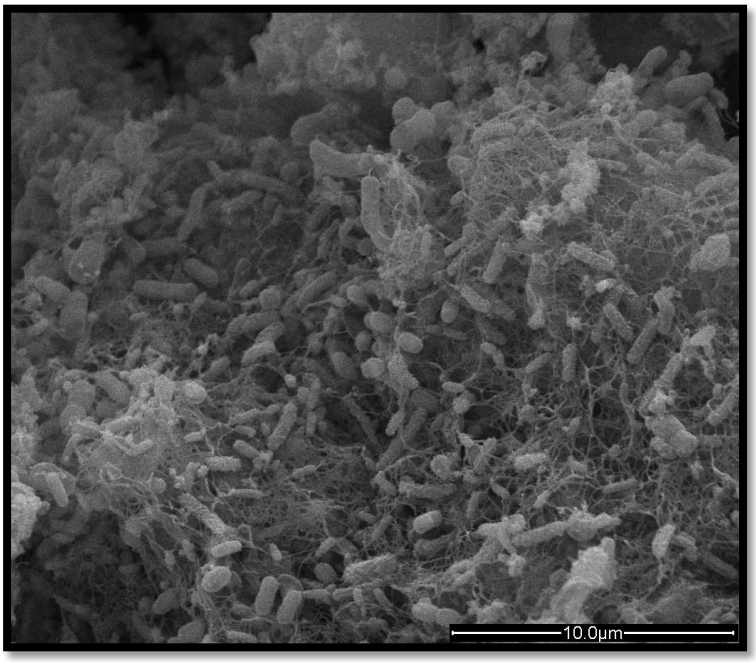

Figure 5.6: Scanning electron micrograph of the planktonic as well as the sessile (biofilm) phase of experiment 4 (4 COC and 1.2 m/s LFV). A) Planktonic phase (15 000x magnification), and B) Sessile phase (biofilm) (10 000x magnification).

By comparing Figure 5.6 (A and B) with previous images shown (Figure 5.3 – 5.5), it is evident that there were more bacilli shaped cells rather than cocci shaped cells. This is especially true for the micrograph of the sessile community (Figure 5.6; B). Experiment 4 (as well as experiment 3) had the highest fouling rates according to the results from Table 4.4.

There is a high amount of slime present within the biofilm (Figure 5.6; B) which could be used to support the results found in Table 4.4.

A)

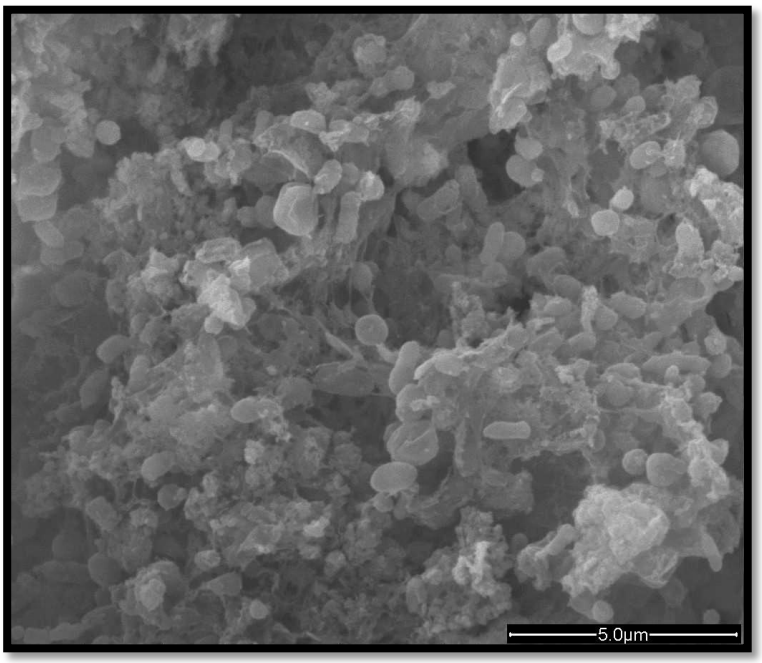

B)

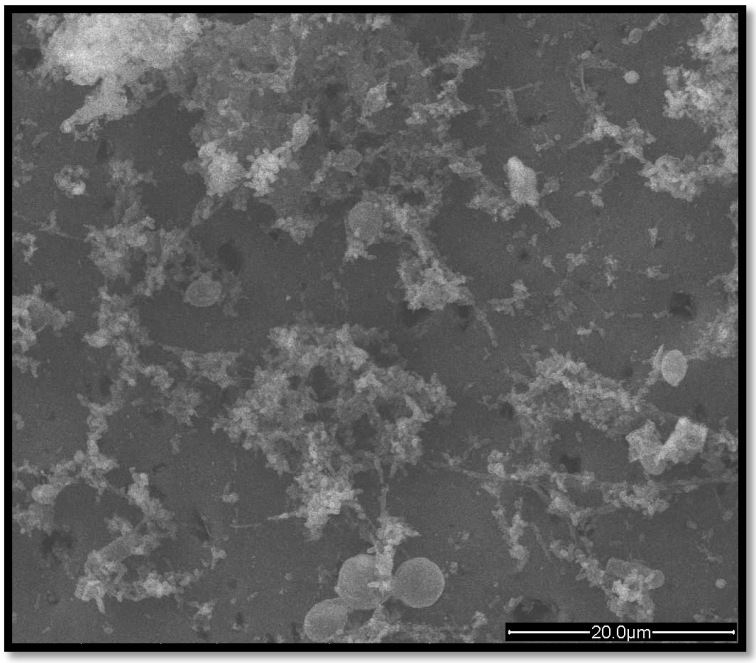

Figure 5.7: Scanning electron micrograph of the planktonic as well as the sessile (biofilm) phase of experiment 5 (4 COC and 0.6 m/s LFV). A) Planktonic phase (16 000x magnification), and B) Sessile phase (biofilm) (4 000x magnification).

The microbial cell morphology from Figure 5.7 (A) was similar to previous planktonic samples (Figure 5.3-5.6) where cocci and bacilli shaped cells are visible. There are also some yeast cells visible. The cell morphology of organisms found within the biofilm (Figure 5.7; B) was difficult to identify because of the thick EPS matrix where these organisms are embedded in. There are also large circular structures (± 10 µm) visible that are potentially biological.

Scanning electron microscopy results for this study supported the results from the conventional microbiological techniques, where Figure 5.6 (A and B) illustrated an increase in bacilli shaped cells as well as an increased amount of slime in the planktonic and sessile samples. Experiment 4 also had the highest heterotrophic aerobic bacterial counts (planktonic and sessile samples). Also, in Chapter 4 (Table 4.4), experiment 4 had some of the highest fouling rates observed during this study. It also supported the fact organisms found within the sessile samples were indeed found within a biofilm community.

5.4.3 Culture independent methods: PLFA results

During this study, three distinct groups of PLFAs were obtained; (i) normal saturated fatty acids (Nsats), (ii) monounsaturated fatty acids (Monos) and (iii) polyunsaturated fatty acids (Polys). Nsats are a general microbial biomarker found in prokaryotic and eukaryotic kingdoms, whilst Monos represent Gram negative bacteria. Yeast and fungi are presented by Polys (McKinley *et al.*, 2005; Church *et al.*, 2007).

A bar chart representing the results from the GC profile obtained is shown in Figure 5.8. This figure (Figure 5.8) represents the microbial community structure results for both phases (planktonic and sessile), as determined through GC analysis, during each experimental run. The major phospholipid fatty acid groups found within each community (sample) is indicated as a percentage of the total microbial community.

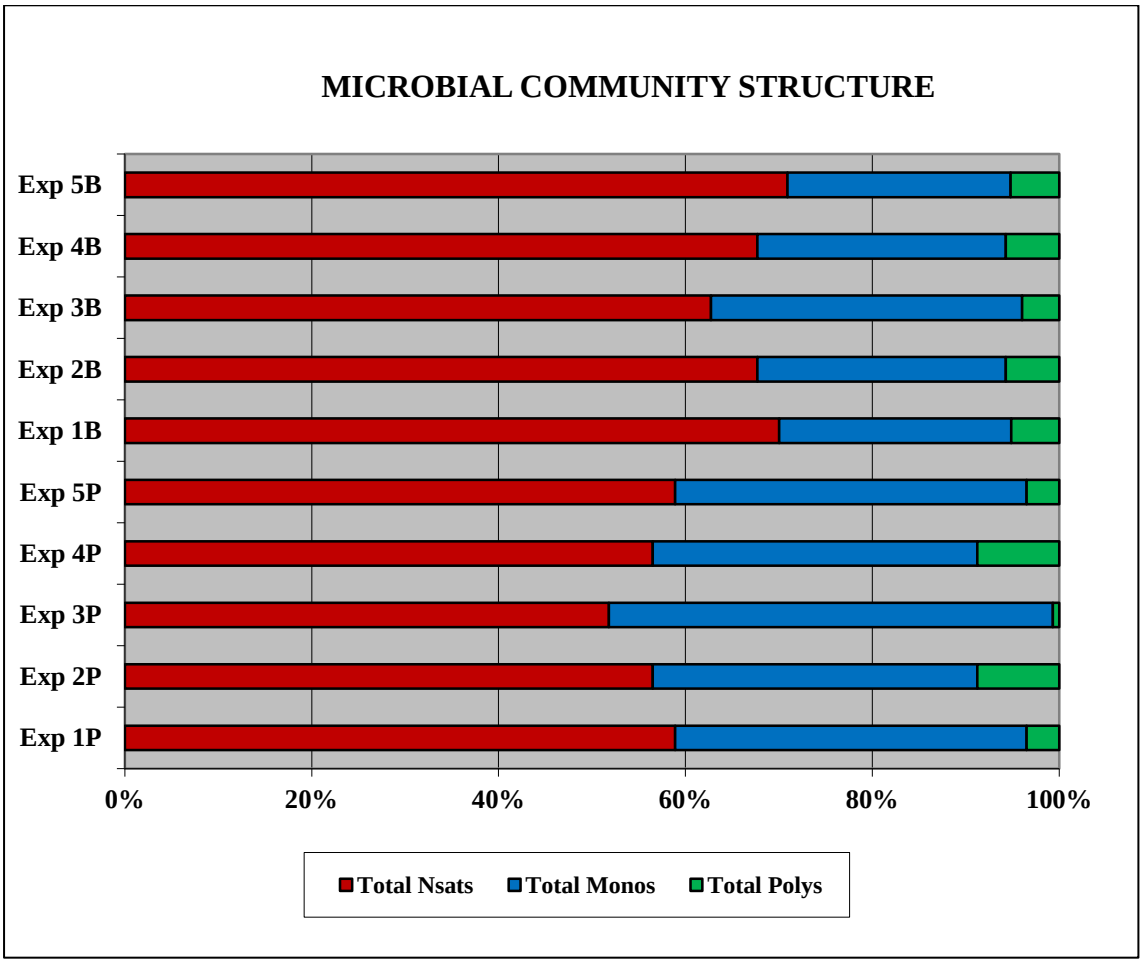

Figure 5.8: Microbial community structure on the basis of the mol percentage fraction of the major phospholipid fatty acid groups that was found during the different experimental runs of this study.

In Figure 5.8 it is demonstrated that during all experimental runs the Nsats contributed the most (more than 50 %) to the microbial community in both planktonic and sessile phases. This was expected as Nsats is the general microbial biomarker for prokaryotic and eukaryotic organisms (McKinley *et al.*, 2005). Gram negative bacteria (shown as Monos, Figure 5.8) had the next highest percentage contribution towards the microbial communities of each experiment. Fungi and yeast (Polys) made up a smaller proportion of the community of microorganisms found throughout the study and ranged between 1 % and 9 % of the total microbial community. In all the samples, bacterial groups dominated the system by making up more than 90 % of the microbial community. The planktonic sample from experiment 3 (2 COC and 1.2 m/s LFV) contained very little fungi within the sample. This is in accordance with the data obtained through conventional microbiological techniques (Figure

5.1), where experiments 3P and 5P had the least amount of fungi and yeast cells. Experiment 1 and 5 was operated at the same low LFV (0.6 m/s) and at 2 and 4 COC, respectively. Planktonic and sessile community structures at experiments 1 and 5 were similar. This leads to the deduction that LFV (as operational parameter) had a greater effect on microbial community structure than COC. However, experiments 2 and 4 (Figure 5.8) was operated at different LFV (0.9 and 1.2 m/s, respectively), but the COC of both experiments was high (3 and 4 COC, respectively). In this case the microbial community structures were similar to each other, demonstrating that COC also had an effect. A study by Rochex *et al.* (2008) also found that higher hydrodynamic stress (which includes fluid velocity) resulted in definite changes within the microbial community structure.

Total estimated viable biomass (pmol/g) of each sample was determined and can be seen in Figure 5.9. According to the results from Figure 5.9, the highest viable biomass was found in the sessile samples from experiments 1 and 5. Both experiments were operated at very low LFV (0.6 m/s). This may be attributed to the fact that lower LFV facilitates the formation of biofilm (Anon, 1994). Also during these experiments (1 and 5), the planktonic communities had the lowest viable biomass found during this study. Studies done by Ilhan-Sungur and Çotuk (2010) on biofilm communities within recirculating cooling tower systems showed that some types of bacteria grow faster within a biofilm than in bulk water. This could explain the higher biomass found within the biofilm. According to conventional microbiological techniques (Figure 5.2) the highest fungal counts were found during these experiments (1 and 5), suggesting that under low fluid velocities, fungi might grow faster than other microorganisms within biofilms.

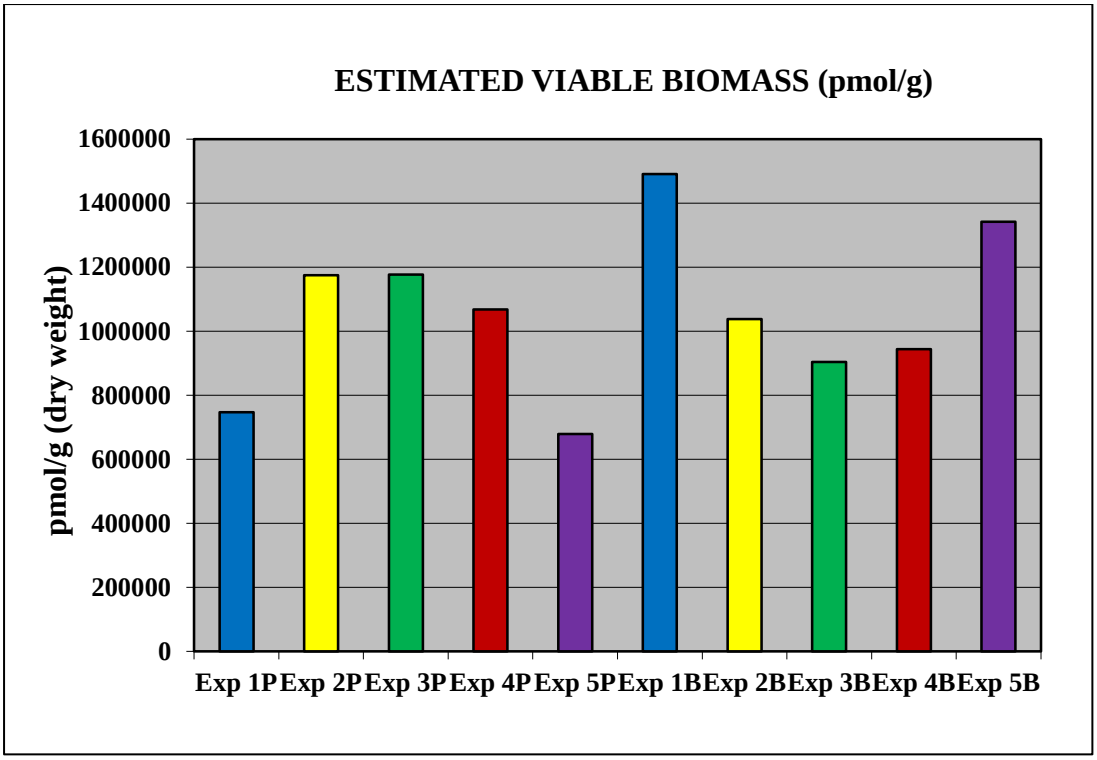

Figure 5.9: Estimated viable biomass (pmol/g) of the planktonic and sessile (biofilm) phases during the different experimental runs. Key: Exp. 1 = 2 COC, 0.6 m/s; Exp. 2 = 3 COC, 0.9 m/s; Exp. 3 = 2 COC, 1.2 m/s; Exp. 4 = 4 COC, 1.2 m/s; Exp. 5 = 4 COC, 0.6 m/s. P = Planktonic; B = Sessile.

Planktonic communities from experiments 2, 3 and 4 had a higher viable biomass than the sessile communities from the same experiments. These experiments were operated at higher LFV (0.9 – 1.2 m/s). This might be due to two different scenarios: 1) the fact that high LFV deters biofilm formation (Bott, 1998), or 2) an increase of the biofilm cohesion strength in response to high detachment caused by the high fluid velocity (Rochex *et al.*, 2008). Biomass does not necessarily affect the corrosion rate of steel surfaces, but rather the composition of the sessile community found adhering to the steel surfaces play an important role with regard to corrosion rates (Jack *et al.*, 1992; Angell *et al.*, 1997). This was mirrored in the results found when comparing the data from Table 4.4 to the data from Figure 5.8 and 5.9. The highest overall biomass (Figure 5.9) was found at experiments 1 and 5. When these data sets are compared to corrosion data from Table 4.4, it is evident that the lowest corrosion rates were found during these experiments (experiments 1 and 5). Also, microbial community structures that were similar (Figure 5.8), had more or less the same corrosion rates (Table 4.4), for example experiments 1 and 5, or experiments 2 and 4 (Figure 5.8). This suggests that community structure rather than biomass affected the corrosion rate.

An RDA ordination was done (Figure 5.10) to demonstrate the correlation between the different PLFA groups found during the various experiments, in relation to the fouling, scaling and corrosion rates as discussed in Section 4. During this study, COC and LFV were the major parameters evaluated. The RDA ordination (Figure 5.10) distinguished the various experimental runs as separate and distinct groupings. Both the major parameters (COC and LFV) establish a gradient in the groupings observed. In the correlation matrix from the ordination, LFV had the highest correlation (77 %) to the first ordination axes of all the parameters used. The COC correlation matrix showed the highest correlation (60.8 %) with the second ordination axis. Thus, LFV as a parameter had a greater influence on the observed PLFA groupings and COC to a lesser degree. The Monte Carlo permutation test, the test of significance for all the canonical axes, had a p-value of 0.002. This indicates that the variation captured by the ordination is statistically significant ($p \leq 0.05$).

The DO value in the sump correlated with the biomarkers for the planktonic organisms. This was expected since microorganisms found within the bulk phase of the cooling water are mostly aerobic. On the other hand, biofilm creates an environment for the sessile microorganisms where both aerobic and anaerobic conditions are present (Lutterbach and De França, 1997; Viera *et al.*, 1999, Keresztes *et al.*, 2001). Linear flow velocity (LFV) correlated with the planktonic microbial community and to a lesser degree with the biomarkers observed in the sessile community (biofilm). According to studies done by Rochex *et al.* (2008) on the effect of hydrodynamic forces on the diversity, composition and dynamics of biofilm communities, higher LFV might lead to a decrease in biofilm diversity but an increase in microbial growth rate.

Cycles of concentration (COC) showed correlation with the scaling observed for mild steel as well as stainless steel (corrosion coupons and heat exchanger tubes). An increase in COC resulted in higher mineral ions within the cooling tower than in the make-up water which in turn can lead to higher scaling rates within the system (Lee and Young, 2002).

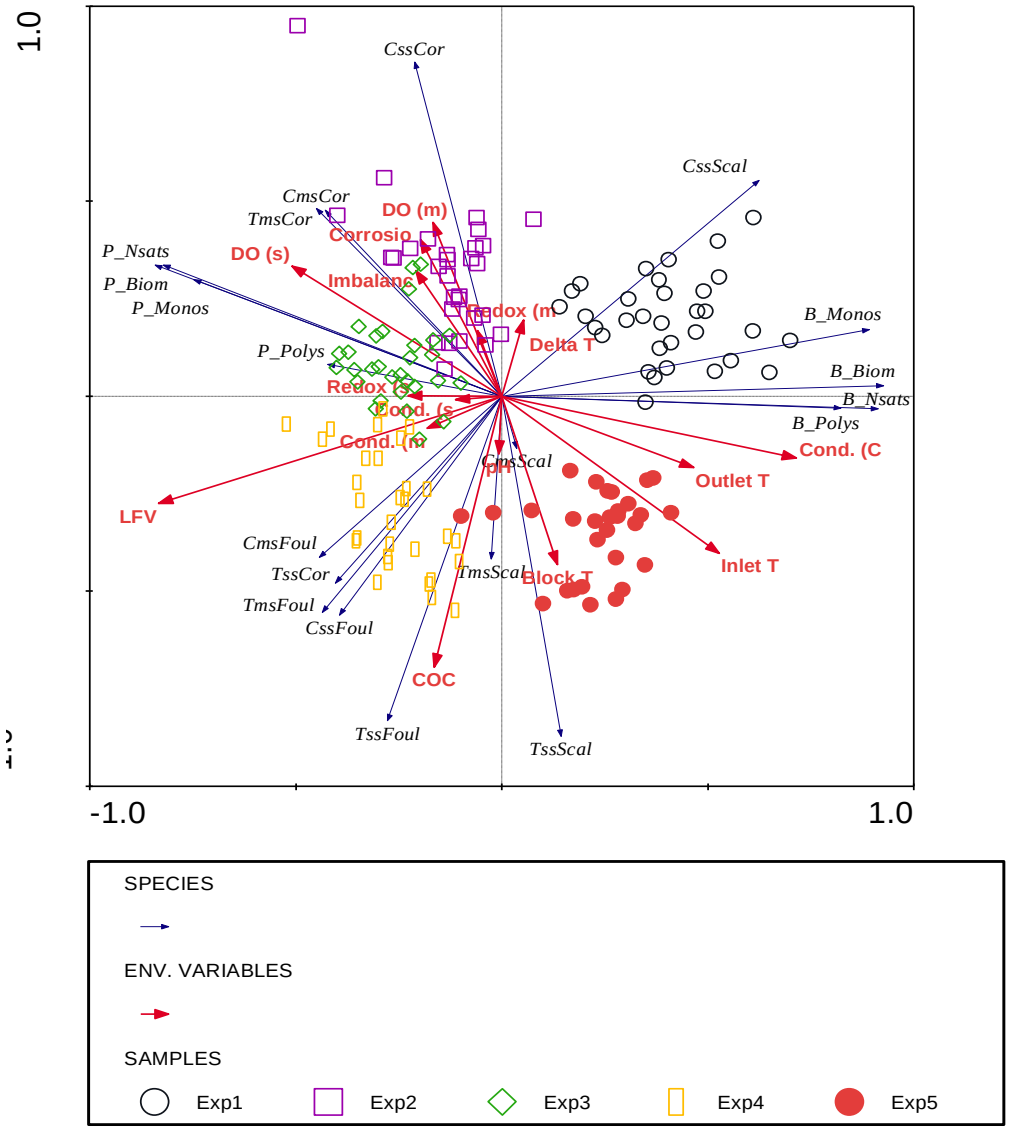

Figure 5.10: Redundancy analysis (RDA) ordination of the physical-chemical data and the observed fouling, scaling, corrosion and PLFA profiles for the various experiments. Eigen values for the first two axes are 0.346 (34.6 %) and 0.226 (22.6 %) respectively.

5.4.4 Culture independent methods: DGGE results

Denaturing gradient gel electrophoresis is one of the most broadly used molecular techniques in the study of microbial communities. It is useful to monitor changes within microbial communities (Sanz and Köchling, 2006). During this study, individual bands found during DGGE were used to provide relative abundance of melting types (Operational Taxonomic units or species) found.

5.4.4.1 DNA concentrations

The quality and concentration of DNA was determined spectrophotometrically, by calculating the A_{260}:A_{280} ratios with the use of a NanoDropTM 1000 Spectrophotometer (Thermo Fischer Scientific, US). An A_{260}:A_{280} of 1.8 – 2.1 was considered acceptable for PCR-based procedures (Neria-González *et al.*, 2006). In the present study the A_{260}:A_{280} ratios were found to be between 1.42 and 1.83, whilst the average for DNA concentration was 1 302.52 ng/µl.

5.4.4.2 PCR and DGGE analyses

Extracted DNA from the planktonic and sessile samples was subjected to PCR as described in Section 5.2.2.3.4. Electrophoresis was done on a 1 % agarose gel to determine whether PCR amplification was successful and to confirm the amplified fragment sizes.

The amplified microbial community 16S rDNA gene fragments are shown in Figure 5.11 (A and B). From the images (Figure 5.11) it is evident that the planktonic (P) as well as the sessile (B) samples amplified successfully. The size of the amplified microbial community 16S rDNA gene fragments (Figure 5.11) was ± 550 base pairs.

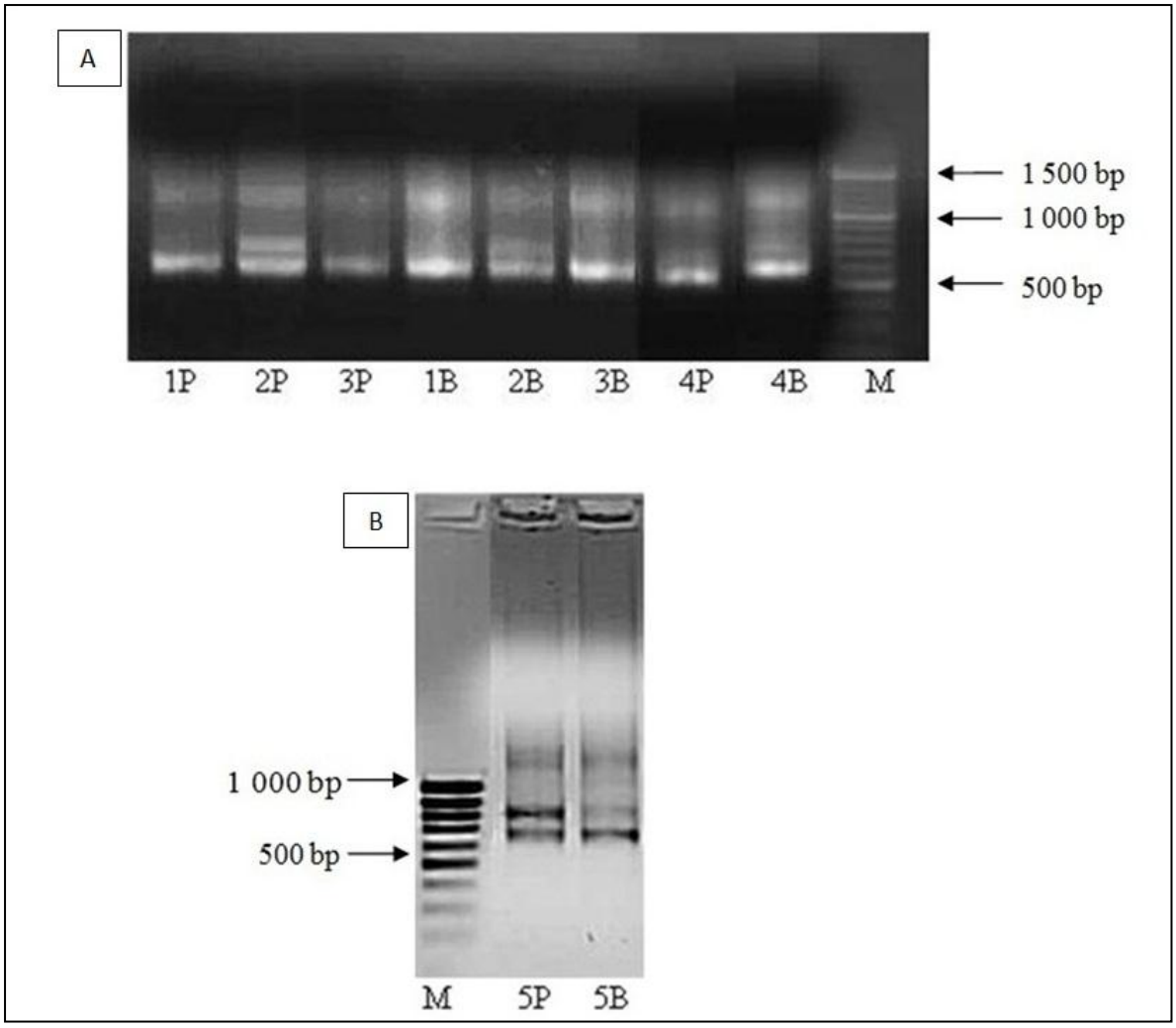

Figure 5.11: Examples of agarose gel of the amplified microbial community 16S rDNA gene fragments. A) 16S rDNA gene fragments for experiments 1 – 4 (planktonic and biofilm). This represent an ethidium bromide stained gel. B) 16S rDNA gene fragments for experiment 5 (planktonic and biofilm). This represents a negative image of an ethidium bromide stained gel.

5.3.3.3 Community profile analysis (DGGE)

In this study number of bands and percentage contribution to each profile was determined and results presented in Figures 5.12 and 5.13. The PCR amplified 16S rDNA planktonic samples from experiments 3 and 5 did not provide analysable profiles and are thus not included in Figures 5.12 and 5.13.

There were a total of 11 band positions and most of these were in the higher denaturant concentration area of the gel. By comparing the profiles from Experiments 1, 2 and 4 (Figure 5.12) it is evident that there were distinct differences in community structure. All of the 11 bands found during 16S rDNA DGGE were present in the sessile samples, whilst the planktonic samples contained only 5 of the 11 possible bands. Band 6 was present during all the experiments (planktonic and sessile phases) apart from the sessile samples from experiment 2 and 4 both experiments was run at higher LFV (0.9 and 1.2 m/s, respectively) and higher COC (3 and 4 COC, respectively). Band 2 was present in all the sessile samples except at experiment 3B (2 COC, 1.2 m/s LFV). The sessile samples from experiment 4 and 5 had a completely different bacterial community structure compared to the other sessile samples (both were run at 4 COC).

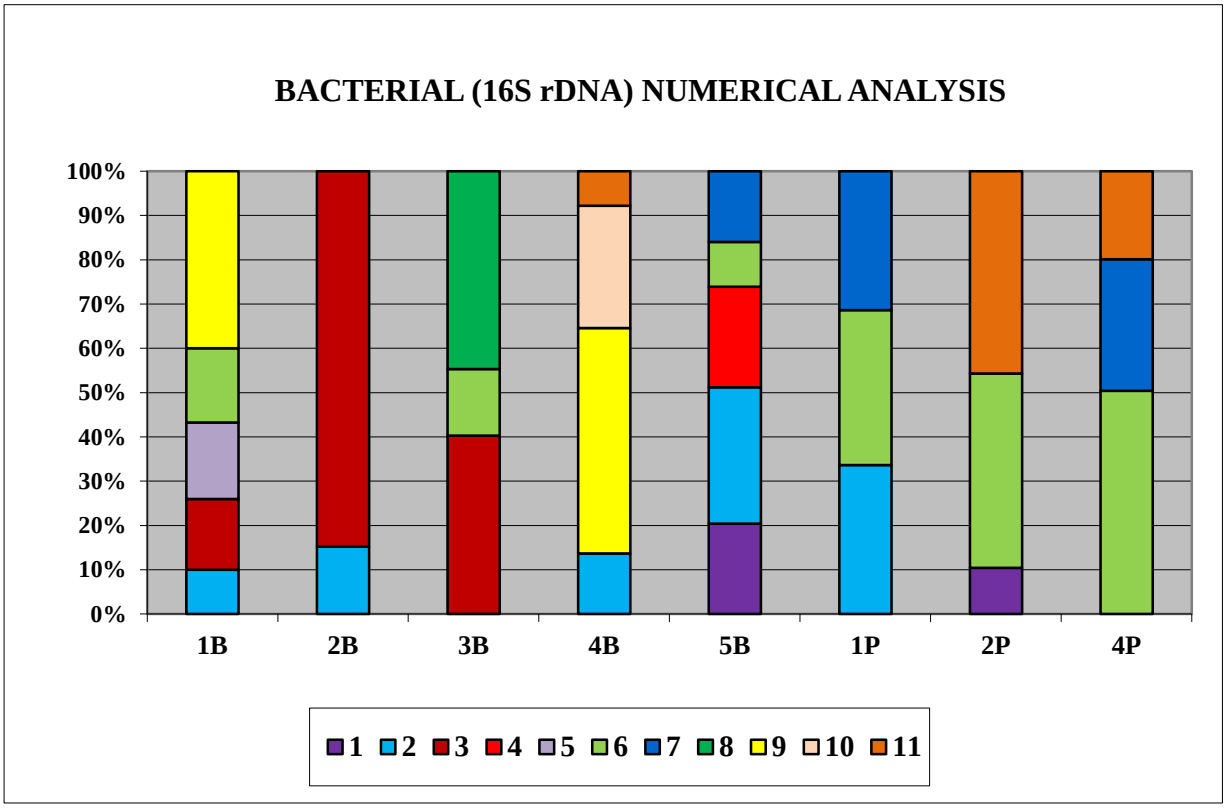

Figure 5.12: Numerical analysis of bacterial (16S rDNA) DGGE data showing relationship between the different experiments as well as phases (planktonic and sessile).

The extracted planktonic and sessile DNA samples were also subjected to 18S rDNA PCR and electrophoresis on a 1 % agarose gel was performed. Amplification of all sessile samples

was successful, but out of all the planktonic samples only experiment 2 and 4 amplified successfully and could be subjected to DGGE analysis.

Results from the 18S rDNA DGGE are summarised in Figure 5.13. This figure illustrates the relationship between the different samples (planktonic as well as the sessile phases).

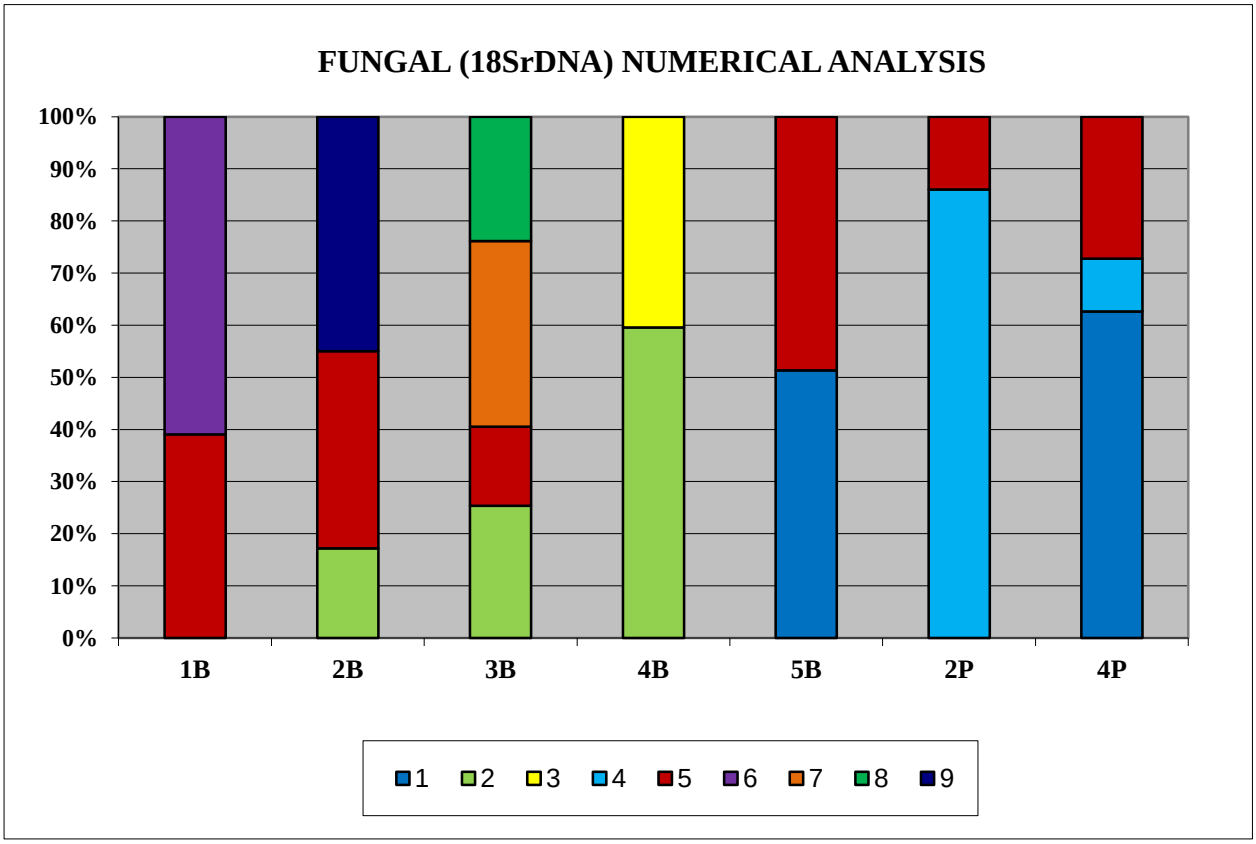

Figure 5.13: Numerical analysis of fungal (18S rDNA) DGGE data showing the relationship between different experiments and phases (planktonic and sessile).

A total of 9 band positions were observed in the 18S rDNA DGGE gel. Band 5 was present in all samples (planktonic and sessile) apart from the sessile sample from experiment 4 (4 COC, 1.2 m/s LFV). Band 2 was present in all sessile samples apart from experiment 1 and 5 (both experiments were run at 0.6 LFV). Sessile samples from experiment 2, 3 and 4 (all of which had band 2 within their profile) were run at higher LFV (0.9 and 1.2 m/s, respectively). As was found in the bacterial community structure results (Figure 5.12), the planktonic and sessile samples differed markedly from each other. Eight (8) out of the possible 9 bands

found during 18S rDNA DGGE was present in the sessile sample, whilst the two planktonic samples had only 3 of the 9 bands present.

5.3.3.4 Microbial diversity (Planktonic and Sessile)

Microbial diversity of the planktonic as well as the sessile phases of the experiments was determined by using the Shannon-Weaver diversity index. Each band in a DGGE profile was accepted to correspond to a single species and the density of each band represent the abundances of that species in the sample (Zhang *et al.*, 2010). The Shannon-Weaver index should rather be seen as a measurement of band pattern diversity, rather than providing actual community diversity. Shannon-Weaver index values for bacterial diversity are presented in Figure 5.14. The figure illustrates that the planktonic bacterial communities had a higher level of diversity than the sessile bacterial communities. From Figure 5.14 it is also evident that the bacterial diversity within the planktonic samples remained relatively constant with a Shannon-Weaver index of ± 0.7 throughout the experiments 1, 2 and 4.

Sessile bacterial community diversity ranged between 0.6 and 0.7 throughout the study, except at experiment 2 (3 COC, 0.9 m/s LFV) where the Shannon-Weaver index value was ± 0.3.

The same level of diversity was found for sessile bacterial communities of experiments 4B and 5B. Both these experiments were run at high COC (4 COC) which indicates that cycles of concentration had an effect on sessile bacterial diversity. Higher COC suggests higher nutrient concentrations, which according to the study by Melo and Bott (1997) on biofouling in water systems would affect the biofilm thickness and ultimately results in increased biofilm diversity. A slightly lower level of diversity (than 4B and 5B) was found at experiments 1B which was run at the same low fluid velocity than experiment 5B (0.6 m/s LFV). Thus, LFV also had an effect on the sessile bacterial community diversity.

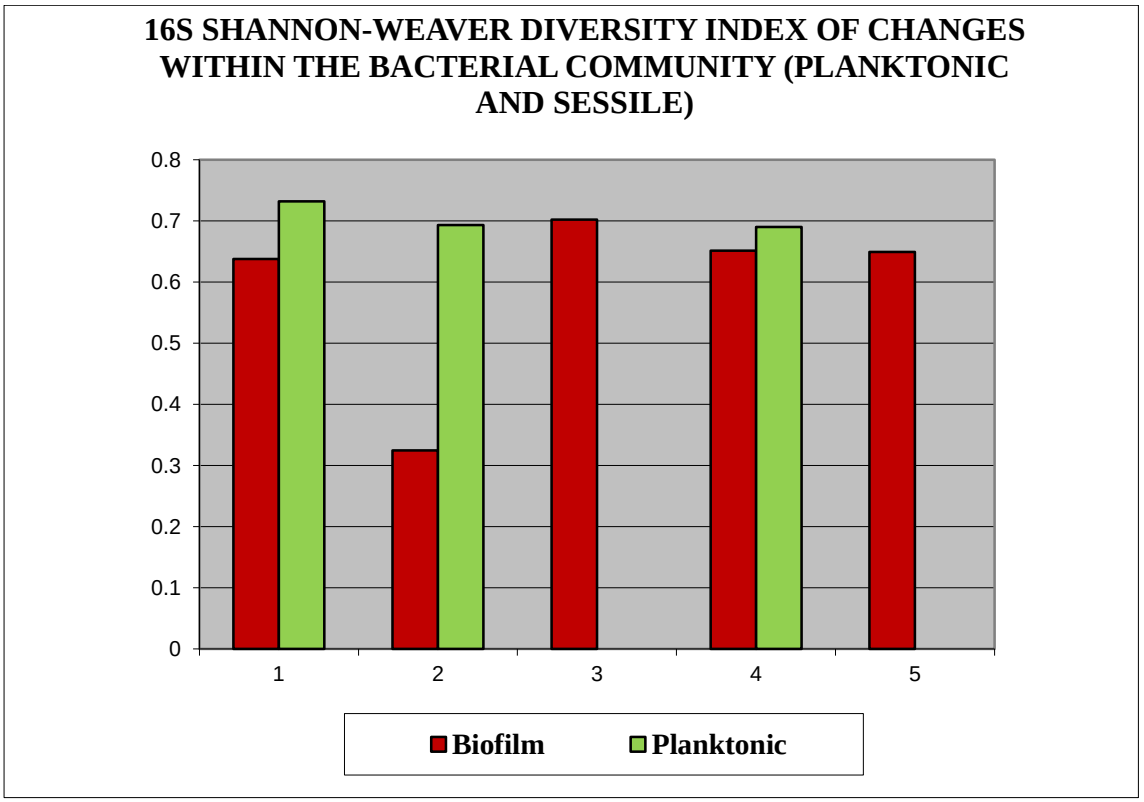

Figure 5.14: Graph of Shannon-Weaver results for the bacterial samples (16S rDNA). The graph indicates the level of bacterial diversity that was found during the different experiments in both the planktonic and the sessile phases.

The fungal community diversity was also determined by using the Shannon-Weaver diversity index. Results obtained are illustrated in Figure 5.15.

Fungal community diversity within the two planktonic samples was not similar to each other, as was the case with the bacterial community diversity (Figure 5.14). Also in Figure 5.15 there seems to be higher community diversity in the sessile samples than in the planktonic samples. The highest diversity was observed in the sessile fungal community of experiment 3B (Shannon-Weaver index of ± 1.2). Operational parameters during this experiment were 2 COC and 1.2 m/s LFV. Experiment 2B also yielded high fungal community diversity (Shannon-Weaver index of ± 0.9) and was run at 3 COC and 0.9 m/s LFV. Similar to what was observed in Figure 5.14, the level of diversity within the sessile samples from experiment 1, 4 and 5 (Figure 5.15) were the same, indicating that both the COC and the LFV affected the sessile fungal and bacterial community diversity.

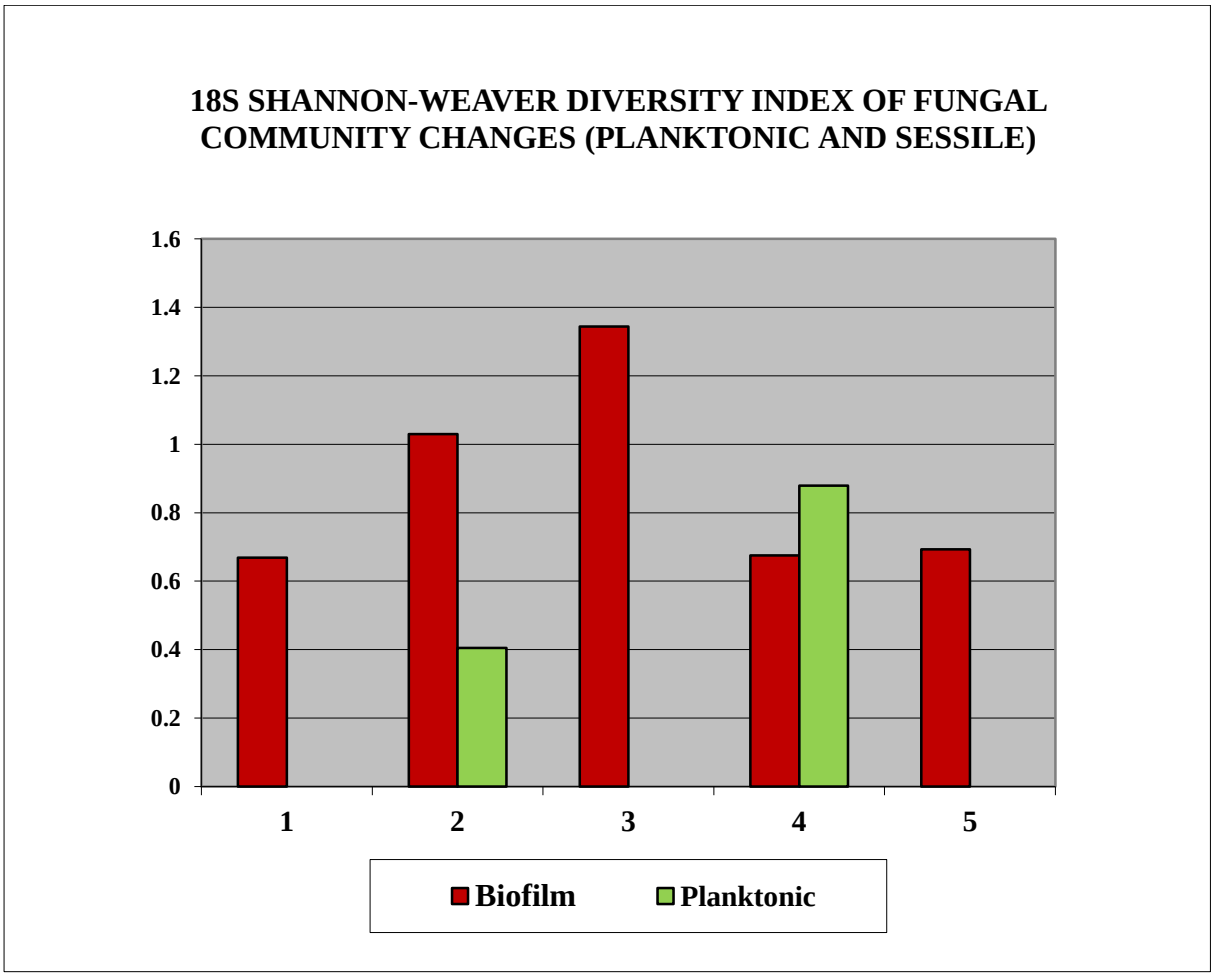

Figure 5.15: Graph of Shannon-Weaver results for the fungal samples (18S rDNA). The graph indicates the level of fungal diversity that was found during the different experiments in both the planktonic and the sessile phases.

By comparing the results of the bacterial community diversity (Figure 5.14) to the fungal community (Figure 5.15), it is evident that there was a much higher level of fungal diversity than bacterial diversity within the sessile phase of the experiments where there were results. This was also found during the conventional microbiological techniques (Figures 5.1 and 5.2).

5.4 CONCLUSION

This section of the study was done to determine the impact of varying two operational parameters (COC and LFV) on the functional and structural diversity of microbial communities within a cooling tower system, using CNP corrected PCBs as make-up water. A combination of culture dependent and culture independent methods was used to achieve this. Firstly, cultural dependent methods (Plate counts and MPN) were employed to determine the different types of organisms and their levels within the cooling tower after operating the system for 30 days.

Results from Figure 5.1 and 5.2 suggest that there were both aerobic as well as anaerobic organisms present in all samples (planktonic and sessile). According to culture dependent techniques the group with the highest bacterial counts during all experiments were the heterotrophic aerobes. The highest heterotrophic aerobe levels in the planktonic phase occurred in experiment 3 (2 COC and 1.2 m/s LFV) and 4 (4 COC and 1.2 m/s LFV), and the highest levels in the sessile phase at experiment 4 (4 COC and 1.2 m/s LFV). Experiments 3 and 4 also had the highest fouling - and COD removal rates (Table 4.4 and 4.5, respectively). The highest SRB count was found in the sessile phase of experiment 5 (Figure 5.2). This experiment also had high SO_4 levels (907.51 mg SO_4/L – Figure 4.2). Sulphate levels in cooling water may be indicative of SRBs actively participating in the microbial community (Peng and Park, 1994; Lutterbach and De França, 1997). Because of the known role of SRBs in microbial induced corrosion (Lutey, 1996; Morikawa, 2006; Xu *et al.*, 2007) one would expect that the corrosion rate found during this experiment was high. However, experiment 5 had a low corrosion rate (0.031 mm/y for mild steel coupons and 0.047 mm/y for stainless steel (Table 4.4). It can therefore be said that the combination of SRBs with other microorganisms found in the biofilm, rather than the SRBs alone can affect the corrosion rate. This is in accordance with previous research by Ilhan-Sungur and Çotuk (2010). Their study on microbial corrosion in cooling tower systems revealed that the corrosion of steel was caused by a variety of microorganisms as well as SRBs within a mixed species biofilm. Results from conventional techniques and PLFA analysis in the present study suggested that the levels of fungi and yeast increased with lower LFV (Figures 5.1, 5.2, 5.8).

Viable biomass as determined by PLFA (Figure 5.8) was similar to the results from culture dependent methods. There were, however, some exceptions. These exceptions could be

explained by the fact that most bacterial species cannot be isolated through conventional techniques. Zhang *et al* (2010) performed a study on the quantification and comparison of bacterial communities in MBRs treating wastewater, and opted to rather use PCR-DGGE than conventional microbiological techniques. Furthermore, the study by Soares *et al.* (2006) on nitrogen fixing bacterial communities using conventional techniques as well as molecular methods revealed that conventional techniques lead to an underestimation of bacterial levels within a microbial community. In the present study, PLFA results (Figure 5.9) indicated that experiments 1 and 5 had the highest sessile mass, whilst experiments 2P, 3P and 4P had similar results. Experiments 1 and 5 were operated at 0.6 m/s LFV and experiments 2, 3 and 4 were operated at 0.9 and 1.2 m/s LFV, respectively. This demonstrated that LFV had a greater effect on biomass than COC.

Phospholipid fatty acid analyses were also used to determine the microbial community structure of the planktonic and the sessile phases. Both the planktonic as well as the sessile communities were dominated by bacteria. In Figure 5.8 it is demonstrated that experiments that were operated at the same LFV had similar community structures (experiments 1 and 5, and experiments 2 and 4) suggesting that LFV was the principal operating parameter affecting community structure. Cycles of concentration as operational parameter also affects community structure, but to a lesser degree than the LFV. This observation is supported by the study performed by Burgess *et al.* (1999) on the role of micronutrients in the biotreatment of industrial effluents. Burgess *et al.* (1999) found that the availability of nutrients influenced the community structure. Furthermore, the study by Melo and Bott (1997) also found that although nutrients affect the microbial community structure, there is an interaction between the nutrient concentration (COC) and the fluid velocity. These authors (Melo and Bott, 1997) stated that higher fluid velocity may counteract the effect of nutrients on community structure.

The biomass and community structure (Figures 5.8 and 5.9) results from the present study were compared to the corrosion rate data illustrated in Section 4 (Table 4.4). This comparison showed that the lowest corrosion rates were found during experiments 1 and 5, and similar results were also found during experiments 2 and 4. It can therefore be deduced that the corrosion rate is not affected by the biomass, but by the biofilm community structure. Jack *et al.* (1992) did a study on corrosion rates of different types of steel in the presence of varying microbial communities. Results from their study (Jack *et al.*, 1992) were similar to

those found in the present study, demonstrating that the corrosion rate is not caused by the total biomass but is affected by different community structures within the biofilm.

Diversity of the microbial communities was determined through DGGE. Denaturing gradient gel electrophoresis data were used to obtain Shannon-Weaver diversity values for the various experiments. Planktonic samples had the highest bacterial diversity (Figure 5.14), whilst the sessile samples had higher fungal diversity (Figure 5.15). Experiments 4 and 5 had similar sessile bacterial (Figures 5.14) and fungal (Figure 5.15) communities (Figure 5.15) diversities. These experiments (4 and 5) were both operated at high COC, suggesting that higher COC lead to higher community diversity. Clarity regarding this phenomenon can be found in the results from the study by Burgess *et al.* (1999) who suggested that higher nutrient availability (COC) can eliminate the need for high levels of competition between microorganisms and in time would result in low community diversity, which in time would lead to high community diversity. High COC can also affect the thickness of biofilm (Melo and Bott, 1997), thus creating an environment where both anaerobic and aerobic organisms can grow which in turn results in higher diversity. Linear flow velocity (LFV) also affected the community diversity, for example the sessile community diversity (bacterial and fungal) found at experiment 1 was slightly lower but similar to the sessile community diversity of experiments 4 and 5 (Figure 5.14 and 5.15). Experiment 1 and 5 were run at low LFV (0.6 m/s), therefore lower LFV resulted in higher community diversity. This observation and deduction is supported in the results found by Rochex *et al.* (2008), who examined the effect of shear stress (including fluid velocity) on biofilm diversity, found that increased LFV would decrease biofilm diversity.

The use of scanning electron microscopy to validate microbial biomass and diversity results throughout the study proved to be successful. Various bacterial morphologies, EPS, as well as the adhesion of microbial cells to form biofilms could be seen in all experiments (Figure 5.3 – Figure 5.7). Changes in microbial community structure were also observed in Figure 5.6 (Experiment 4), which was the experiment with the highest heterotrophic aerobe (Figure 5.1) levels as well as the highest fouling rates (Table 4.4) and high COD removal rates (Table 4.5). Therefore, SEM can be viewed as a useful method to observe the community structure of a given sample.

Not only did both of the two operational parameters (COC and LFV) affect the microbial dynamics within the cooling tower system, it also influenced the chemical properties of the cooling water. Therefore it can be stated that the fouling, scaling and corrosion rates are affected by both the chemical properties (Chapter 4) as well as the microbial dynamics found in the cooling tower. Experiments 3 and 4 were operated at high LFV (1.2 m/s) and had the highest fouling rates (Table 4.4) and bacterial counts (Figures 5.1 and 5.2). It can therefore be concluded that high fouling was caused by microbial activities (biofouling). Corrosion rates were affected by the microbial community structure (Figure 5.8) and not the viable microbial biomass (Figure 5.9). Lowest corrosion rates (Table 4.4) were observed during experiment 1 and 5 (0.6 m/s LFV). High community diversity (Figure 5.14 and 5.15) was also found during these experiments. High COC had a bigger effect on community diversity than the LFV. It can therefore be deduced that lower LFV and higher COC leads to higher corrosion rates.

CHAPTER 6 - FINAL DISCUSSION, CONCLUSIONS AND RECOMMENDATIONS

6.1 DISCUSSION

During this study a laboratory scale mini cooling tower test rig was operated using CNP corrected (100:10:1) synthetic Fischer-Tropsch gas-to-liquid Primary Column Bottoms. This was done in order to appraise the suitability of this effluent as process cooling water. A further goal was to determine the effect of microbial diversity on fouling, scaling and corrosion and to determine under which operational condition the cooling tower system will act optimally as a bioreactor. In order to achieve this, three objectives were formulated. These objectives will serve as headers:

6.1.1 Optimisation of cooling tower operational conditions

Optimisation of operational conditions was achieved by determining the fouling, scaling and corrosion rates during accelerated corrosion tests on both stabilised and non-stabilised water. Fouling, scaling and corrosion rates were determined by using corrosion and scaling indices, as well as measured chemical water quality data. Results from the accelerated corrosion tests indicated that the various corrosion and scaling indices should be used to predict scaling. The data also demonstrated that corrosion tendencies were insufficient in predicting the actual scaling and corrosion observed. Although the stabilised water resulted in higher fouling and corrosion rates than the non-stabilised water, these rates were within the SASOL guidelines. Scaling rates, however, were much higher in the non-stabilised water than in the stabilised water and did not fall within the SASOL guidelines. The objective as set out was achieved and details can be found in Chapter 3. Based on the outcomes of the experiment it was decided that stabilised water and that 2, 3 and 4 instead of 2, 4 and 6 cycles of concentration should be used in the cooling tower experiments.

6.1.2 The effect of operational parameters on the rate of fouling, scaling and corrosion

Stabilised, synthetic PCBs were used as process cooling water in each of the five experiments. The PCB was CNP corrected to 100:10:1 and experiments were operated at various selected cycles of concentration and linear flow velocities. Each experiment lasted 30 days. The fouling, scaling and corrosion rates for mild steel as well as 316 L stainless steel corrosion coupons and heat exchanger tubes were determined, using various indices as well as water chemical data. Results obtained showed negligible fouling, scaling and corrosion rates for all stainless steel coupons and heat exchanger tubes (Xu *et al.*, 2007). Predicted corrosion and scaling rates corresponded well to actual corrosion and scaling rates, especially for the scaling rates (Swart and Engelbrecht, 2007). High cycles of concentration lead to increased scaling, fouling and corrosion (Swart and Engelbrecht, 2007). Linear flow velocity had the same effect as cycles of concentration (higher LFV lead to increased fouling and scaling), but to a lesser degree (Melo and Bott, 1997). However, lower linear flow velocity resulted in decreased corrosion rates. All five experiments demonstrated that COD could be removed in the cooling towers. When both of the operational parameters were simultaneously increased it was accompanied by increased fouling, scaling and corrosion rates. Experiment 3 and 4 had the highest percentage COD removal rates (89.35 % and 80.89 % respectively). Both these experiments were operated at 1.2 m/s LFV but differed with regards to COC (2 and 4 respectively). Even though there is a small difference in % COD removal under the specified operating conditions, the fouling, scaling and corrosion rates observed favour operating conditions found in experiment 4. These fouling, scaling and corrosion rates compared well with the SASOL guidelines and current operational conditions at SASOL (Swart and Engelbrecht, 2007). Obtaining >80 % COD removal meant even if operated under high LFV and COC conditions the cooling tower could act as a bioreactor. Therefore it is recommended that operational parameters should be applied as in experiment 4.

6.1.3 The functional and structural diversity of planktonic and sessile microbial communities

During this study, a combination of culture dependent and culture independent methods were used to determine the functional and structural diversity of the planktonic as well as the sessile microbial communities. Scanning electron microscopy (SEM) data also proved useful

in the observation of microbial morphology and microbial community structures, both within the sessile and planktonic phase. Results from culture dependent techniques showed heterotrophic aerobic bacteria were the most abundant during all experiments. Overall the heterotrophic aerobic bacterial counts corresponded well with the % COD removal, with the highest bacterial counts for this group observed at experiment 3 and 4.

PLFA analysis illustrated that LFV affected the microbial biomass as well as the microbial community structure to a greater extent than COC. Higher LFV ultimately lead to lower sessile biomass (Melo and Bott, 1997). Results also indicated that corrosion rate was more profoundly affected by microbial community structure, but to a lesser extent by biomass (Jack *et al*., 1992). Denaturing gradient gel electrophoresis (DGGE) was used to determine the microbial community diversity. These results showed that increased COC and decreased LFV lead to higher microbial diversity (Burgess *et al.*, 1999; Rochex *et al*., 2008). According to the culture dependent and independent methods, both operational parameters (COC and LFV) affected the functional and structural diversity of the microorganisms although not to the same extent.

6.2 CONCLUSION

This study showed that the Fischer-Tropsch gas-to-liquid Primary Column Bottoms can be used as process cooling water. It is, however, important that the water be stabilised. If the purpose is to use the cooling tower as a bioreactor then the water should be CNP corrected as no nitrate and phosphorous occur naturally in PCB. Both operational parameters (LFV and COC) affected microbial community function and structure as well as fouling, scaling and corrosion rates. Fouling was mostly influenced by LFV. Experiments with high LFV also had the highest fouling rates as well as bacterial counts. Thus fouling found within the system was mostly caused by microorganisms (biofouling). Corrosion on the other hand increased with higher COC and lower LFV. Community diversity had the greatest effect on the corrosion rate. For overall best results, the cooling tower should be CNP corrected, stabilised, and run at high COC (4) and high LFV (1.2 m/s). These conditions resulted in an 80.89 % COD removal, demonstrating that the cooling tower can act as a bioreactor. In a parallel study (Slabbert, 2006), a laboratory scale mini-cooling tower test rig was operated under the exact same conditions as in this study. However, in that study PCB was used without CNP correction. In that case no COD was removed and it was observed that nutrient

levels consistently increased in all experiments (Slabbert, 2006). Also, fouling, scaling and corrosion rates were higher than observed in the present study.

6.3 RECOMMENDATIONS

From the results obtained in this study the following recommendations are made:

1. For the operation of the cooling towers it is advantageous to use stabilised water in the process.
2. For optimal COD removal, nutrient correction is advised with 4 cycles of concentration and a high linear flow velocity (1.2 m/s) recommended as the target operation parameters for the cooling tower system.

For further studies into the possible application of cooling towers as bioreactors the following are recommended:

1. To facilitate a better evaluation of the effect of varying cycles of concentration it is recommended to include operating the cooling tower system at 3 and 5 cycles of concentration to better delineate the optimal operational conditions.
2. Based on the favourable results obtained in this study, especially for COD removal, other effluent streams should also be considered. Examples may include high nitrogenous streams and food industry effluents.
3. As a further measure to control scaling in the cooling water system, preventative crystallisation could be investigated.
4. DGGE band excision should be performed to allow for sequencing analyses of the microbial populations. This should supply valuable information as to the role and performance of the bacteria present in the system under the various operating conditions.

REFERENCES:

Adewumi, J.R., Ilemobade, A.A. and Van Zyl, J.E. (2010) Treated wastewater reuse in South Africa: Overview, potential and challenges. *Resources, Conservation and Recycling*. **55**, 221 – 231.

Aguilera, A, Gómez, F., Lospitao, E. and Amils, R. (2006) A molecular approach to the characterization of the eukaryotic communities of an extreme acidic environment: Methods for DNA extraction and denaturing gradient gel electrophoresis analysis. *Systematic and Applied Microbiology*. **29**, 593 - 605.

Al-Ahmad, M., Aleem, F.A.A., Mutiri, A. And Ubaisy, A. (2000) Biofouling in RO membrane systems. Part 1: Fundamentals and control. *Desalination.* **132**, 173 – 179.

Almeida, M.A.N. and de França, F.P. (1998) Biofilm formation on brass coupons exposed to a cooling system of an oil refinery. *Journal of Industrial Microbiology & Biotechnology*. **20**, 39 – 44.

Al-Rawajfeh, A.E. (2010) $CaCO_3$-CO_2-H_2O system in falling film on a bank of horizontal tubes: Model verification. *Journal of Industrial and Engineering Chemistry*. **16(6)**, 1050 – 1058.

Alva-Argáez, A., Kokossis, A.C. and Smith, R. (2007) The design of water-using systems in petroleum refining using a water-pinch decomposition. *Chemical Engineering Journal.* **128**, 33 - 46.

Andermark, P.J., Lee, J.J. and Seeley, H.W. (1991) Microbes in action: A laboratory manual of Microbiology. New York: W.H. Freeman and Company. 450 p.

Angell, P., Machowski, W.J. Paul, P.P., Wall, C.M. and Lyle, F.F. (1997) A multiple chemostat system for consortia studies on microbially influenced corrosion. *Journal of Microbiological Methods*. **30(3)**, 173 – 178.

Angell, P. and Urbanic, K. (2000) Sulphate-reducing bacterial activity as a parameter to predict localized corrosion of stainless alloys. *Corrosion Science*. **42**, 897 - 912.

Anon, (1994) The industrial water society (lWS) Cooling water treatment: A code of practice. Tamworth. 85 p.

Anon, (2001a) International Water Association (IWA). Yearbook 2001. Management. London, United Kingdom. 13 p.

Anon, (2001b) International Water Association (IWA). Yearbook 2001. Recycling. London, United Kingdom. 19 p.

Anon, (2004)

[Web:] http://www.nace.org

[Date of access 26 November 2007]

Anon, (2005)

[Web:] http://www.thermidaire.on.ca

[Date of access 25 May 2005]

Anon, (2006a)

[Web:] http://ewr.cee.vt.edu/environmental/tech/wtprimer/corrosion/corroion.html#link4

[Date of access 2 October 2006]

Anon, (2006c)

[Web:] http://www.corrosionsource.com

[Date of access 2 October 2006]

Anon, (2006d)

[Web:] http://www.frenchcreeksoftware.com

[Date of access 2 October 2006]

Antony, A., Low, J.H., Gray, S., Childress, A.E., Le-Clech, P. and Leslie, G. (2011) Scale formation and control in high pressure membrane water treatment systems: A review. *Journal of Membrane Science*. **383**, 1 – 16.

APHA, (American Public Health Association), AWWA (American Water Works Association), WPCF (Water Pollution Control Federation) **(1985)** Standard methods for the examination of water and wastewater. 16th. Ed. APHA. USA.1268 p.

Ataei, A., Panjeshahi, M.H. and Gharaie, M. (2009) New method for industrial water reuse and energy minimization. *International Journal of Environmental Research*. **3(2)**, 289 – 300.

Azis, P.K.A., Al-Tisan, 1. and Sasikumar, N. (2001) Biofouling potential and environmental factors of seawater at a desalination plant intake. *Desalination*. **135**, 69 - 82.

Beloti, V. De Souza, J.A., De Agular Ferreira Barros, M., Nero, L.A., de Mattos, M.R., Gusmao, V.V. and de Moraes, L.B. (2003) Evaluation of petrifilm EC and HS for total coliforms and *Escherichia coli* enumeration in water. *Brazilian Journal of Microbiology*. **34**, 301 - 304.

Benzaoui, A. and Bouabdallah, A. (2004) Desalination and biological wastewater treatment process. *Desalination*. **165**, 105 - 110

Bligh, E.G. and Dyer, W.J. (1959) A rapid method of total lipid extraction and purification. *Canadian Journal of Biochemistry and Physiology*. **37**, 911 – 917.

Bott, T.R. (1998) Techniques for reducing the amount of biocide necessary to counteract the effects of biofilm growth in cooling water systems. *Applied Thermal Engineering*. **18**, 1059 - 1066.

Burgess, J.E., Quarmby, J. and Stephenson, T. (1999) Role of micronutrients in activated sludge-based biotreatment of industrial effluents. *Biotechnology Advances*. **17**, 49 - 70.

Chen, L.M. and Chai, L.H. (2006) A theoretical analysis on self-organized formation of microbial biofilms. *Physica A*. **370**, 793 - 807.

Chen, M.J., Zhang, Z. and Bott, T.R. (2005) Effects of operating conditions on the adhesive strength of *Pseudomonas fluorescens* biofilms in tubes. *Colloids and Surfaces B: Biointerfaces*. **43**, 61 – 71.

Choi, D., You, S. and Kim, J. (2002) Development of an environmentally safe corrosion, scale, and microorganism inhibitor for open recirculating cooling systems. *Materials Science and Engineering A*. **335**, 228 - 236.

Chongdar, S., Gunasekaran, G. and Kumar, P. (2005) Corrosion inhibition of mild steel by aerobic biofilm. *Electrochimica Acta.* **50**, 4655 – 4665.

Choudary, S.G. (1998) Emerging microbial control issues in cooling water systems. *Hydrocarbon Processing.* **77**, 91 – 102.

Church, C.D., Wilkin, R.T., Alpers, C.N., O Rye, R. and McCleskey, R.B. (2007) Microbial sulphate reduction and metal attenuation in pH 4 acid mine water. *Geochemical Transactions.* **8(10)**, 1 – 14.

Cloete, T.E., Brözel, V.S., de Bruyn, E.E. and Pietersen, B. (1994) Optimisation of biofouling control in industrial water systems. WRC Report. No 3181/94.

Cochran, W.G. (1950) Estimation of bacterial densities by means of the "Most Probable Number". *International Biometric Society*. **6(2)**, 105 – 116.

Cresson, R., Carrère, H., Delgenès, J.P. and Bernet, N. (2006) Biofilm formation during the start-up period of an anaerobic biofilm reactor – Impact of nutrient complementation. *Biochemical Engineering Journal*. **30**, 55 – 62.

Dhamole, P.B., Nair, R.R., D'Souza, S.F. and Lele, S.S. (2009) Simultaneous removal of carbon and nitrate in an airlift bioreactor. *Bioresource Technology*. **100**, 1082 – 1086.

Doche, M.L., Hihn, J.Y. Mandroyan, A., Maurice, C., Hervieux, O. and Roizard, X. (2006) A novel accelerated corrosion test for exhaust systems by means of power ultrasound. *Corrosion Science*. **48**, 4080 - 4093.

Dry, M.E. (1999) Fischer-Tropsch reactions and the environment. *Applied Catalysis A: General*. **189**, 185 - 190.

Dry, M.E. (2002) The Fischer-Tropsch process: 1950 – 2000. *Catalysis Today*. **71**, 227 – 241.

Dubey, R.S. and Upadhyay, S.N. (2001) Microbial corrosion monitoring by an amperometric microbial biosensor developed using whole cell of *Pseudomonas* sp. *Biosensors and Bioelectronics*. **16**, 995 - 1000.

Dubiel, M., Hsu, C.H., Chien, C.C., Mansfeld, F., and Newman, D.K. (2002) Microbial Iron Respiration Can Protect Steel from Corrosion. *Applied and Environmental Microbiology.* **68(3)**, 1440 – 1445.

DWAF, (Department of Water Affairs and Forestry), (2004) National Water Research Strategy. Proposed first edition. 150p.

Dzierzewicz, Z., Cwalina, E., Chodurek, E. and Wilczok, T. (1997) The relationship between microbial metabolic activity and biocorrosion of carbon steel. *Research in Microbiology*. **148**, 785 - 793.

Englert, G.E. and Müller, LL. (1996) The corrosion behaviour of mild steel and type 304 stainless steel in media from an anaerobic biodigester. *International Biodeterioration & Biodegradation*. **37(3-4)**, 173 – 180.

Ercolini, D. (2004) PCR-DGGE fingerprinting: novel strategies for detection of microbes in food. Review article. *Journal of Microbiological Methods.* **56**, 297 – 314.

Feng, Y.Y., Hoe, W.C., Hu, J.Y., Ng, W.J., Ong, S.L. and Tan, X.L. (2005) Investigation into biofilms in a local drinking water distribution system. *Biofilms*. **2(1)**, 19 – 25.

Flemming, H.E. (1997) Reverse Osmosis membrane biofouling. *Experimental Thermal and Fluid Science*. **14**, 382 - 391.

Forney, L.J., Liu, W.-T., Guckert, J.B., Kumagai, Y., Namkung, E., Nishihara, T. and Larson, R.J. (2001) Structure of microbial communities in activated sludge: Potential implications for assessing the biodegradability of chemicals. *Ecotoxicology and Environmental Safety*. **49(1)**, 40 - 53.

Gagnon, G.A. and Slawson, R.M. (1999) An efficient biofilm removal method for bacterial cells exposed to drinking water. *Journal of Microbiological Methods.* **34**, 203 – 214.

Garcia-Armisen, T. and Servais, P. (2004) Enumeration of viable E.coli in rivers and wastewaters by fluorescent *in situ* hybridization. *Journal of Microbiological Methods*. **58**, 269 - 279.

Gelsomino, A., Keijzer- Wolters, A.C., Cacco, G. and van Elsas, l.D. (1999) Assessment of bacterial community structure in soil by polymerase chain reaction. *Journal of Microbiological Methods*. **38**, 1 - 15.

George, R.P., Marshall, D. and Newman, R.C. (2003) Mechanism of a MIC probe. *Corrosion Science*. **45**, 1999 - 2015.

Gonzalez, J.E.G., Santana, F.J.H. and Mirza-Rosca, J.C. (1998) Effect of bacterial biofilm on 316 SS corrosion in natural seawater by EIS. *Corrosion Science*. **40**, 2141- 2154.

Gunson, A.J., Klein, B., Veiga, M. And Dunbar, S. (2012) Reducing mine water requirements. *Journal of Cleaner Production*. **21**, 71 – 82.

Hallberg, K.B., Grail, B.M., du Plessis, C.A. and Johnson, D.B. (2011) Reductive **dissolution** of ferric iron minerals: A new approach for bio-processing nickel laterites. *Minerals Engineering*. **24**, 620 – 624.

Hawthorn, D. (2009) Heat transfer: Solving scaling problems at the design stage. *Chemical Engineering Research and Design.* **87**, 193 – 199.

Herrera, L.K. and Videla, H.A. (2009) Role of iron-reducing bacteria in corrosion and protection of carbon steel. *International Biodeterioration & Biodegradation*. **63(7)**, 891 – 895.

Hill, G.T., Mitkowski, N.A., Aldrich-Wolfe, L., Emele, L.R., Jurkonie, D.D., Ficke, A., Maldonado-Ramirez, S., Lynch, S.T. and Nelson, E.B. (2000) Methods for assessing the composition and diversity of soil microbial communities. *Applied Soil Ecology*. **15**, 25 - 36.

Ilhan-Sungur, E. and Çotuk, A. (2010) Microbial corrosion of galvanized steel in a simulated recirculating cooling tower system. *Corrosion Science.* **52(1)**, 161 – 171.

Ishii, S.K.L. and Boyer, T.H. (2011) Evaluating the secondary effects of magnetic ion exchange: Focus on corrosion potential in the distribution system. *Desalination*. **274**, 31 – 38.

Iverson, W.P. (1987) Advances in applied microbiology. Volume 32. Academic Press. New Jersey. p. 1 – 37.

Jack, R.F., Ringelberg, D.B. and White, D.C. (1992) Differential corrosion rates of carbon steel by combinations of *Bacillus* sp., *Hafnia alvei* and *Desulfovibrio gigas* established by phospholipid analysis of electrode biofilm. *Corrosion Science*. **33**, 1843 – 1853.

Jacques, M., Lagacé, L., Mafu, A.A. and Roy, D. (2006) Compositions of maple sap microflora and collection system biofilms evaluated by scanning electron microscopy and denaturing gradient gel electrophoresis. *International Journal of Food Microbiology*. **109(2)**, 9 – 18.

Jewitt, G.P.W., Garratt, J.A., Calder, I.R. and Fuller, L. (2004) Water resource planning and modeling tools for the assessment of land use change in the Luvuvhu Catchment, South Africa. *Physics and Chemistry of the Earth*. **29**, 1233 - 1241

Johansson, L. and Saastomoinen, T. (1999) Investigating early stages of biocorrosion with XPS: AISI 304 stainless steel exposed to *Burkholderia* species. *Applied Surface Science.* **114**, 244 - 248.

Johnson, D.A. (2001) Operate cooling towers correctly at high cycles of concentration. *Chemical Engineering Progress*.

Kampas, P., Parsons, S.A., Pearce, P., Ledoux, S., Vale, P., Cartmell, E. and Soares, A. (2009) An internal carbon source for improving biological nutrient removal. *Bioresource Technology*. **100**, 149 – 154.

Karlberg, L. and Penning de Vries, F.W.T. (2004) Exploring potentials and constraints of low-cost drip irrigation with saline water in sub-Saharan Africa. *Physics and Chemistry of the Earth*. **29**, 1035 - 1042.

Keresztes, Z., Felhösi, I. and Kálmán, E. (2001) Role of redox properties of biofilms in corrosion processes. *Electrochimica Acta*. **46**, 3841 - 3849.

Khatami, H.R., Ranjbar, M., Schaffie, M. and Emady, M.A. (2010) Development of a fuzzy saturation index for sulfate scale prediction. *Journal of Petroleum Science and Engineering.* **71**, 13 – 18.

Kim, J., Savulescu, L. and Smith, R. (2001) Design of cooling systems for effluent temperature reduction. *Chemical Engineering Science.* **56**, 1811 - 1830.

Koppol, A.P.R., Bagajewicz, M.J., Dericks, B.J. and Savelski, M.J. (2003) On zero water discharge solutions in the process industry. *Advances in Environmental Research*. **8**, 151 - 171.

Kosińska, K. and Miśkiewicz, T. (2009) Performance of an anaerobic bioreactor with biomass recycling, continuously removing COD and sulphate from industrial wastes. *Bioresource Technology*. **100**, 86 – 90.

Lagacé, L., Jacques, M., Mafu, A.A. and Roy, D. (2006) Compositions of maple sap micro flora and collection system biofilms evaluated by scanning electron microscopy and denaturing gradient gel electrophoresis. *International Journal of Food Microbiology*. **109**, 9 - 18.

Lapara, T.M., Nakatsu, C.H., Pantea, L.M. and Alleman, J.E. (2001) Aerobic biological treatment of a pharmaceutical wastewater: Effect of temperature on COD removal and bacterial community development. *Water Research*. **35**, 4417 – 4425.

Lazarova, V. and Manem, J. (1995) Biofilm characterization and activity analysis in water and wastewater treatment. *Water Research*. **29**, 2227 - 2245.

Le Blay, G., Fliss, I. and Lacroix, C. (2004) Comparative detection of bacterial adhesion to $CaCO_2$ cells with ELISA, radioactivity and plate count methods. *Journal of Microbiological Methods*. **59**, 211 - 22l.

Lee, S.H. and Young, I.C. (2002) Velocity effect on electronic-antifouling technology to mitigate mineral fouling in enhanced-tube heat exchanger. *International Journal of Heat and Mass Transfer*. **45**, 4163 - 4174.

Lei, F. and VanderGheynst, J.S. (2000) The effect of microbial inoculation and pH on microbial community structure changes during composting. *Process Biochemistry*. **35**, 923 - 929.

Li, H., Hsieh, M-K., Chien, S-H., Monnell, J.D., Dzombak, D.A. and Vidic, R.D. (2011) Control of mineral scale deposition in cooling systems using secondary-treated municipal wastewater. *Water Research.* **45(2)**, 748 – 760.

Li, H., Yang, M., Zhang, Y. and Kamagata, Y. (2006) Nitrification performance and microbial community dynamics in a submerged membrane bioreactor with complete sludge retention. *Journal of Biotechnology*. **123**, 60 - 70.

Ludensky, M. (2003) Control and monitoring of biofilms in industrial applications. *International Biodeterioration and Biodegradation*. **51**, 255 - 263.

Lutey, R.W. (1996) Applied industrial microbiological control. Buckman Laboratories International. Memphis: USA. 23 p.

Lutey, R.W. (1998) A Review of current technologies for the control of MIC in Industrial waters. International workshop on biofouling and biocorrosion. September 10 - 11, Pretoria: South Africa.

Lutterbach, M.T.S. and De França, F.P. (1997) Biofilm formation in water cooling systems. *World Journal of Microbiology & Biotechnology*. **12**, 391 – 394.

MacDonald, R. and Brözel, V.S. (2000) Community analysis of bacterial biofilms in a simulated recirculating cooling-water system by fluorescent *in situ* hybridization with rRNA-targeted oligonucleotide probes. *Water Research*. **34**, 2439 - 2446.

Macnaughton, S.J., Jenkins, T.L., Wimpee, M.H., Cormiér, M.R. and White, D.C. (1997) Rapid extraction of lipid biomarkers from pure culture and environmental samples using pressurized accelerated hot solvent extraction. *Journal of Microbiological Methods*. **31**, 19 – 27.

Mamlouk, D., Hidalgo, C., Torija, M-.J. And Gullo, M. (2011) Evaluation and optimisation of bacterial genomic DNA extraction for no-culture techniques applied to vinegars. *Food Microbiology*. **28(7)**, 1374 – 1379.

Marín-Cruz, J., Cabrera-Sierra, R., Pech-Canul, M.A. and González, I. (2006) EIS study on corrosion and scale processes and their inhibition in cooling system media. *Electrochimica Acta*. **51**, 1847 – 1854.

McKinley, V.L., Peacock, A.D. and White, D.C. (2005) Microbial community PLFA and PHB responses to ecosystem restoration in tallgrass prairie soils. *Soil Biology & Biochemistry*. **37**, 1946 – 1958.

McLeod, E.S., MacDonald, R. and Brözel, V.S. (2002) Distribution of *Shewanella putrefaciens* and *Desulfovibrio vulgaris* in sulphidogenic biofilms of industrial cooling water systems determined by fluorescent *in situ* hybridization. *Water South Africa*. **28(2)**, 123 – 128.

Meesters, K.P.H., Van Groenestijn, J.W. and Gerritse, J. (2003) Biofouling reduction in recirculating cooling systems through biofiltration of process water. *Water Research*. **37**, 525 - 532.

Melidis, P., Sanozidou, M., Mandusa, A. and Ouzounis, K. (2007) Corrosion control by using indirect methods. *Desalination*. **213,** 152 – 158.

Melo, R.F. and Bott, T.R. (1997) Biofouling in Water Systems. *Experimental Thermal and Fluid Science*. **14**, 375 – 381.

Miller, G.W. (2006) Integrated concepts in water reuse: managing global water needs. *Desalination*. **187**, 65 – 75.

Milovanovic, M. (2007) Water quality assessment and determination of pollution sources along the Axios/Vardar River, Southeastern Europe. *Desalination*. **213**. 159 - 173.

Mohsen, M.S., (2004) Treatment and reuse of industrial effluents: Case study of a thermal power plant. *Desalination*. **167**, 75 - 86.

Morikawa, M. (2006) Beneficial biofilm formation by industrial bacteria *Bacillus subtilus* and related species. *Journal of Bioscience and Bioengineering*. **101**, 1 - 8.

Muyzer, G., De Waal, E. and Uitterlinden, A.G. (1993) Profiling of complex microbial populations by denaturing gradient gel electrophoresis analysis of polymerase chain reaction - amplified genes coding for 16S rRNA. *Applied and Environmental Microbiology*. **59**, 695 - 700.

Nakagawa, T., Fukui, M., Sato, S. And Yamamoto, Y. (2002) Successive changes in community structure of an ethylbenzene-degrading sulfate-reducing consortium. *Water Research*. **36**, 2813 – 2823.

Neria-González, I., Wang, E.T., Ramírez, F., Romero, J.M. and Hernández-Rodríguez, C. (2006) Characterization of bacterial community associated to biofilms of corroded oil pipelines from the southeast of Mexico. *Anaerobe*. **12**, 122 - 133.

Neu, T.R and Lawrence, J.R (1997) Development and structure of microbial biofilms in river water studied by confocal laser scanning microscopy. *FEMS Microbiology ecology*. **24**, 11 - 25.

Ojumu, T.V., Hansford, G.S. and Petersen, J. (2009) The kinetics of ferrous-iron oxidation by *Leptospirillum ferriphilum* in continuous culture: The effect of temperature. *Biochemical Engineering Journal*. **46**, 161 – 168.

Okabe, S., Matsudat, T., Satoh, H., Itoh, T. and Watanabe, Y. (1998) Sulfate reduction and sulfide oxidation in aerobic mixed population biofilms. *Water Science Technology*. **37**, 131 - 138.

Omar, W., Chen, J. And Ulrich, J. (2010) Reduction of seawater scale forming potential using the fluidized bed crystallization technology. *Desalination*. **250**, 95 – 100.

Overett, M.J., Hill, R.O. and Moss, J.R. (2000) Organometallic chemistry and surface science: mechanistic models for the Fischer-Tropsch synthesis. *Coordination Chemistry Reviews*. **206 - 207**, 581 - 605.

Palojarvi, A., Sharman, S., Rangger, A., Von Lutzow, M. and Insam, H. (1997) Comparison of Biolog and phospholipid fatty acid patterns to detect changes in microbial community. *In*: Microbial communities. Microbial communities – Functional versus structural approaches. Springer verlag, New York. p. 37 - 48.

Panjeshahi, M.A. and Ataei, A. (2008) Application of an environmentally optimum cooling water system design to water and energy conservation. *International Journal of Environment Science and Technology*. **5(2)**, 251 – 262.

Papassiopi, N., Vaxevanidou, K. And Paspaliaris, I. (2010) Effectiveness of iron reducing bacteria for the removal of iron from bauxite ores. *Minerals Engineering*. **23**, 25 – 31.

Pasmore, M., Todd, P., Smith, S., Baker, D., Silverstein, J., Coons, D. and Bowman, C.N. (2001) Effects of ultrafiltration membrane surface properties on *Pseudomonas*

aeruginosa biofilm initiation for the purpose of reducing biofouling. *Journal of Membrane Science.* **194**, 15 - 32.

Pathak, A., Dastidar, M.G., Sreekrishnan, T.R. (2009) Bioleaching of heavy metals from sewage sludge by indigenous iron-oxidizing microorganisms using ammonium ferrous sulfate and ferrous sulfate as energy sources: A comparative study. *Journal of Hazardous Materials*. **171(1-3)**, 273 – 278.

Pelz, O., Chatzinotas, A., Zarda-Hess, A., Abraham, W. and Zeyer, J. (2001) Tracing toluene-assimilating sulfate-reducing bacteria using ^{13}C- incorporation in fatty acids and whole-cell hybridization. *FEMS Microbiology Ecology*. **38**, 123 - 131.

Peng, C. and Park, J.K. (1994) Electrochemical mechanisms of corrosion influenced by sulphate- reducing bacteria in aquatic systems. *Water Research*. **28**, 1681 - 1692.

Perni, S., Jordan, S.J., Andrew, P.W. and Shama, G. (2006) Biofilm development by *Listeria innocua* in turbulent flow regimes. *Food Control*. **17**, 875 – 883.

Prescott, L.M., Harley, J.P. and Klein, D.A. (2002) Microbiology. 5th.Ed.. McGraw- Hill. New York. 1026 p.

Prisyazhniuk, V.A. (2007) Prognosticating scale-forming properties of water. *Applied Thermal Engineering*. **27**, 1637 - 1641.

Prisyazhniuk, V.A. (2009) Physico-chemical principles of preventing salts crystallization on heat-exchange surfaces. *Applied Thermal Engineering*. **29**, 3182 – 3188.

Qureshi, B.A. and Zubair, S.M. (2006) A complete model of wet cooling towers with fouling in fills. *Applied Thermal Engineering*. **26**, 1982 - 1989.

Rakanta, E., Daflou, E. and Batis, G. (2007) Evaluation of corrosion problems in a closed air-conditioning system: a case study. *Desalination*. **213**, 9 - 17.

Ranjard, L., Poly, F. and Nazaret, S. (2000) Monitoring complex bacterial communities using culture-independent molecular techniques: application to soil environment. *Research in Microbiology.* **151**, 167 – 177.

Rao, T.S., Sairam, T.N., Viswanathan, B. and Nair, K.V.K. (2000) Carbon steel corrosion by iron oxidising and sulphate reducing bacteria in a freshwater cooling system. *Corrosion Science*. **42**, 1417 - 1431.

Reasoner, D.J. (2004) Heterotrophic plate count methodology in the United States. *International Journal of Food Microbiology*. **92**, 307 - 315.

Rebhun, M. And Engel, G. (1998) Reuse of wastewater for industrial cooling systems. *Journal Water Pollution Control*. **60(2)**, 237 – 241.

Rochex, A., Godon J.-J., Bernet, N. and Escudié, R. (2008) Role of shear stress on composition, diversity and dynamics of biofilm bacterial communities. *Water Research*. **42**, 4915 – 4922.

Rolleke, S., Gurtner, c., Drewello, U, Drewello, R., Lubitz, W. and Weissmann, R. (1999) Analysis of bacterial communities on historical glass by denaturing gradient gel electrophoresis of PCR-amplified gene fragments coding for 16S rRNA. *Journal of Microbiological Methods*. **36**, 107 - 114.

Saha, N.K., Balakrishnan, M. and Batra, V.S. (2005) Improving industrial water use: case study for an Indian distillery. *Resources, Conservation and Recycling*. **43**, 163 - 174.

Sanz, J.L. and Köchling, T. (2007) Molecular biology techniques used in wastewater treatment: An overview. *Process Biochemistry*. **42**, 119 - 133.

Schmidt, C.A.B., Barbosa, M.C. and De Almeida, M.S.S. (2007) A laboratory feasibility study on electrokinetic injection of nutrients on an organic, tropical, clayey soil. *Journal of Hazardous Materials*. **143(3)**, 655 - 66l.

Schwartz, T., Jungfer, C., Heißler, S., Friedrich, F., Faubel, W. and Obst, U. (2009) Combined use of molecular biology taxonomy, Raman spectrometry, and ESEM imaging to study natural biofilms grown on filter materials at waterworks. *Chemosphere*. **77**, 249 – 257.

Shreir, L.L., Jarman, R.A. and Burstein, G.T. (2000) Corrosion. Volume 1: Metal/Environment Reactions. 3rd. revised Ed. Butterworth-Heinemann. Oxford. 1432 p.

Silbert, M. & Associates (2006) W-Index – Water Index calculations Version 5.0 for Excel. Date of Access: 21 October 2011. [http://www.silbert.org/W-index-Spreadsheet.pdf]

Singh, R., Paul, D. and Jain, R.K. (2006) Biofilms: implications in bioremediation. *Trends in Microbiology*. **14**, 389 - 397.

Skopek, T.R, Glaab, W.E., Monroe, J.1., Kort, K.L. and Schaefer, W. (1999) Analysis of sequence alterations in a defined DNA region: comparison of temperature-modulated heteroduplex analysis and denaturing gradient gel electrophoresis. *Mutation Research*. **430**, 13 - 2l.

Slabbert, S.S. (2007) Evaluation of Fischer-Tropsch GTL Primary Column Bottoms as process cooling water: Analysis of microbial community dynamics, fouling, scaling and corrosion. Masters Dissertation, North West University, Potchefstroom, South Africa.

Smith, C.A., Phiefer, C.B., Macnaughton, S.J., Peacock, A., Burkhalter, R.S., Kirkegaard, R. and White, D.C (2000) Quantitative lipid biomarker detection of unculturable microbes and chlorine exposure in water distribution system biofilms. *Water Research*. **34**, 2683 - 2688.

Soares, R.A., Roesch, L.F.W., Zanatta, G., De Oliveira Camargo, F.A. and Passaglia, L.M.P. (2006) Occurrence and distribution of nitrogen fixing bacterial community associated with oat (*Avena sativa*) assessed by molecular and microbiological techniques. *Applied Soil Ecology*. **33**, 221 - 234.

Statsoft, Inc. (2011). Statistica (Data analysis software system), version 10. www.statsoft.com

Swart, J.S. and Engelbrecht, J.P. (2007) Pilot scale evaluation of mine water (MW) as a cooling medium. *Water SA*. **30(5)**, 145 – 148.

Tanji, Y., Morono, Y., Soejima, A., Hori, K. And Unno, H. (1999) Structural analysis of a biofilm which enhances carbon steel corrosion in nutritionally poor aquatic environments. *Journal of Bioscience and Bioengineering*. **88(5)**, 551 – 556.

Tempelhoff, J.W.N. (2009) Civil society and sanitation hydropolitics: A case study of South Africa's Vaal River Barrage. *Physics and Chemistry of the Earth*. **34**, 164 – 175.

TerBraak, C.J.F. (1988) CANOCO – an extension of Decorana to analyze spatial-environment relationships. *Vegetation*. **75(3)**, 159 – 160.

Van der Bruggen, B. and Braeken, L. (2006) The challenge of zero discharge: from water balance to regeneration. *Desalination*. **188**, 177 - 183.

Videla, H.A. (2002) Prevention and control of biocorrosion. *International Biodeterioration and Biodegradation*. **49**, 259 - 270.

Viera, M.R., Guiamet, P.S., De Mele, M.F.L. and Videla, H.A. (1999) Use of dissolved ozone for controlling planktonic and sessile bacteria in industrial cooling systems. *International Biodeterioration & Biodegradation.* **44**, 201 – 207.

Villanueva, L., Navarrete, A., Urmeneta, J., White, D.C. and Guerrero, R. (2004) Combined Phospholipid Biomarker-16S rRNA Gene Denaturing Gradient Gel Electrophoresis Analysis of Bacterial Diversity and Physiological Status in an Intertidal Microbial Mat. *Applied and Environmental Microbiology*. **70(11)**, 6920 – 6926.

Wang, G., Jin, J., Xu, M., Pan, X. and Tang, C. (2007) Inoculation with phosphate-solubilizing fungi diversifies the bacterial community in rhizospheres of maize and soybean. *Pedosphere*. **17(2)**, 191 - 199.

Wang, J., Wang, Z.Y. and Ke, W. (2010) Corrosion behavior of weathering steel in diluted Qinghai salt lake water in a laboratory accelerated test that involved cyclic wet/dry conditions. *Materials Chemistry and Physics*. **124**, 952 – 958.

Wang, J., Li, S., Xiong, G. And Cang, D. (2011) Application of digital technologies about water network in steel industry. *Resources, Conservation and Recycling*. **55**, 755 – 759.

Wang, Z., Fan, Z., Xie, L. And Wang, S. (2006) Study of integrated membrane systems for the treatment of wastewater from cooling towers. *Desalination*. **191**, 117 – 124.

Wepener, V., van Dyk, C., Bervoets, L., O'Brien, G., Covaci, A. And Cloete, Y. (2011) An assessment of the influence of multiple stressors on the Vaal River, South Africa. *Physics and Chemistry of the Earth*. **36**, 949 – 962.

Werker, A.G. and Hall, E.R. (1998) Using microbial fatty acids to quantify, characterize and compare biofilm and suspended microbial populations in wastewater treatment systems. *Water Science Technology*. **38**, 273 - 280.

White, D.C. and Ringelberg, D.B. (1998) Signature Lipid Biomarker Analysis. In: Burlage, R.S., Atlas, R., Stahl, D., Greesey G., Sayler, G. (Eds.), *Techniques in microbial ecology*, Oxford University Press, New York. p.255 – 272.

White, D.C., Palmer, R.J., Zinn, M., Smith, c.x., Burkhalter, R., Macnaughton, S.J., Whitaker, K.W. and Kirkegaard, R. (1999) Manipulation of biofilm microbial ecology. Proceedings of the Eighth International Symposium on Microbial Ecology. Halinax: Nova Scotia. August 9 - 14, 1995.

Widmer, F., FlieBbach, A., Laczkó, E., Schulze-Aurich, J. and Zeyer, J. (2001) Assessing soil biological characteristics: a comparison of bulk community DNA-, PLFA-, and Biolog^{TM} - analyses. *Soil Biology and Biochemistry*. **33**, 1029 - 1036.

Winch, S., Praharaj, T., Fortin, D. and Lean, D.R.S. (2008) Factors affecting methylmercury distribution in surficial acidic, base-metal mine tailings. *Science of the Total Environment*. **392**, 242-251.

Xu, C., Zhang, Y., Cheng, G. and Zhu, W. (2007) Localized corrosion behavior of 316 L stainless steel in the presence of sulfate-reducing and iron-oxidizing bacteria. *Materials Science and Engineering A*. **443**, 235 - 241.

Yan, H., Liu, L., Yang, F., Takaoka, D. and Wang, C. (2010) Operational optimization of air conditioning cooling water system with UF-RO desalination. *Desalination.* **251(1-3)**, 53 – 57.

Yang, H. and Abbaspour, K.C. (2007) Analysis of wastewater reuse potential in Beijing. *Desalination*. **212**, 238 - 250.

Yang, Q., Liu, Y., Gu, A., Ding, J. and Shen, Z. (2002) Investigation of induction period and morphology of $CaC0_3$ fouling on heated surface. *Chemical Engineering Science*. **57**, 921 - 931.

You, S., Tseng, D. and Guo, G. (2001) A case study on the wastewater reclamation and reuse in the semiconductor industry. *Resources, Conservation and Recycling*. **32**, 73 - 81.

Zhang, B., Baosheng, S., Min, J., Huina, L. and Xianhua, L. (2010) Quantification and comparison of ammonia-oxidizing bacterial communities in MBRs treating various types of wastewater. *Bioresource Technology*. **101**, 3054 – 3059.

Zhao, x., Wang, Y., Ye, Z., Borthwick, A.G.L. and Ni, J. (2006) Oil field wastewater treatment in biological aerated filter by immobilized microorganisms. *Process Biochemistry*. **41**, 1475 - 1483.

Appendix A1

Table A1: Water chemistry of raw feed (PCB) as well as the different COC stabilised and non-stabilised water during the accelerated corrosion process.

Variable	Units	PCB	2COC,S	4COC,S	6COC,S	2COC,N	4COC,N	6COC,N
Total alkalinity	(mg $CaCO_3$/L)	**10.00**	605.00	930.00	1050.00	125.00	235.00	87.50
Total hardness	(mg $CaCO_3$/L)	**391.00**	428.00	784.00	958.00	561.00	958.00	1792.00
TDS	(mg/L)	**-**	1000.00	1700.00	2300.00	1300.00	2000.00	5400.00
TSS	(mg/L)	**-**	42.00	92.00	59.00	31.00	61.00	117.00
Total iron	(mg Fe/L)	**2.26**	1.06	4.25	3.37	1.60	3.37	7.24
Chloride	(mg Cl/L)	**33.20**	68.00	152.00	2.92	265.00	508.60	2364.50
Sulphate	(mg SO_4/L)	**121.60**	132.10	343.00	575.70	142.10	261.80	386.10
Dissolved oxygen	(mg/L)	**-**	0.90	0.30	0.29	0.74	0.56	0.23
Electrical conductivity	(mS/cm)	**0.79**	2.12	3.30	4.24	1.85	2.94	8.72
pH		**4.40**	8.16	8.30	8.38	7.43	7.51	7.10
Key: COC = Cycles of concentration; S = Stabilised water; N = Non-stabilised water								